SUSTAINABLE ENERGY SYSTEMS WITH HVDC TRANSMISSION

Thesis submitted in the partial fulfillment for the award of the degree of

Master of Engineering
in
Power Systems & Electric Drives

Thapar University, Patiala

By
Ashima Taneja
Roll No: 800941005

Under the supervision of

Dr. Sanjay K. Jain
Associate Professor, EIED

JULY 2011

ELECTRICAL & INSTRUMENTATION ENGINEERING DEPARTMENT
THAPAR UNIVERSITY
PATIALA-147004

CERTIFICATE

I hereby certify that the work which is being presented in the thesis entitled, "**Sustainable Energy Systems with HVDC Transmission**" in partial fulfillment of the requirement for the award of degree of Master of Engineering in ***Power Systems & Electric Drives*** submitted in Electrical & Instrumentation Engineering Department of Thapar University, Patiala, is an authentic record of my own work carried out under the supervision of **Dr. Sanjay K. Jain**, Associate Professor, EIED.

The matter presented in this thesis has not been submitted for the award of any other degree of this or any other university.

Ashima 04/07/11

(Ashima Taneja)
Roll No: 800941005

It is certified that the above statement made by the student is correct and true to the best of my knowledge and belief.

Sanjay 04/07/2011

(Dr. Sanjay K. Jain)
Associate Professor
EIED, Thapar University
Patiala

Countersigned by

S. Ghosh

(Dr. Smarajit Ghosh)
Professor & Head
Electrical & Instrumentation Engg. Department
Thapar University,
Patiala

(Dr. S.K. Mohapatra)
Dean (Academic Affairs)
Thapar University,
Patiala

ACKNOWLEDGEMENT

On completion of my thesis work, it is my proud privilege to express my deep sense of gratitude towards **Dr. Sanjay K. Jain, Associate Professor, EIED** for his invaluable guidance, constant encouragement, suggestions, great patience, and continuous technical support which helped me to survive through crest and troughs of my thesis work and complete it successfully. It is a great privilege to work under him, who motivated me in every course of my work and made me believe in myself.

It is a great pleasure to express my special thanks to **Dr. Smarajit Ghosh, Professor and Head of EIED.**, for his suggestions and encouragement which helped me in completing this thesis work successfully. I also thank **Dr. Yaduvir Singh, P.G. Coordinator** and all faculty members of EIED for their encouragement.

Much appreciations is expressed to **Dr. Abhijit Mukherjee, Director, Thapar University, Dr. K.K. Raina, Deputy Director, Thapar University** and **Dr. S.K. Mohapatra, Dean of Academic Affairs** for providing moral support during my M.E. Thesis work.

I am very happy to express salutations to my parents because, my success, my failure, indeed everything I own, belongs to them. I would also like to express my deep affection and best wishes to my loving sister Miss. Geetika Taneja.

Ashima

Ashima Taneja

800941005

ABSTRACT

Power generation using conventional resources like coal, natural gas etc. is well accepted over the years and mostly preferred for large capacity plants. Due to various environmental concerns like global warming and depleting fossil fuels, it has become necessary not only to upgrade our technology but to explore renewable resources like wind, small hydro, solar for generation of electricity. The renewable resources are available in abundance and their usage can be advantageous to supply various consumers and especially during peak demand. Availability of renewable resources at large distant locations suggests their integration through grid for better exploration. For low capacity renewable resources, the HVDC link can be utilized for their integration with grid.

In this work, mathematical modeling and simulation of various sources like PV, hydro, wind, diesel and thermal generators have been carried out. Also, the modeling of a monopolar HVDC transmission line has been derived and implemented in MATLAB Simulink environment. Every generator is integrated through independent HVDC link and the respective output is brought to a common grid individually. The performance of the system is studied with individual resource and transmission line connected to the grid and with all the generating resources feeding their energy to the grid collectively.

TABLE OF CONTENTS

LIST OF FIGURES

5.16(c)	Single Phase AC Voltage of Steam HVDC System obtained at common grid after interconnection	81

CHAPTER 1

INTRODUCTION

1.1 OVERVIEW

As known to us, the non renewable resources of energy like coal, petroleum, natural gas, etc. are depleting day by day, however, the dependency on electrical energy is increasing continuously. Therefore, the renewable sources of energy like wind, solar, hydro, nuclear, tidal, etc. are to be harnessed. Sustainable energy generation like hydro, wind, sun and waves are depending on the geographic features and may not always be located close to the consumption. This fact makes transmission of the power as almost as essential as the generation. Such problem does not arise normally during the electricity generation with the non sustainable resources like coal, oil, gas etc. because they can be and are being transported. Thus, hydro, wind, sun and wave energy have to be transmitted as electricity.

Electricity has been used for more than 100 years mainly by alternating current. However, transmission of large amounts of power over long distances the use of high voltage direct current; HVDC has in many cases been found very economical.

HVDC was first used commercially 50 years ago. Since then a growing number of transmission schemes have been constructed around the world. Apart from being economical for transmission of power over long distances the use of high voltage direct current has the following advantages over ac transmission:

- The two stations can be connected to networks that are not synchronized or do not even have the same frequency.
- Power can be transmitted over very long distances without compensation for the reactive power.

- Only two conductors are needed (or even one conductor if the ground or the sea is used as return) for HVDC compared to three conductors for alternating current.

A new type of HVDC using thyristors for the ac/dc conversion has been developed. By using components that can not only switch on the current but also switch it off, making it possible to build voltage source converters (VSC).This type of converters offer many advantages when it comes to transmission of power especially from sustainable energy systems. The HVDC systems using VSC has the following advantages:

- Simultaneous control of both active and reactive power. The ac voltage can be controlled at both stations.
- No need for short circuit power for commutation. It can operate against even black networks.
- It can operate without communication between the stations.
- It can operate from control the power continuously from one direction.
- No change of voltage polarity when the power direction is changed. This makes easier to build multi terminal schemes.

The **wind power** is an important sustainable source for generating electricity. It is available in abundance normally in coastal areas. The large capacity output through wind farms is poised to many challenges like identification of sites for big wind parks with good wind conditions, opposition due to people because of their displacement. Such problems are normally not experienced for small capacity plants. The wind can be harnessed using the synchronous or induction generators. The induction generator can be operated as doubly fed induction generator (DFIG) or self-excited induction generator (SEIG) depending on the type of rotor construction i.e. wound rotor or cage rotor construction. The generated AC output can be fed directly to the grid or can be fed to grid through HVDC transmission line.

Another most important generation of sustainable energy comes from **hydropower**. Generally conventional large capacity hydro projects are situated away from the population. The implementation of large hydro project has faced many techno-economic challenges like resistance through people, long implementation period etc. The small or mini hydro resources are available in abundance in the hilly regions like north-eastern states, Uttrakhand in India. There

are situations when hydro resources are located around thousand kilometers away from the consumption end. For example, large hydro resources available in Assam are used to supply Punjab, Gujarat etc. For medium capacity generation, the synchronous generators with excited and governor control can be used. For small distances, ac transmission is sufficient. However, for large distances the power transfer through HVDC transmission lines is suited.

Another sustainable energy resource is solar power which has not being harnessed up to the optimum level as compared to the available capacity. The reasons for the under utilization of solar power is the lesser efficiency of the solar panels and arrays. Solar power is captured by large number of solar cells connected in series/parallel to give desired power. Each solar cell works on the principle of photovoltaic that is conversion of light radiation into electricity. The power available from solar cells is dc in nature which is converted to ac for facilitating high voltage transmission. The dc is converted into ac by use of a power electronic inverter employing line commutation which is made possible by the use of power IGBT's and transistors. The tremendous development in power electronics and advent of PWM technology are vital improvements towards increase in efficiency of solar cells. Also, suitable sites for solar plants are most certainly located in deserts where the efficiency will be the best and the land is not used for agriculture, forestry or urban settlement. For deserts, the overhead lines are not suited due to the risk of salt contamination on the insulators and therefore cable transmission can be used. For such situations, the HVDC, which is suited for cable transmission, can be employed to transmit very large amounts of power over long distances.

1.2 LITERATURE SURVEY

The literature on renewable energy generation and HVDC transmission is very much diversified; a brief review is presented in the following section.

Variable generation technologies generally refer to generating technologies whose primary energy source varies over time and can't reasonably be stored to address such variation. Variable generation sources which include wind, solar, ocean and some hydro generation resources are all renewable. There are two major attributes of a variable generator that distinguish it from conventional forms of generation and may impact the bulk power system planning and operations: variability and uncertainty [3].

The main reasons for using renewable energy are: fuel saving, supplying remote places and environmental considerations. The effect of Wind Energy Converters (WECS) in small autonomous power systems has been mostly investigated**.** The transient stability of isolated power systems with WECS has been examined to great extend in order to determine the optimum penetration level at which the power system remains stable. [4].

MATLAB/Simulink is used to model the system and apportion the electrical production between the inverter and diesel engine generator. A self-tuning PID controller was designed to control a small to medium sized diesel engine model. The equations of synchronous generator are obtained from Park equations [5].

An electro-hydraulic speed-control mechanism provides flexibility through the use of electronic circuits in place of mechanical components in the low-power portions has been simulated. [6-10].

The stand-alone renewable green wind energy system is connected to the local load bus over a radial transmission line comprising the following main components: wind turbine, gear box, asynchronous generators, etc has been proposed. [11-12].

This paper describes the dynamic behavior of a typical fixed speed wind turbine connected to the grid; the model is developed in the simulation tool MATLAB/ Simulink and created as a modular structure. The pitch control system is used for stabilization of the wind turbine at grid faults. [13-17].

New models including the widespread use of electric-hydraulic speed control both in new construction and in modernization of older power plants are developed. Models describing the actual equipment rather than making approximations to fit existing mechanical governor models are simulated. [18-24].

An exact small signal linear model of the HVDC converter has been recently published, and this paper describes two applications of the model. The first application is the calculation of steady state harmonic levels in the presence of unbalanced ac systems. The second application is the calculation of the dynamics of HVDC systems, particularly within the frequency range from 2 to

200Hz. Both applications are in excellent agreement with time domain simulations using PSCAD/EMTDC [31].

1.3 OBJECTIVE OF WORK

The objective of the present work is to study and simulate modeling of various energy generating resources namely PV generator, asynchronous wind generator, salient pole synchronous hydro generator, diesel generator set and steam driven cylindrical rotor alternator. Along with the generating resources, the aim is to study and simulate a long distance HVDC system to transmit the energy generated by these resources for load located at far distant locations. The interconnection of these resources feeding energy collectively to the grid has been simulated.

1.4 ORGANIZATION OF THESIS

The work carried out in this thesis has been summarized in six chapters The **Chapter 1** summarized the overview of the thesis, brief literature review, objectives of work and organization of the thesis. The **Chapter 2** deliberates the various renewable energy sources like wind, diesel, hydro, solar and coal. The **Chapter 3** discussed the mathematical modeling and simulations of the various resources discussed in Chapter 2. The **Chapter 4** details the basics of HVDC Transmission along with its mathematical and Simulink model. The **Chapter 5** presents the results and discussions on the work done. The conclusions and the scope of further work are detailed in **Chapter 6**.

CHAPTER 2

ELECTRICITY GENERATION FROM VARIOUS RESOURCES

In recent years there has been increasing interest in the production of electric energy from the renewable energy sources, especially wind, solar and hydro. The main reasons for using them are: fuel saving, supplying remote places and environmental considerations.

Various resources of energy like wind, solar, hydro, coal and diesel etc. have been explored for generation of electricity. The availability of these resources and the methods by which these sources can be tapped to generate electricity and the basic components used for the generation has been discussed below.

2.1 ELECTRIC POWER GENERATION FROM WIND

Wind energy is the fastest growing source of renewable clean, reliable, and efficient pollution free green electricity in the world. It is rapidly expanding and is powering homes and businesses. Wind is a renewable resource because it is inexhaustible. It is a result of the sun shining unevenly on the earth. The corresponding daily and seasonal changes in temperature consistently generate wind, producing a energy source that can never be depleted.

The economic viability of constructing a wind turbine at the site depends mostly on the quality of wind resource. Generally, average annual wind speeds of at least 4.0–4.5 m/s are needed for a small wind turbine to produce enough electricity to be cost-effective. The basic components of a typical wind energy system are shown on Figure 2.1.These basic components include:

- A **rotor** consists of blades with aerodynamic surfaces. When the wind blows over the blades, the rotor turns, causing the generator or alternator in the turbine to rotate and produce electricity.
- A **gearbox** matches the rotor speed to that of the generator/alternator.
- An enclosure or **nacelle** protects the gearbox, generator and other components of the turbine from the elements.
- A **tail vane** or yaw system aligns the turbine with the wind.

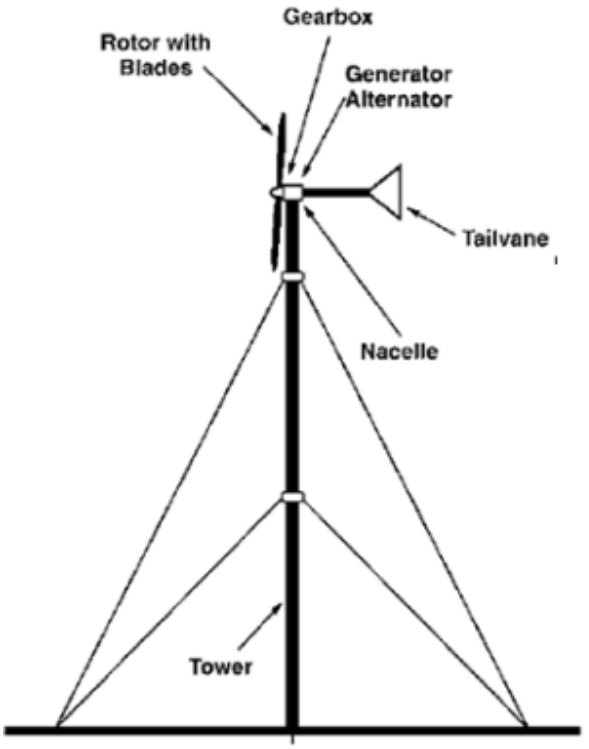

Figure 2.1: Wind Turbine

Several types of towers are available:

- **Guyed lattice towers,** where the tower is permanently supported by guy wires.
- **Guyed tilt-up towers** can be raised and lowered for easy maintenance and repair.
- **Self-supporting towers** do not have guy wires.

The power in the wind is proportional to:

- Area of windmill being swept by the wind
- Cube of the wind speed
- Air density - which varies with altitude

The wind power is expressed as:

$$P = ½.\rho.A.V^3 \quad (2.1)$$

Where,

P is power in watts (W)

ρ is the air density in kilograms per cubic meter (kg/m^3)

A is the swept rotor area in square meters (m^2)

V is the wind speed in meters per second (m/s)

Although the equation (2.1), provide the power in the wind, the actual power that can be extracted from the wind is significantly less. The actual power depends on several factors, such as the type of machine and rotor used the sophistication of blade design, friction losses, and the losses in the pump or other equipment connected to the wind machine. Therefore, the wind power will be:

$$P = ½.C_p.\rho.A.V^3 \qquad (2.2)$$

Where, C_p is defined as the c proportion of the power in the wind that the rotor can extract.

- **Start-up wind speed:** the wind speed that will turn an unloaded rotor
- **Cut-in wind speed:** the wind speed at which the rotor can be loaded
- **Rated wind speed:** the wind speed at which the machine is designed to run (this is at optimum tip speed ratio)
- **Maximum design wind speed:** the wind speed above which damage could occur to the machine.

The **tip speed ratio** is defined as the ratio of the speed of the extremities of a windmill rotor to the speed of the free wind.

2.2 ELECTRICITY GENERATION USING DIESEL DRIVEN ALTERNATOR

Though a lot of renewable energy resources are gaining a lot of popularity today; but still power generation by using diesel engine as prime mover has its own place in the commercial power generation.

A diesel generator is the combination of a diesel engine with an electrical generator to generate electric energy. Diesel generating sets are used in places without connection to the grid or as emergency power-supply if the grid fails. Small portable diesel generators ranging from about 1

KVA to 10 KVA may be used as power supplies on construction sites, or as auxiliary power for vehicles such as mobile homes.

The diesel internal combustion engine uses highly compressed, hot air to ignite the fuel. Only air is initially introduced into the combustion chamber. The air is then compressed with a compression ratio typically between 15:1 and 22:1 resulting in 40-bar pressure. This high compression heats the air to 550 °C. Then fuel is injected directly into the compressed air in the combustion chamber. The fuel injector ensures that the fuel is distributed evenly. The heat of the compressed air vaporizes fuel from the surface of the droplets. The vapor is then ignited by the heat from the compressed air in the combustion chamber, the droplets continue to vaporize from their surfaces and burn, getting smaller, until all the fuel in the droplets has been burnt.

A diesel engine burns diesel fuel in order to produce motion for the generator, which converts the motion into electricity by using electromagnets. The small internal combustion engine of a diesel generator operates just like any other small engine; though a number of fuels can be used to power similar engines, diesel is generally preferred for generators because of its ability to burn but not explode. A throttle and governor are used to keep the speed of the diesel engine under control in order to standardize the power output of the generator while also preventing damage to components that could be caused by the engine operating at too high of a speed.

As the diesel engine turns the crankshaft that connects to the generator, the central axle of the generator is spun within a chamber containing electromagnets. This high-speed motion causes an electric current, which is then available for use by any equipment that is plugged in to the diesel generator. The governor switch that helps to control the diesel engine's speed allows for increases in engine speed when the produced electricity is being used, leading to the engine revving up as needed in order to make sure that the amount of electricity provided by the diesel generator doesn't drop suddenly whenever plugged-in power tools or other electronic devices are in use.

2.3 HYDROELECTRIC POWER GENERATION

Hydropower is energy that comes from the force of moving water. The fall and movement of water is part of a continuous natural cycle called the water cycle. Gravity drives the water, moving it from high ground to low ground. Hydropower is called a renewable energy source because the water on the earth is continuously replenished by precipitation.

A typical hydro plant, as shown in Figure 2.2, there are three main parts, a power plant where the electricity is produced, a dam that can be opened or closed to control water flow and a reservoir where water can be stored. To generate electricity, a dam opens its gates to allow water from the reservoir above to flow down through large tubes called penstocks. At the bottom of the penstocks, the fast-moving water spins the blades of turbines. The turbines are connected to generators to produce electricity. The electricity is then transported via huge transmission lines.

The amount of electricity that can be generated at a hydro plant is determined by two factors: head and flow. **Head** is the distance from the highest level of the dammed water to the point where it goes through the power-producing turbine. **Flow** is how much water moves through the system—the more water that moves through a system, the higher the flow. Generally, a **high-head plant** needs less water flow than a **low-head plant** to produce the same amount of electricity.

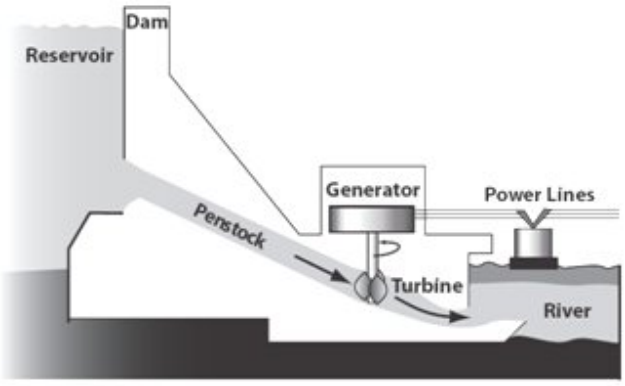

Figure 2.2: Schematic of Hydro electric power plant

One of the biggest advantages of a hydropower plant is its ability to store energy. The water in a reservoir is, after all, stored energy. Water can be stored in a reservoir and released when needed

for electricity production. Some hydro plants use pumped storage systems. The same water is used again and again.

Generating electricity with hydropower is the cheapest way to generate electricity, and the fuel supply that is flowing water is always available. Hydropower is cheapest way to generate electricity today. The cost of electricity (per kWh) is one fourth of the cost due to coal plants and half of the cost due to nuclear plants.

2.4 SOLAR POWER

Among various non-conventional resources, the energy from the sun is a primary one, unbounded by territorial or monopoly limitations. And this energy is readily available during the day for anyone to tap and that too free and without any constraint. The sun generates an enormous amount of energy each second, by converting hydrogen to helium. This energy, called solar radiation is radiated into space and reaches the earth as sunlight. This solar radiation can be "captured" and converted to useful energy. Photovoltaic (PV) cells are the most recent type of technology used to produce electricity directly from sunlight.

The physics of the PV cell is very similar to that of the classical diode with a pn junction. When the junction absorbs light, the energy of absorbed photons is transferred to the electron–proton system of the material, creating charge carriers that are separated at the junction. The charge carriers in the junction region create a potential gradient, get accelerated under the electric field, and circulate as current through an external circuit.

PV cells consist, in essence, of a junction between two thin layers of dissimilar semiconducting materials, known respectively as ‘p’ (positive) type semiconductor band ‘n’ (negative) type semiconductor. n-type semiconductors are made from crystalline silicon that has been ‘doped’ with tiny quantities of an impurity (usually phosphorus) in such a way that the doped material possesses a surplus of free electrons. Electrons are sub-atomic particles with a negative electrical charge, so silicon doped in this way is known as an n (negative) type semiconductor. p-type semiconductors are also made from crystalline silicon, but are doped with very small amounts of a different impurity (usually boron) which causes the material to have a deficit of free electrons. These ‘missing’ electrons are called holes.

Since the absence of a negatively charged electron can be considered equivalent to a positively charged particle, silicon doped in this way is known as a p (positive)-type semiconductor. When the n-types and p-type meet they form a p-n junction. The pn junction to understand the operation of PV cell is shown in Figure 2.3. In pn junction, the holes drift from the p-side to the n-side and free electrons drift in the other direction. This movement produces an electrical field across the junction. There are negative ions left behind when a hole leaves the p-side and positive ions left behind when a free electron leaves the n-side. These create a dipole layer at the junction that produces an electric field that opposes more majority carriers traveling to the opposite side of the p-n junction. This electric field will aid in the generation of electricity.

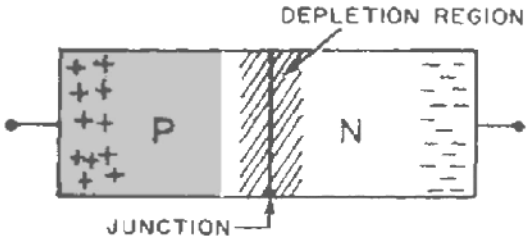

Figure 2.3: pn junction

The light consists of stream of tiny particles of energy called photons. When photons from light of a suitable wavelength fall within the p–n junction, they can transfer their energy to some of the electrons in the material, so 'promoting' them to a higher energy level. Normally, these electrons help to hold the material together by forming so called 'valence' bonds with adjoining atoms, and cannot move. In their 'excited' state, however, the electrons become free to conduct electric current by moving through the material. In addition, when electrons move they leave behind holes in the material, which can also move.

The PV cell is the elementary unit, the interconnection of the number of PV cell forms the module and similarly PV array is formed by combining the number modules. The PV hierarchy is shown in Figure 2.4.

PV Cell

PVs generate electric power when illuminated by sunlight or artificial light. To illustrate the operation of a PV cell the p-n homo junction cell is used.

- **PV Module**

  For the majority of applications multiple solar cells need to be connected in series or in parallel to produce enough voltage and power. Individual cells are usually connected into a series string of cells (typically 36 or 72) to achieve the desired output voltage. The complete assembly is usually referred to as a module shown in Figure 2.4 and manufacturers basically sell modules to customers.

- **PV Array**

  An array is a structure that consists of a number of PV modules shown in Figure 2.4, mounted on the same plane with electrical connections to provide enough electrical power for a given application. Arrays range in power capacity from a few hundred watts to hundreds of kilowatts. To increase the voltage, modules are connected in series and to increase the current they are connected in parallel.

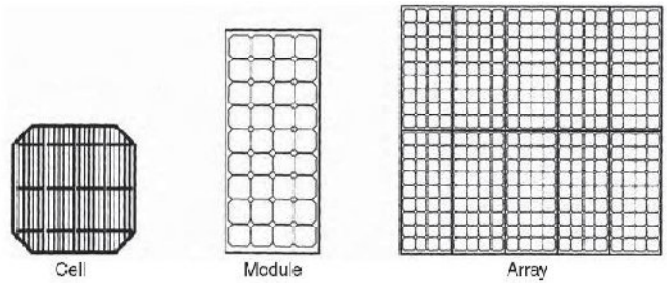

Figure 2.4: Illustration of PV cell, module and array

2.5 THERMAL POWER GENERATION

Electricity has been produced from coal from a very long time. It's the most conventional method of producing electricity. Despite of its various short comings like low efficiency and pollution, it's still being popularly used. The reasons are easily available fuel and simpler technology to generate power with lower costs.

The components and working of thermal power plant are explained as follows:

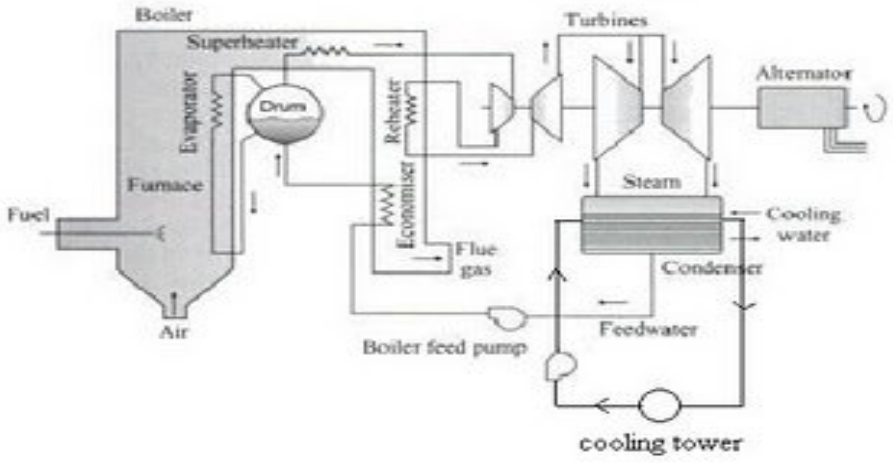

Figure 2.5: Layout of Simplified Thermal Power Plant

The various components of thermal power plant as shown in Figure 2.5 are coal conveyor**,** stoker, pulverizer, boiler**,** coal ash, air preheater, electrostatic precipitators, smoke stack, turbine, condenser, transformers, cooling towers, and generator and high voltage power lines.

- With a **Coal conveyor** coal is transported from coal storage place in power plant to the place nearby boiler.
- A **stoker** is a mechanical device for feeding coal to a furnace.
- A **pulverizer** is a device for grinding coal for combustion in a furnace in a power plant. Pulverized coal is put in boiler furnace.
- **Boiler** is an enclosed vessel in which water is heated and circulated until the water is turned into steam at required pressure.
- Sometimes this steam is further heated in a **superheater** as higher the steam pressure and temperature the greater efficiency the engine will have in converting the heat in steam in to mechanical work. This steam at high pressure and temperature is used directly as a heating medium, or as the working fluid in a prime mover to convert thermal energy to mechanical work, which in turn may be converted to electrical energy. Some of the heat of superheated steam is used to rotate the turbine where it loses some of its energy.
- **Reheater** is also steam boiler component in which heat is added to this intermediate-pressure steam, which has given up some of its energy in expansion through the high-pressure turbine.

The steam after reheating is used to rotate the second steam turbine where the heat is converted to mechanical energy. This mechanical energy is used to run the alternator, which is coupled to turbine, there by generating electrical energy.

- Steam after rotating steam turbine comes to **condenser**. Condensers are heat exchangers which convert steam from its gaseous to its liquid state, also known as phase transition. In doing so, the latent heat of steam is given out inside the condenser.
- The condensate formed in the condenser after condensation is initially at high temperature. This hot water is passed to **cooling towers**. It is a tower- or building-like device in which atmospheric air (the heat receiver) circulates in direct or indirect contact with warmer water (the heat source) and the water is thereby cooled. Water, acting as the heat-transfer fluid, gives up heat to atmospheric air, and thus cooled, is recirculated through the system, affording economical operation of the process.
- Flue gases coming out of the boiler carry lot of heat. Function of **economizer** is to recover some of the heat from the heat carried away in the flue gases up the chimney and utilize for heating the feed water to the boiler. It is placed in the passage of flue gases in between the exit from the boiler and the entry to the chimney.
- The remaining heat of flue gases is utilized by **air preheater**. It is a device used in steam boilers to transfer heat from the flue gases to the combustion air before the air enters the furnace.
- **Electrostatic precipitator** is a device which removes dust or other finely divided particles from flue gases by charging the particles inductively with an electric field, then attracting them to highly charged collector plates. It's also known as precipitator. The process depends on two steps. In the first step the suspension passes through an electric discharge.
- A **chimney** is a system for venting hot flue gases or smoke from the boiler, stove and furnace to outside the atmosphere.
- An **alternator** is an electromechanical device that converts mechanical energy to alternating current electrical energy.

CHAPTER 3

MATHEMATICAL MODELING AND SIMULATIONS

In these sections, the mathematical models of various generating systems namely wind generator system, diesel driven alternator, hydro electric generator, PV cells and thermal generator, have been derived. The implementation of these mathematical models under Simulink has also been described.

3.1 WIND GENERATOR MODEL

In this section, the electrical and mechanical components of wind generator system are modeled. The aerodynamic model has been used to represent the Fixed Speed Wind Turbine (FSWT). The induction generator is represented by dq model.

3.1.1 MATHEMATICAL MODEL OF THE WIND TURBINE

The wind turbine continuously extracts kinetic energy from the wind by decelerating the air mass, and feeds it to the generator as mechanical power. The aerodynamic model of the wind turbine is necessary because it gives a coupling between the wind speed and the mechanical torque produced by the wind turbine. The mechanical power, P_M, produced by the wind turbine rotor can be defined as:

$$P_m = C_p(\lambda, \beta)\, P_v = \frac{1}{2}\rho_{air} v^3 A C_p(\lambda, \beta) \qquad (3.1)$$

Where

A	=	swept wind turbine rotor area,
C_p	=	performance coefficient of the wind turbine,
P_v	=	wind power available in the rotor swept area,
v	=	wind speed,
ρ_{air}	=	air density,
λ	=	tip speed ratio of the rotor blade tip speed to wind speed,
β	=	blade pitch angle.

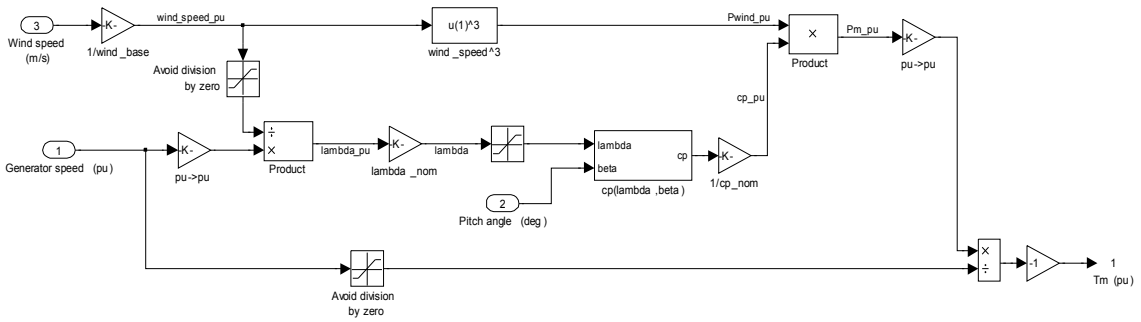

Figure 3.1: Simulation of Wind Turbine Block

The mathematical model of wind turbine simulated in MATLAB/Simulink is shown in Figure 3.1.The relation between C_P and λ is normally established by the C_P/λ curve. This curve can be approximated using the power/wind curve, provided by wind turbine manufacturers. To perform this calculation, it is supposed that the rotor speed does not depend on wind speed in steady-state operation. Here, a generic equation is used to model the performance coefficient, $C_P(\lambda, \beta)$. This equation, based on the turbine model characteristics, is:

$$C_p(\lambda, \beta) = f_1(u) = C_1 \left(\frac{C_2}{\lambda} - C_3\,\beta - C_4\right) e\left(\frac{-C_5}{\lambda}\right) + C_6 \qquad (3.2)$$

Also,

$$1/\lambda_i = f(u) = 1/(\lambda + 0.08\,\beta) - 0.035/(\beta^3 + 1) \qquad (3.3)$$

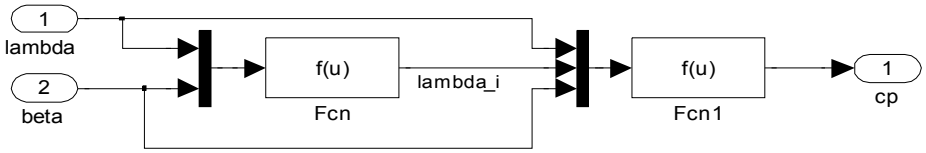

Figure 3.2: Simulation Model for Obtaining λ_i and C_p

Above equations (3.2) and (3.3) are simulated as shown in Figure 3.2.

3.1.2 INDUCTION GENERATOR MODEL

The electrical part of the machine is represented by a fourth-order state-space model and the mechanical part by a second-order system. All electrical variables and parameters are referred to the stator. All stator and rotor quantities are in the arbitrary two-axis reference frame (dq frame)

The voltage equations and flux equations for induction generator are described as follows:

$$V_{qs} = R_s i_{ds} + \frac{d\varphi_{qs}}{dt} - \omega\varphi_{qs} \quad (3.4a)$$

$$V_{ds} = R_s i_{ds} + \frac{d\varphi_{qs}}{dt} - \omega\varphi_{qs} \quad (3.4b)$$

$$V'_{qr} = R_r i'_{qr} + \frac{d\varphi'_{dr}}{dt} + (\omega - \omega_r)\varphi'_{dr} \quad (3.4c)$$

$$V'_{dr} = R_r i'_{dr} + \frac{d\varphi'_{qr}}{dt} - (\omega - \omega_r)\varphi'_{qr} \quad (3.4d)$$

$$\varphi_{qs} = L_s i_{qs} + L_m i'_{qr} \quad (3.5a)$$

$$\varphi'_{dr} = L'_r i'_{dr} + L_m i_{ds} \quad (3.5b)$$

$$\varphi_{ds} = L_s i_{ds} + L_m i'_{dr} \quad (3.5c)$$

$$\varphi'_{qr} = L'_r i'_{qr} + L_m i_{qs} \quad (3.5d)$$

$$T_e = 1.5p(\phi_{ds} i_{qs} - \phi_{qs} i_{ds}) \quad (3.6)$$

$$L_s = L_{ls} + L_m \quad (3.7a)$$

$$L'_r = L'_{lr} + L_m \quad (3.7b)$$

$$\frac{d\theta_m}{dt} = \omega_m \quad (3.8a)$$

$$\frac{d\omega_m}{dt} = \frac{1}{2H}(T_e - F\omega_m - T_m) \quad (3.8b)$$

The q axis and axis equivalent of the induction machine electrical model are shown in Figure 3.3 & Figure 3.4.

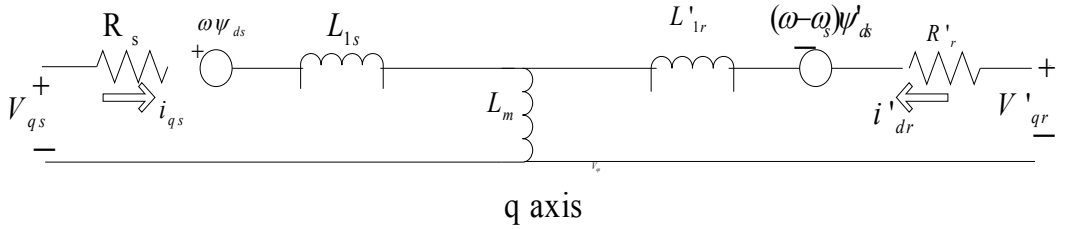

Figure 3.3: q axis equivalent of induction generator

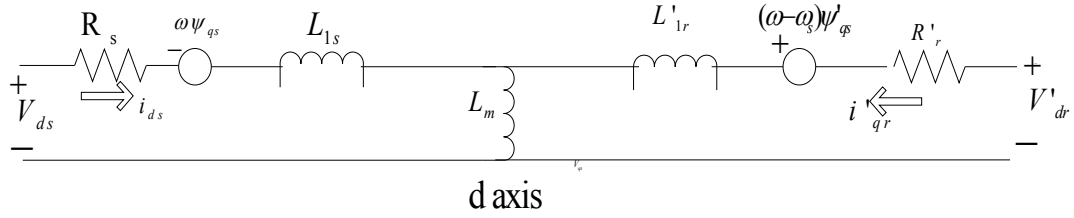

Figure 3.4: d axis equivalent of induction generator

The electrical model suggests that the stator and rotor fluxes are obtained using the numerical integration. However, the stator and rotor currents are obtained using the computed fluxes and the inductance parameters. Further, the above model is a dq variable model and therefore the outcome will be dq axes fluxes and currents. For the clarity, the dq variables are to be converted back into the phase variables. For computing the fluxes the stator and rotor voltages, which are the input, are to be represented into the dq variables.

Therefore, the implementation is shown in Figure 3.5 carried out using the following steps:

1) The dq axes stator and rotor voltages v_{ds}, v_{qs}, v_{dr} and v_{qr} are obtained from phase variables, v^s_{abc} and v^r_{abc} through the following sub-steps:

- Sine and cosine values for Θ, ωr and β are calculated where, ω_r is angular speed of rotor, Θ is rotor angle and $\beta = \Theta - \Theta_r$.
- The stator & rotor voltages (v^s_{abc} , v^r_{abc}) are transformed into $_{dq}$ axes to form v^s_{dq} and v^r_{dq} using Park transformation to form equation 3.4a to 3.4d.

2) The mutual fluxes in equations 3.9a and 3.9b for q and d axes are calculated by using rotor and stator dq axes fluxes φ_{dq}^{s} & i_{dq}^{r} and inductances L_{lr} & L_{ls} from equation no 3.5a to 3.5d.

$$\varphi_{mq} = \left(\frac{\varphi_{qr}}{L_{lr}} + \frac{\varphi_{qs}}{L_{ls}} \right) L_{aq} \tag{3.9a}$$

$$\varphi_{md} = \left(\frac{\varphi_{dr}}{L_{lr}} + \frac{\varphi_{ds}}{L_{ls}} \right) L_{ad} \tag{3.9b}$$

3) The currents for stator and rotor side i^{s}_{dq} & i^{r}_{dq} are calculated by using following equations from 3.10a to 3.10d.

$$i_{qr} = k\left(\varphi_{qr} - \varphi_{mq} \right) \tag{3.10a}$$

$$i_{dr} = k\left(\varphi_{dr} - \varphi_{md} \right) \tag{3.10b}$$

$$i_{qs} = k\left(\varphi_{qs} - \varphi_{mq} \right) \tag{3.10c}$$

$$i_{ds} = k\left(\varphi_{ds} - \varphi_{md} \right) \tag{3.10d}$$

4) Finally, the rotor and stator side currents are transformed into phase currents.

5) Torque is calculated as shown in above equation 3.6.

6) From the mechanical model of the induction generator, equation 3.8a & 3.8b is formed. Simulink representation of mechanical model is shown in Figure 3.6.

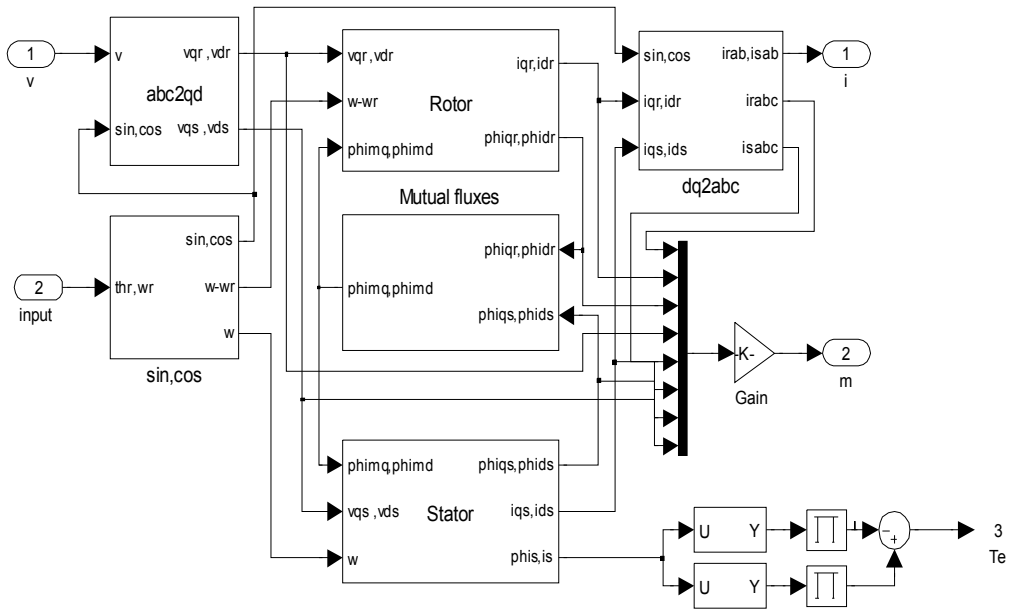

Figure 3.5: Simulink model representation of electrical model of induction generator

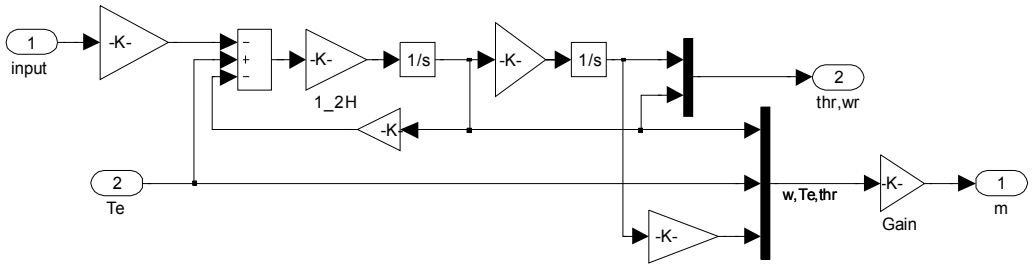

Figure 3.6: Simulink model representation of mechanical model of induction generator

3.2 DIESEL GENERATOR MODEL

A diesel electricity generator is simulated by using an alternator having its mechanical energy from diesel engine. Also, alternator gets its field voltage from an excitation system.

3.2.1 DIESEL ENGINE MODEL

To simulate the complete dynamics of a diesel engine system, a very large order model will be required. However for most studies on speed dynamics of internal combustion engines, it is

sufficient to use a lower order model. Similar approaches have been adopted in diesel engine simulation studies. The engine consists of three parts: the actuator, the engine and the flywheel. The speed control system designed to control the speed of diesel engine is shown in Figure 3.7.

Diesel engines in the range of 100 to 1000 horsepower are generally referred to as small to medium sized diesel engines. When being used to drive electrical gen sets, a Proportional, Integral, Derivative (PID) controller typically controls this type of engine. Suitable values for the three gains in a PID compensator are usually found by trial and error.

PID controller is the Laplace transform of the classic:

$$u(s) = Pe(s) + \frac{Ie(s)}{s} + \frac{Dse(s)}{\mu s + 1} \tag{3.11}$$

Where e(s) is the input to the controller which is difference of reference value given and feedback value obtained and u(s) is the output of the controller.

A lag has been added to the denominator of the derivative term, because high frequency noise tends to dominate a pure derivative function. The time constant of this lag, μ, is typically made much smaller than the time constants of any modeled system dynamics.

A dead time T_D in Figure 3.7 represents unmodeled high frequency dynamics, as well as the almost pure dead time associated with an engine.

This dead time is the result of having several cylinders. Not all cylinders will be in a position to accept more fuel at a given instant. The dead time T_D is largely made up of the time required for all cylinders to come into position to be filled with more or less fuel. This parameter is fixed in this model, and is set to 0.04 seconds. This parameter cannot vary because the parameter estimation technique utilized by this controller cannot tolerate varying dead time.

In the simulated system, speed control for diesel engine and supplying the torque obtained from it to a synchronous generator. Diesel engine is assumed to be simulated and the speed obtained from it is basically controlled by designing a speed control system for it.

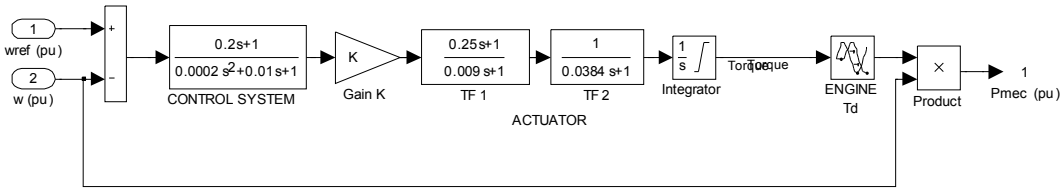

Figure 3.7: Speed Control of Diesel Engine

The blocks basically take speed of engine as input and gives mechanical power as its output. The speed of the diesel engine is same as that of the synchronous generator. To the summing block of the control system, the reference angular speed ω provided is 1 pu. The actual speed of the diesel engine is provided from the measurement port of the synchronous machine which happens to be same for both the engine and generator. The speed error is provided to the PID controller with transfer function:

$$H(s) = \frac{40(1+0.2s)}{1+0.01s+0.0002s^2} \tag{3.12}$$

The control system passes the output signal to the actuator, which converts it to a torque signal. The transfer function of the actuator is given by the two transfer function blocks in cascade and the resultant transfer function is given by:

$$G(s) = \frac{1+0.25s}{s(1+0.009s)(1+0.0384s)} \tag{3.13}$$

The control signal after passing through the integrator is made to have a delay of 0.024 units. The integrator takes care that torque remains between the limits from 0 to 1.2.

$$T_D = e^{-0.024s} \tag{3.14}$$

The time delay block, which is referred to as the input dead time of the system, comprises of three parts:

(i) Time from a load disturbance to time when the cylinders respond;

(ii) Time between the fuel rack change and when a certain amount of fuel has been injected into the chamber;

(iii) Time for fuel to burn and the generation of torque required.

Usually, the first one is called a “power-stroke delay” and the latter two are regarded as an “ignition delay”. The engine dead time is a function of the engine speed and can be considered as a nonlinear part of the system.

The torque signal obtained is then fed to a product box along with the velocity; the result of which gives the mechanical power, which is then fed to the synchronous machine.

$$P_{mec} = \text{Torque X angular velocity} \qquad (3.15)$$

3.2.2 SYNCHRONOUS GENERATOR MODEL

The electrical part of the machine is represented by a sixth-order state space model. The model takes into account the dynamics of the stator, field, and damper windings. The equivalent circuit of the model is represented in the rotor reference frame (dq frame). All rotor parameters and electrical quantities are viewed from the stator. They are identified by prime variables.

The voltage equations and flux equations for synchronous generator are described as follows:

$$V_d = R_s i_d + \frac{d\varphi_d}{dt} - \omega_r \varphi_q \qquad (3.16a)$$

$$V_q = R_s i_q + \frac{d\varphi_q}{dt} + \omega_r \varphi_d \qquad (3.16b)$$

$$V_{kd} = R'_{kd}\, i'_{kd} + \frac{d\varphi'_{kd}}{dt} \qquad (3.17)$$

$$V'_{kq1} = R'_{kq1}\, i'_{kq1} + \frac{d\varphi'_{kq1}}{dt} \qquad (3.18a)$$

$$V'_{kq2} = R'_{kq2}\, i'_{kq2} + \frac{d\varphi'_{kq2}}{dt} \qquad (3.18b)$$

$$\varphi_d = L_d i_d + L_{md}(i'_{fd} + i'_{kd}) \qquad (3.19a)$$

$$\varphi_q = L_q i_q + L_{md} i'_{kq} \qquad (3.19b)$$

$$\varphi_{fd} = L_{fd} i_{fd} + L_{md}(i'_d + i'_{kd}) \qquad (3.19c)$$

$$\varphi_{kd} = L_{kd} i_{kd} + L_{md}(i'_d + i'_{fd}) \quad (3.19d)$$

$$\varphi_{kq1} = L_{kq1} i_{kq1} + L_{mq} i_q \quad (3.19e)$$

$$\varphi_{kq2} = L_{kq2} i_{kq2} + L_{mq} i_q \quad (3.19f)$$

$$\Delta\omega(t) = \frac{1}{2H}\int_0^t (T_m - T_e)dt + Kd\Delta\omega(t) \quad (3.20a)$$

$$\omega(t) = \Delta\omega(t) + \omega_o \quad (3.20b)$$

$$\Theta_e = [\frac{\omega}{P_m} - T_e - \omega_e]/2H \quad (3.21)$$

The q axis and d axis equivalent of the synchronous machine electrical model are shown in Figure 3.8 & Figure 3.9.

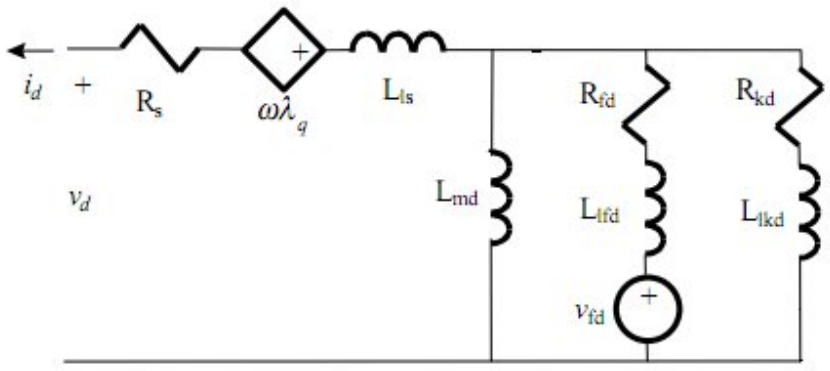

Figure 3.8: q axis equivalent of synchronous generator

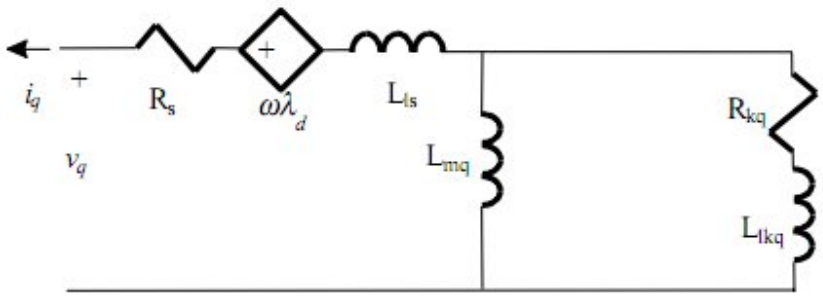

Figure 3.9: d axis equivalent of synchronous generator

The electrical model suggests that the stator and rotor fluxes are obtained using the numerical integration. However, the stator and rotor currents are obtained using the computed fluxes and the inductance parameters. Further, the above model is a dq variable model and therefore the outcome will be dq axes fluxes and currents. For the clarity, the dq variables are to be converted back into the phase variables. For computing the fluxes the stator and rotor voltages, which are the input, are to be represented into the dq variables. Therefore, the implementation is carried out using the following steps:

1) The dq axes field & damper winding voltages v_{kd}, v'_{kq1} and v'_{kq2} are obtained from phase variables v_{abc} through the following sub-steps:

- Sine and cosine values for Θ_e, where Θ_e is rotor angle.
- The voltages (v_a, v_b, v_c) are transformed into dq axes to form v_d and v_q along with v_{kd}, v'_{kq1} and v'_{kq2}using Park transformation to form equations 3.16 to 3.18.

2) The mutual fluxes for q and d axes are calculated by using equations of 3.19a to 3.19f of field and damper winding dq axes fluxes φ_{fdq}, φ_{kd} and φ_{kq} and inductances L_{id} & L_{kq} and represented in 3.22a and 3.22b.

$$\Phi_{mq} = \Phi_q L_{iq} + \Phi_{kq1} L_{ikq1} + V_{kq2} L_{ikq2} \quad (3.22a)$$

$$\Phi_{md} = L_{id}\Phi_d + I_{fd}\Phi_{fd} \quad (3.22b)$$

3) The currents for dq axes field & damper winding i_{dq}, i_{fdq} and i_{kdq} are calculated by using following equations from 3.23a to 3.23g.

$$i_q = L_i[\Phi_q - \Phi_{mq}] \quad (3.23a)$$

$$i_d = L_i[\Phi_d - \Phi_{md}] \quad (3.23b)$$

$$i_{fd} = L_{ifd}(\Phi_{fd} - \Phi_{md}) \quad (3.23c)$$

$$i_{fq} = L_{ifq}(\Phi_{fq} - \Phi_{mq}) \quad (3.23d)$$

$$i_{kq1} = L_{ikq1}(\Phi_{kq1} - \Phi_{mq}) \quad (3.23e)$$

$$i_{kq2} = L_{ikq2} (\Phi_{kq2} - \Phi_{mq}) \quad (3.23f)$$

$$i_{kd} = L_{ikd} (\Phi_{kd} - \Phi_{md}) \quad (3.23g)$$

4) Finally, the rotor and stator side currents are transformed into phase currents.

5) Torque is calculated in equation 3.24.

$$T_e = \Phi_d i_q - \varphi_q i_d \quad (3.24)$$

6) The active and reactive power can be obtained from q and d axes voltages V_d & V_q and currents I_d & I_q as:

$$P = V_d I_d + V_q I_q \quad (3.25a)$$

$$Q = V_q I_d - V_d I_q \quad (3.25b)$$

7) From the mechanical model of the synchronous generator, above equation 3.20 and 3.21 are formed. Simulink representation of mechanical model is shown in Figure 3.11.

The implementation of above steps is shown in Simulink model shown in Figure 3.10.

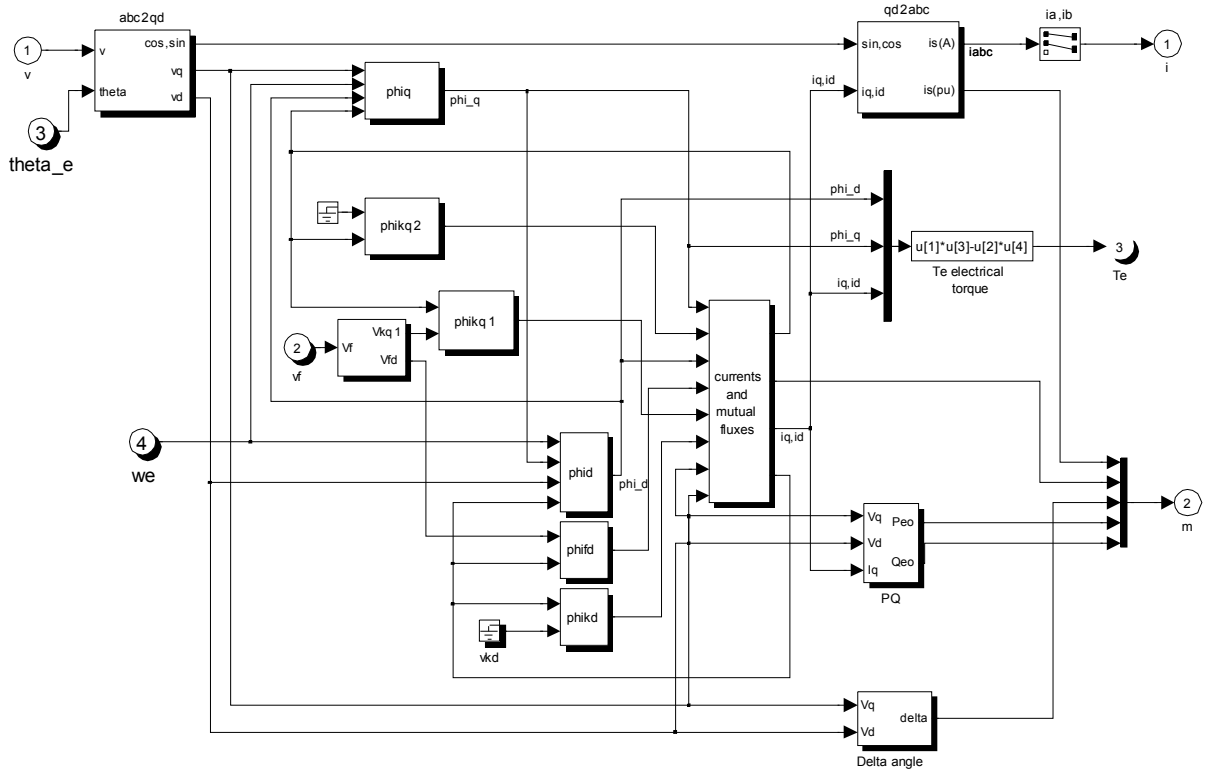

Figure 3.10: Simulink model representation of electrical model of synchronous generator

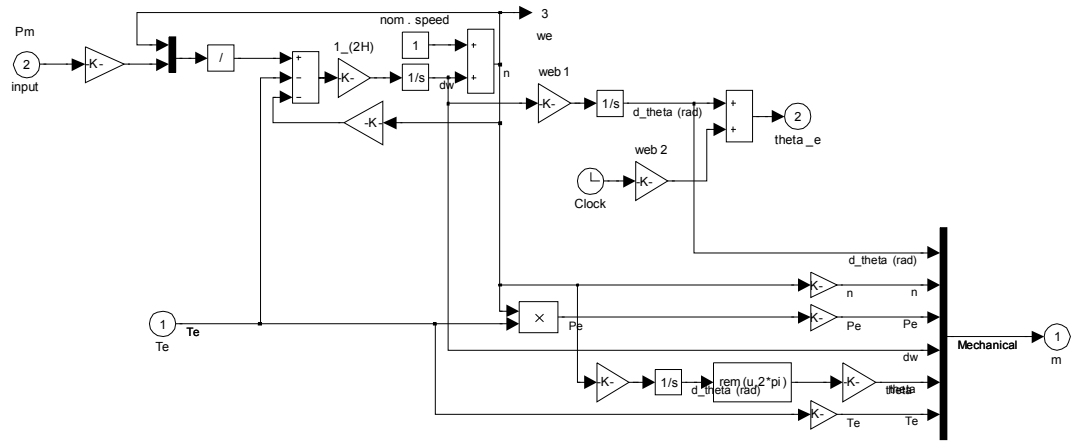

Figure 3.11: Simulink model representation of mechanical model of synchronous generator

3.2.3 EXCITATION SYSTEM OF ALTERNATOR MODEL

This model, described by the block diagram of Figure 3.12(a), is used to represent field-control dc commutator exciters with continuously acting voltage regulators (especially the direct-acting rheostatic, rotating amplifier, and magnetic amplifier types). Because this model has been widely implemented by the industry, it is sometimes used to represent other types of systems when detailed data for them are not available or when a simplified model is required.

The principal input to this model is the output, V_C, from the terminal voltage transducer. At the summing junction, terminal voltage transducer output, V_C, is subtracted from the set point reference, V_{REF}. The stabilizing feedback, V_F, is subtracted and the power system stabilizing signal, V_S, is added to produce an error voltage. In the steady state, these last two signals are zero, leaving only the terminal voltage error signal. The resulting signal is amplified in the regulator. The major time constant, T_A, and gain, K_A, associated with the voltage regulator are showing limits typical of saturation or amplifier power supply limitations. These voltage regulators utilize power sources that are essentially unaffected by brief transients on the synchronous machine or auxiliary buses.

From the block diagram shown in Figure 3.12(a), following equation is obtained:

$$V_{comp} = V_s + V_{uel} - V_c + V_{ref} - Vf \qquad (3.26)$$

Where

V_c = Voltage of Transducer output

V_{ref} = reference Voltage

V_F = st abilizing feedback

V_s = stabilizing signal

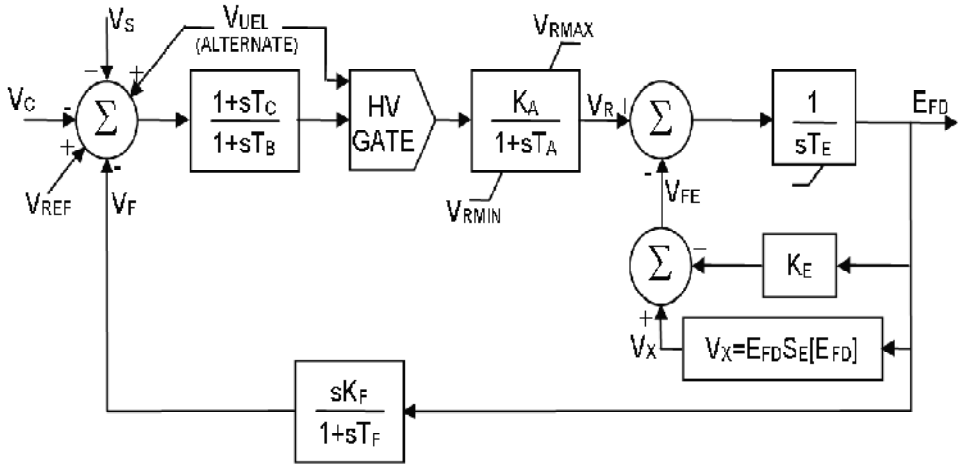

Figure 3.12(a): Field-Controlled DC Commutator Exciters

The voltage regulator output, V_R, is used to control the exciter, which may be either separately excited or self-excited. When a self-excited shunt field is used, the value of K_E reflects the setting of the shunt field rheostat. In some instances, the resulting value of K_E can be negative and allowance should be made for this. Most of these exciters utilize self-excited shunt fields with the voltage regulator operating in a mode commonly termed buck-boost.

The majority of station operators manually track the voltage regulator by periodically trimming the rheostat set point so as to zero the voltage regulator output. This may be simulated by selecting the value of K_E so that initial conditions are satisfied with $V_R = 0$. In some programs, if K_E is entered as zero, it is automatically calculated by the program for self-excitation. If a nonzero value for K_E is provided, the program should not recalculate K_E, as a fixed rheostat setting is implied. For such systems, the rheostat is frequently fixed at a value that would produce self- excitation near rated conditions. Systems with fixed field rheostat settings are in widespread use on units that are remotely controlled. A value for $K_E = 1$ is used to represent a separately excited exciter.

The term $S_E[E_{FD}]$ is a nonlinear function with values defined at two or more chosen values of E_{FD}. The output of this saturation block, V_X, is the product of the input, E_{FD}, and the value of the nonlinear function $S_E[E_{FD}]$ at this exciter voltage.

A signal derived from field voltage is normally used to provide excitation system stabilization, V_F, via the rate feedback with gain, K_F, and time constant, T_F. Implementing the model in Figure 3.12(b) discussed above, following model is been simulated in MATLAB Simulink environment

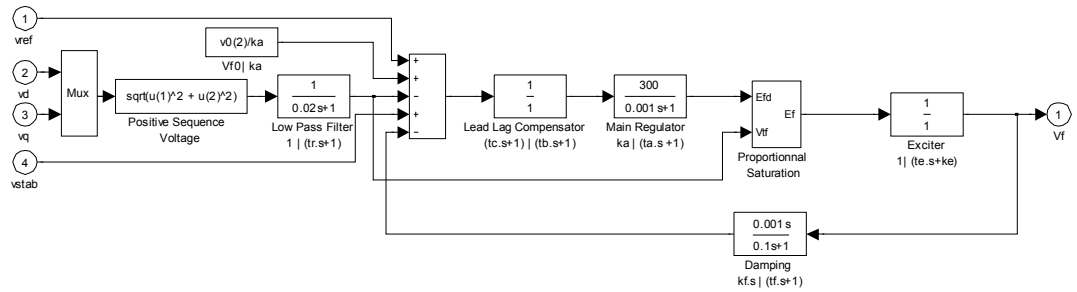

Figure 3.12(b): Simulation of Excitation System

Here also, the input given to the Lead Lag Compensator can be written as:

$$V_{comp} = V_{ref} + V_{fo}/k_a - \sqrt{(V_d^2 + V_q^2)}/(1 + T_r s) + V_{stab} - V_f(k_f s/(1+t_f s)) \qquad (3.27)$$

Where

V_{comp} is the input voltage given to compensator,

V_{ref} is the reference voltage if exciter,

V_{fo} is initial value of field voltage,

k_a is regulator gain,

V_f is field voltage,

k_f is damping function gain,

t_f is filter time constant.

Comparing equations (3.26) and (3.27), it is inferred that:

$V_s = V_{stab} =$ stabilizing voltage signal

And $$V_F = \frac{V_f ks}{1+T_r s}. \qquad (3.28)$$

The terminal field voltage is calculated as:

$$V_{tF} = \frac{\sqrt{V^2_d + V^2_q}}{1+T_r s} \qquad (3.29)$$

Where

V_d and V_q are direct and quadrature axis voltages,

T_rs is Low Pass filter tome constant.

Also, V_c, Voltage of Transducer output is given by:

$$V_c = \frac{V_{fo}}{k_a} \tag{3.30}$$

3.3 HYDRO GENERATOR MODEL

A hydro generator is simulated using a salient pole synchronous generator having its mechanical torque from hydro turbine. Also, excitation system of alternator provides the generator its necessary field voltage.

3.3.1 HYDRO TURBINE AND SPEED GOVERNOR MODEL

New models including the widespread use of electric-hydraulic speed control both in new construction and in modernization of older power plants are required to be developed. It is better to use models describing the actual equipment rather than making approximations to fit existing mechanical governor models. The tremendous increase in computer power eliminates the need for less detailed models.

There are two main types of prime mover models one for prime movers including water supply conduit and the other for prime mover speed controls. The prime mover models include both linear and nonlinear controls. Non-linear models are required where speed and power changes are large, such as in islanding, load rejection, and system restoration studies.

The block diagram of Figure 3.13(a) shows the basic elements of a hydro turbine within the power system environment. Excluded from the scope are models for generation load control and electrical load dynamics.

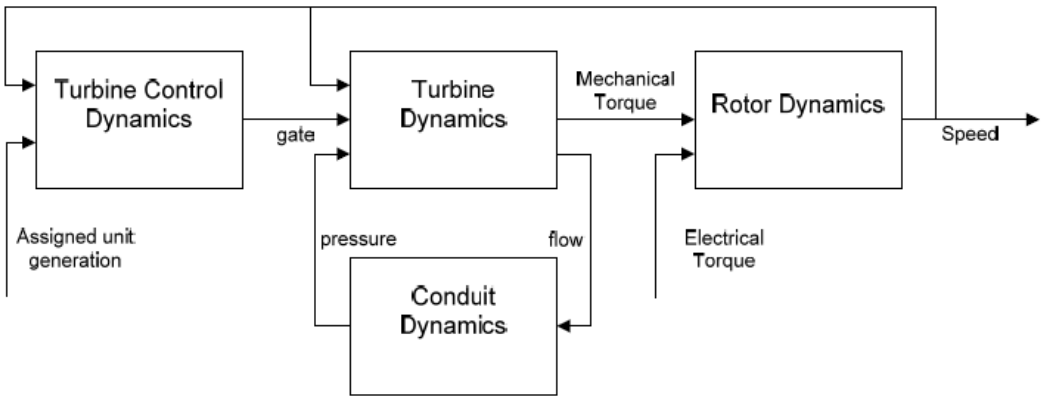

FIGURE 3.13(a): Functional Block Diagram Showing Relationship of Hydro Prime Mover System and Controls to Complete System

Hydro turbines, because of their initial inverse response characteristics of power to gate changes, require provision of transient droop features in the speed controls for stable control performance. The term 'transient droop' implies that, for fast deviations in frequency, the governor exhibits high regulation (low gain) while for slow changes and in the steady state the governor exhibits the normal low regulation (high gain). From a linear control analysis point of view, the case of a hydro turbine generator can be represented by the block diagram of Figure 3.13(a).

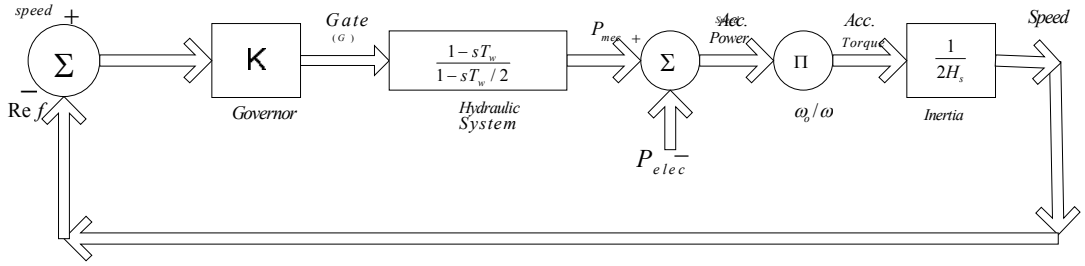

Figure 3.13(b): Linear Model of Hydro Turbine and Speed Controls

Conventional frequency response and Bode plot analysis of this control system shows that a pure proportional controller would have to be tuned with a very low gain for acceptable stability yielding a very poor (high) regulation.

Governors - Proportional Control with Transient Droop

Figure 3.13(c) shows the model block diagram of a typical governor in which the turbine gate is controlled by a two stage hydraulic position servo. The physical meaning of the parameters used in the model is as follows:

T = Pilot valve and servo motor time constant

Q = servo gain

T_g = Main servo time constant

R_p = Permanent droop

R_T = Transient droop

T_R = Reset time or dashpot time constant

The permanent droop determines the speed regulation under steady state conditions. It is defined as the speed drop in percent or per unit required to drive the gate from minimum to maximum opening without change in speed reference. Due to the peculiar dynamic characteristics of the hydraulic turbine, it is necessary to increase the regulation under fast transient conditions in order to achieve stable speed control. This is achieved by the parallel transient droop branch with washout time constant T_R. Because of the choice of the per unit system, with maximum gate opening defined as unity, the speed limits must be defined, for consistency, as fractions of the maximum gate opening per second.

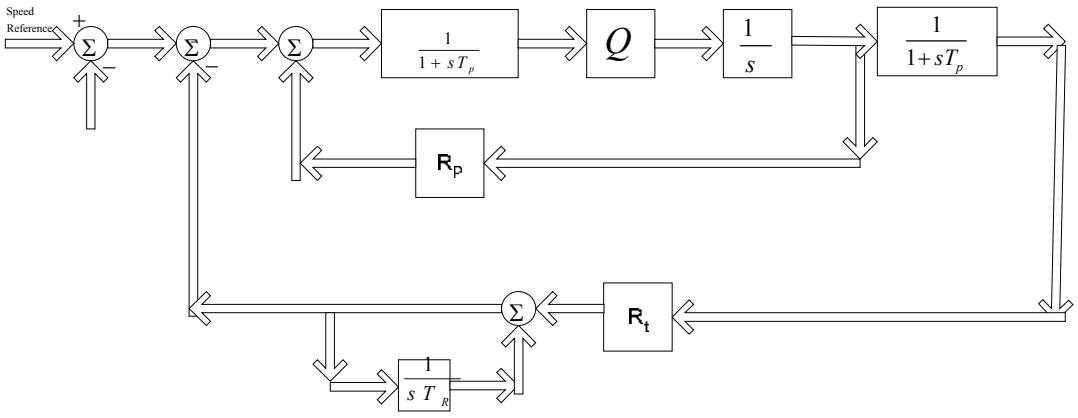

Figure 3.13(c): Model of Typical Hydro-Turbine Governor

The simulated block system of hydro electric generator is been shown in Figure 3.13(d). It shows a salient pole synchronous generator with a separate excitation system. The mechanical power to the machine is provided by a hydraulic governor. This governor controls the speed of turbine and the gate opening.

In the simulated system, the hydraulic governor is simulated by using a non linear hydraulic turbine, PID governor system and a servo motor. The simulated block diagram of hydraulic governor is shown in Figure 3.13(e).

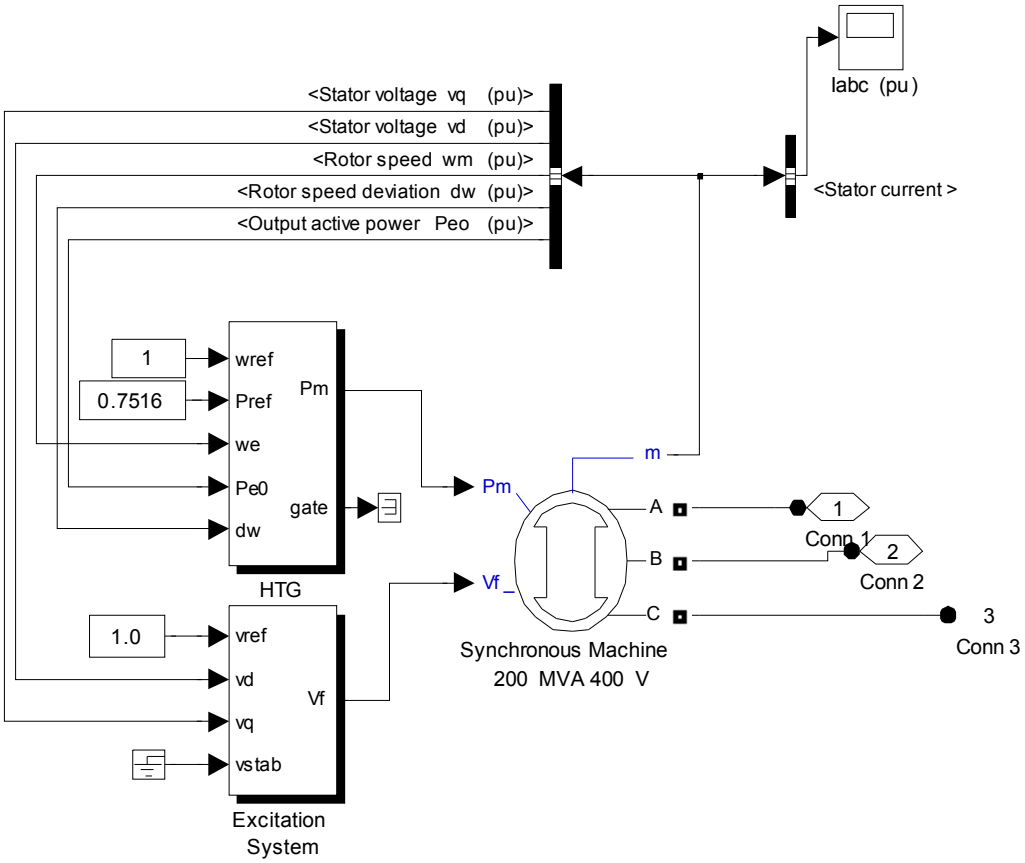

Figure 3.13(d): Modeling of Hydroelectric Generator

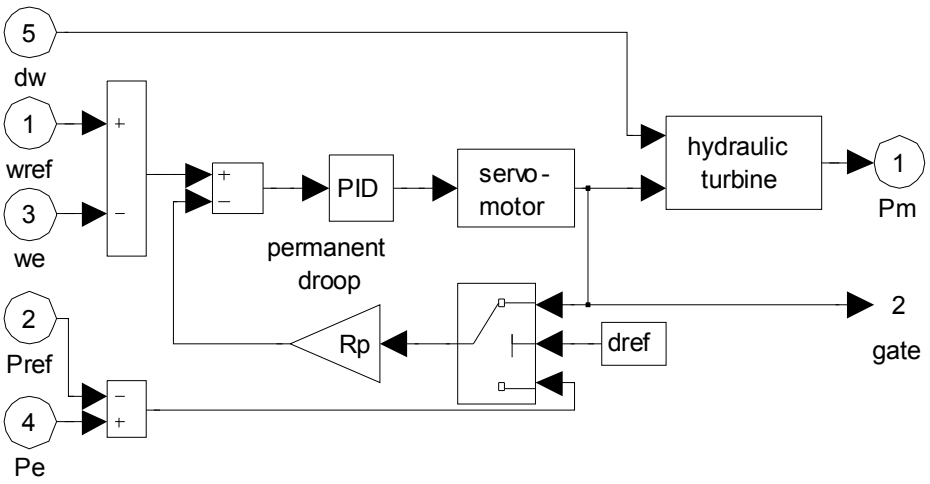

Figure 3.13(e): Simulated hydraulic speed governor

Following equation has been obtained from the simulated model shown in Figure 3.13(e).

$$P_m = [\frac{g^2_{\min}}{g^2_{\max}} \beta d\omega] X \frac{1}{T_\omega} [1 - \frac{g^2_{\min}}{g^2_{\max}} \beta d\omega] \qquad (3.31)$$

A reference speed is provided to turbine equipped with a PID controller. Sensing the error signal, PID controller provided with the permanent droop as explained in the above sections, sends appropriate signal to servo motor to open the gates. Taking into account the gate opening and the rotor speed deviation, turbine produces mechanical power to be fed to synchronous generator.

Figure 3.13(e) shows the simulated model which shows how the servo motor limits its speed for controlling the opening of gate. The limits g_{min} and g_{max} (pu) imposed on the gate opening, and vg_{min} and vg_{max} (pu/s) imposed on gate speed.

The static gain of the governor is equal to the inverse of the permanent droop R_p in the feedback loop. The PID regulator has a proportional gain K_p, an integral gain K_i, and a derivative gain K_d. The high-frequency gain of the PID is limited by a first-order low-pass filter with time constant Td (s). Simulated model of PID controller is shown in Figure 3.13(f).

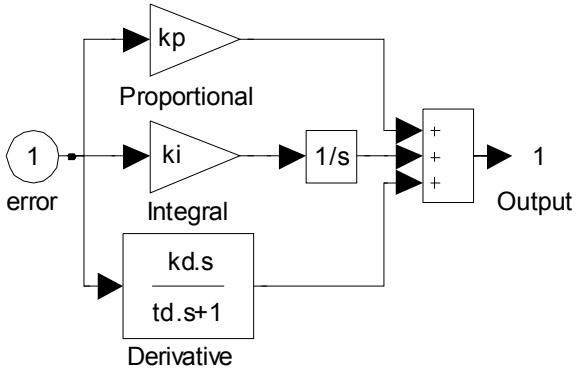

Figure 3.13(f): Simulated PID controller

Following equation is obtained from simulated controller of Figure 3.13(f):

$$u(s) = [\ K_p + K_i/s + K_d/(\ 1 + T_d s)\ ]\ e(s) \qquad (3.32)$$

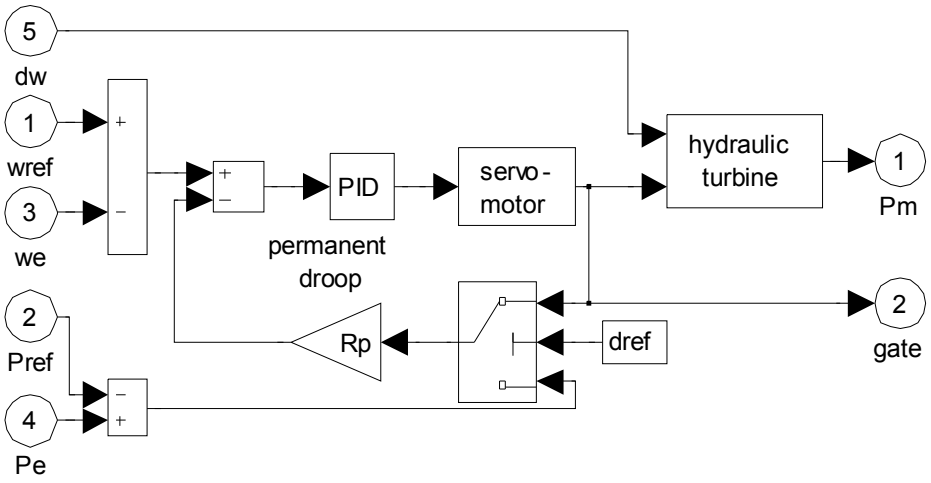

Figure 3.13(g): Speed Control of Servo Motor for Gate Opening

Figure 3.13(g) shows speed control of servo motor for gate opening. Following equation is obtained from simulated controller of Figure 3.13(g):

$$\text{Gate opening} = \int_{g\min}^{g\max} \frac{k_a}{1+T_a s}(u(s)-g) \qquad (3.33)$$

3.3.2 SYNCHRONOUS GENERATOR

The synchronous generator for hydro is modeled in the same way as in case of diesel alternator as explained in section 3.2.2.

EXCITATION SYSTEM OF SYNCHRONOUS GENERATOR

The excitation system of synchronous generator for hydro for providing field voltage is modeled in the same way as in case of diesel alternator as explained in section 3.2.3.

3.4 PV CELL MODEL

The use of equivalent electric circuits makes it possible to model characteristics of a PV cell. The method used here is implemented in MATLAB programs for simulations. The same modeling technique is also applicable for modeling a PV module.

The complex physics of the PV cell can be represented by the equivalent electrical circuit shown in Figure 3.14(a). The circuit parameters are as follows.

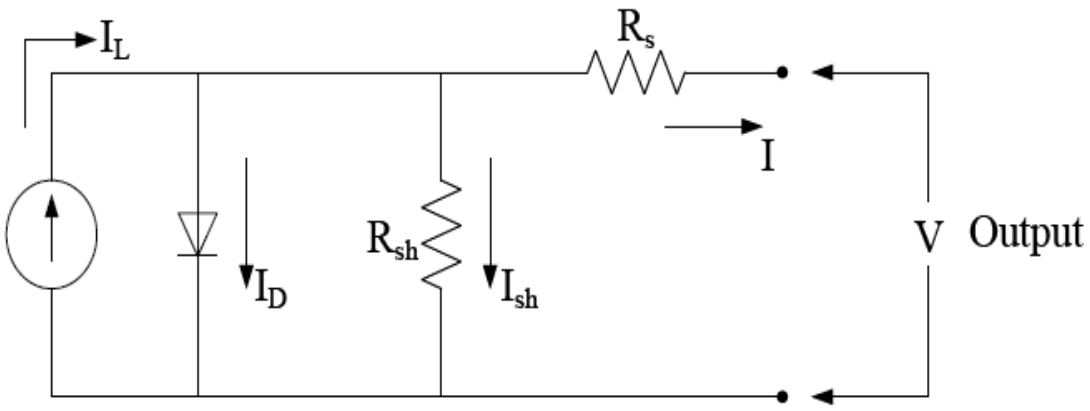

Figure 3.14(a): Equivalent circuit of PV cell showing the diode and ground leakage currents.

The open-circuit voltage V_{OC} of the cell is obtained when the load current is zero, i.e., when I = 0, and is given by the following:

$$V_{oc} = V + IR_{SH} \tag{3.34}$$

The diode current is given by the classical diode current expression:

$$I_d = I_D[\ \exp(\frac{QV_{oc}}{kT}) - 1\ ] \tag{3.35}$$

Where

I_D = the saturation current of the diode

Q = electron charge = 1.6×10^{-19} C

k = Boltzmann constant = 1.38×10-23 J/°K

T = temperature on absolute scale °K

The load current is therefore given by the expression:

$$I = I_L - I_d = I_D[\ \exp(\frac{QV_{oc}}{kT}) - 1\ ] - (\frac{V}{R_{sh}}) \qquad (3.36)$$

The diode-saturation current can therefore be determined experimentally by applying a voltage V_{OC} to the cell in the dark and measuring the current going into the cell. This current is often called the dark current or the reverse diode-saturation current.

The Figure 3.14(b) shows the Simulink model of a PV cell. The cell operate at room temperature, V_T=26mV. The reverse saturation current is I_s = $1x10^{-9}$A. The temperature is constant during simulation.

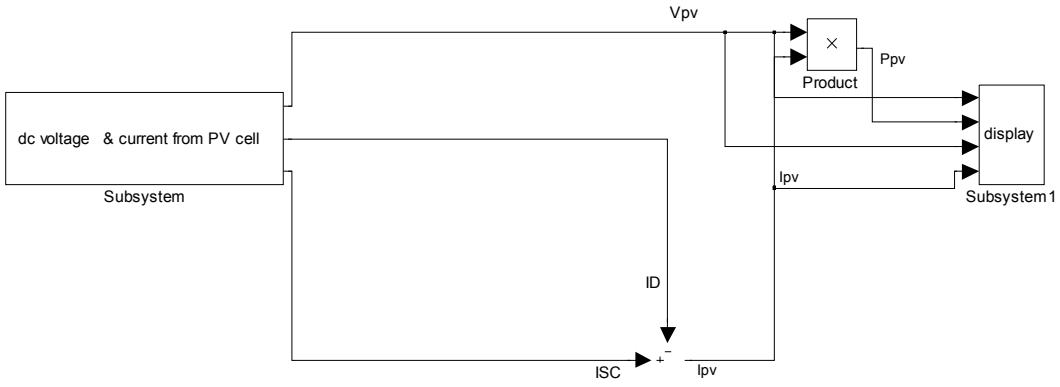

Figure 3.14(b): Simulation of Solar Cell

3.5 STEAM GENERATOR MODEL

A steam generator is simulated using a cylindrical pole alternator having its mechanical power from steam turbine and field voltage from excitation system.

3.5.1 SPEED GOVERNING SYSTEM MODEL

Figure 3.15(a) includes functional blocks for the governor speed changer and for automatic generation control to show their relationship to the speed- governing system. The time span of most stability studies is short compared to the time required to make significant load changes, so that load changing equipment is not represented.

Electro-Hydraulic Control

An electro-hydraulic speed-control mechanism provides flexibility through the use of electronic circuits in place of mechanical components in the low-power portions. The block diagram of Figure 3.15(b) illustrates a typical configuration. The steam flow (or first stage pressure) feedback and the servomotor feedback loop provide for improved linearity over the mechanical-hydraulic system. Figure 3.15(c) shows the modeling of Steam turbine and Governor in Simulink

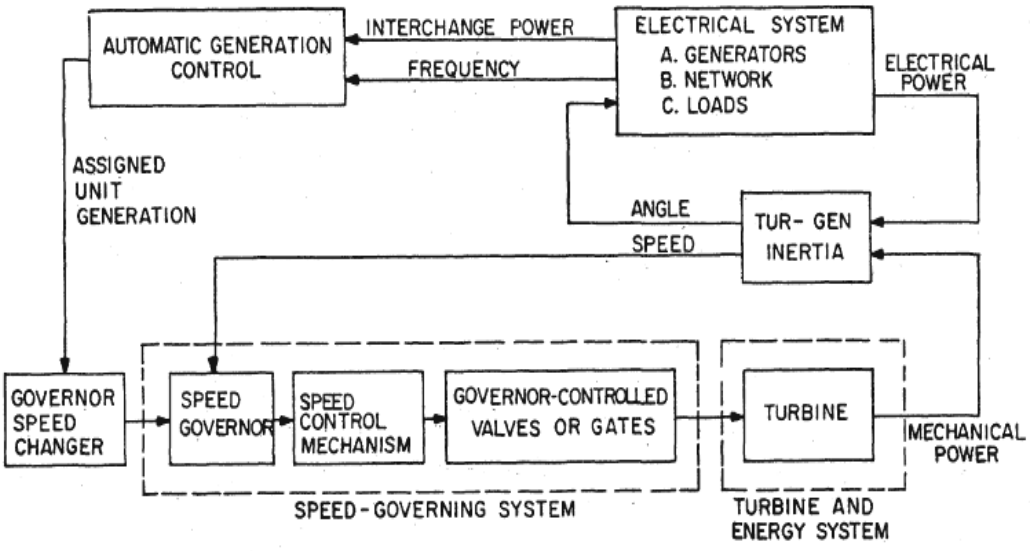

Figure 3.15(a): Functional Block Diagram Showing Location of Speed-Governing System and Turbine Relative to Complete System

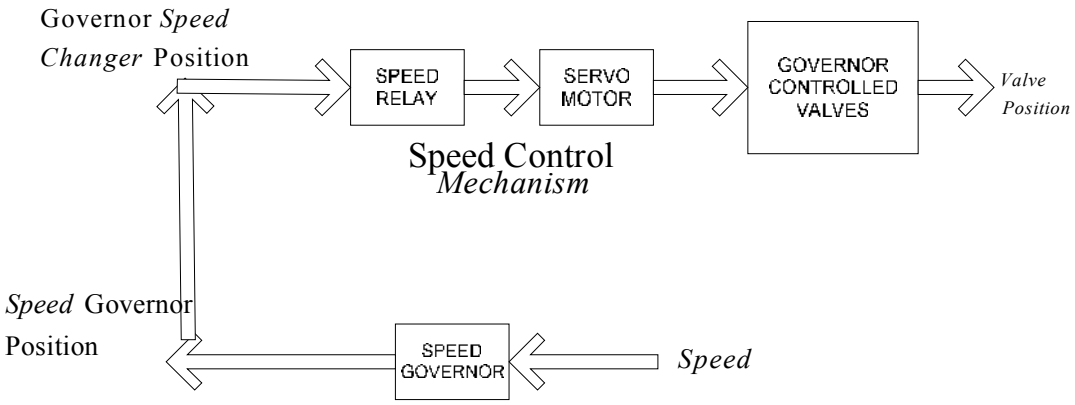

Figure 3.15(b): Electro -Hydraulic Speed-Governing System for Steam Turbines

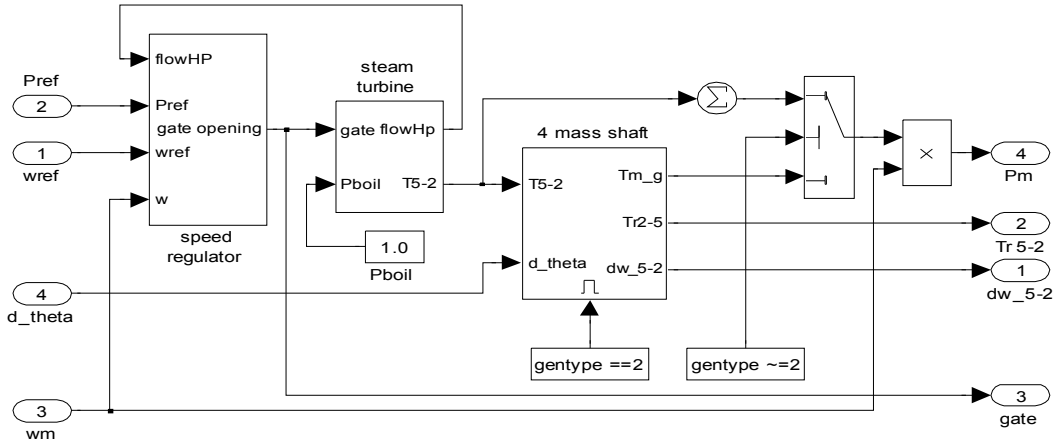

Figure 3.15(c): Modeling of Steam turbine and Governor in Simulink

The speed-governing model of Figure 3.15(d) may be used to represent either a mechanical-hydraulic system or an electro-hydraulic system by means of an appropriate selection of parameters. This model shows the load reference as an initial power P_o. This initial value is combined with the increments due to speed deviation to obtain the total power, P_{GV}, subject to the time lag, T_3, introduced by the servomotor mechanism.

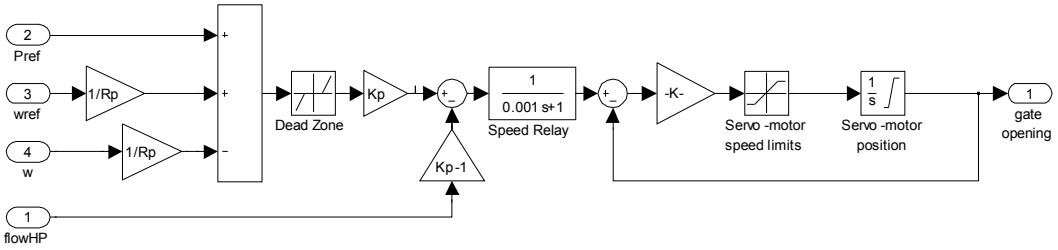

Figure 3.15(d): Simulation of Speed regulator

Following equation is obtained from Simulink model shown in Figure 3.15(c).

$$P_m=(T_2+T_3+T_4+T_5)w_m \tag{3.37}$$

Following Equation was obtained from simulation model shown in Figure 3.15(d).

$$\text{Gate opening} = \int_{g\min}^{g\max} \frac{1}{T_s m}\left(\frac{1}{1+0.01s}\right)\left[Kp\left(P_{ref}+\frac{\omega_{ref}-\omega}{R_p}\right)-(k_p-1)\,flow_{HP}\right] \tag{3.38}$$

3.5.2 STEAM TURBINE SYSTEM

All compound steam turbine systems utilize governor-controlled valves at the inlet to the high pressure (or very high pressure) turbine to control steam flow. The steam chest and inlet piping to the first turbine cylinder and reheaters and crossover piping downstream all introduce delays between valve movement and change in steam flow. The principal objective in modeling, the steam system for stability studies is to account for these delays. Flows into and out of any steam vessel are related by a simple time constant.

Pressure changes at the entrance to the governor-controlled valves may also be important in some stability studies. Boiler controls are designed to regulate valve pressure, but the controlled boiler response is not fast enough to compensate for pressure variations due to the movement of governor controlled valves. It can be assumed that there is a pressure somewhere in the steam generator which does remain constant for the time interval of a stability study, and that a pressure change dependent on the square of steam flow occurs in the boiler tubes from that constant pressure point to the valves. Figure 3.16(a) shows the General Model for Speed-Governing Systems (Steam Turbine Systems) and its simulated block diagram is shown in Figure 3.16(b).

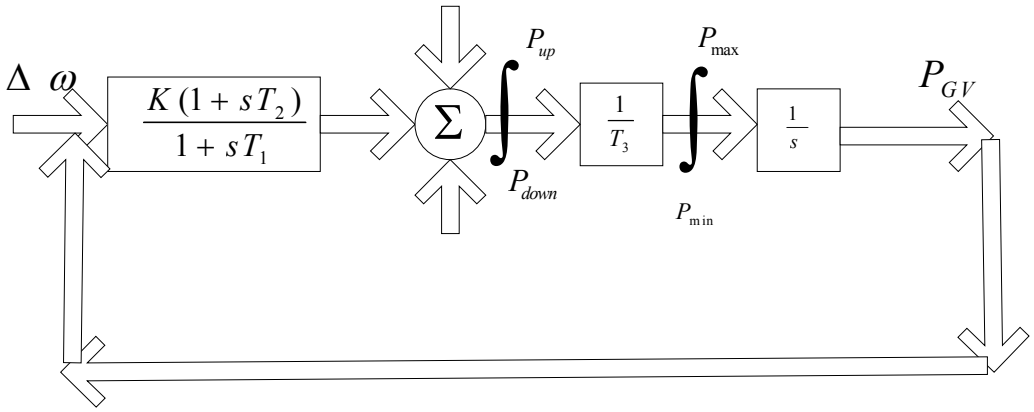

Figure 3.16(a): General Model for Speed-Governing Systems (Steam Turbine Systems)

The following equations are obtained from the simulation of steam turbine.

$$T_5 = P_{boil} \,.\, gate/(0.5s + 1) \quad (3.39a)$$

$$T_4 = T_5/(3.3s+1) \quad (3.39b)$$

$$T_3 = T_4/(10s +1) \quad (3.39c)$$

$$T_2 = T_3/(s+1) \quad (3.39d)$$

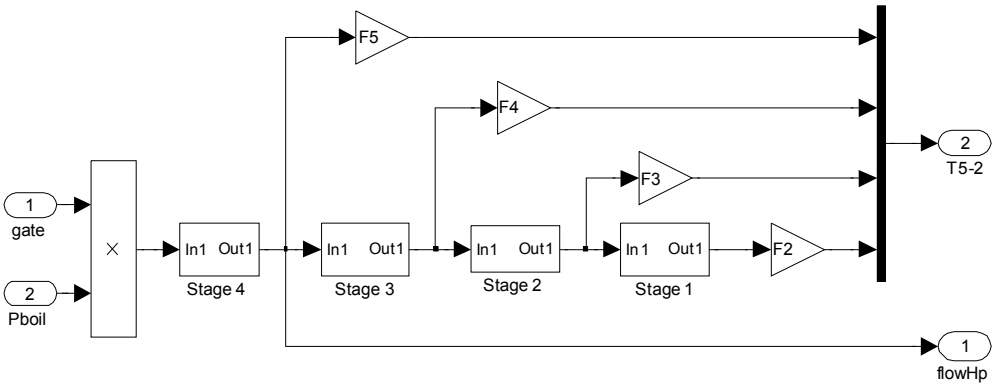

Figure 3.16(b): Simulation of Steam Turbine

3.5.3 SYNCHRONOUS GENERATOR

The synchronous generator for steam is modeled in the same way as in case of diesel alternator as explained in section 3.2.2.

EXCITATION SYSTEM OF SYNCHRONOUS GENERATOR

The excitation system of synchronous generator for hydro for providing field voltage is modeled in the same way as in case of diesel alternator as explained in section 3.2.3.

CHAPTER 4

HVDC TRANSMISSION SYSTEM

4.1 INTRODUCTION

Electrical power is generated as an alternating current (AC). It is also transmitted and distributed as AC and, apart from certain traction and industrial drives and processes, it is consumed as AC. In many circumstances, however, it is economically and technically advantageous to introduce direct current (DC) links into the electrical supply system.

HVDC transmission applications fall into four broad categories and any scheme usually involves a combination of two or more of these categories:

- Transmission of bulk power where AC would be uneconomical, impracticable or subject to environmental restrictions.
- Interconnection between systems which operate at different frequencies, or between non-synchronized or isolated systems which, although they have the same nominal frequency, cannot be operated reliably in synchronism.
- Addition of power in feed without significantly increasing the short circuit level of the receiving AC system.
- Improvement of AC system performance by the fast and accurate control of HVDC power.

It is very much cost effective for a long distance DC power transmission compared to AC power transmission. In case of undersea cables where the intersections of the bold lines are located at a relatively short distance, the DC system is much more economical.

Figure 4.1 illustrates (1) the initial cost for HVAC power transmission and (2) illustrates the initial cost of HVDC power transmission with a bigger initial cost due to a higher valve cost for HVDC transmission. In addition, (3) and (5) represent the cost for transmission line construction in HVAC and HVDC power transmissions, respectively and they demonstrate that HVDC power transmission has a lower cost for transmission line construction. In the case of HVAC power

transmission, a shunt capacitor must be installed typically at every 100 km or 200 km because of its electrostatic capacity. In other words, the increase in total cost for power transmission lines is accompanied by additional costs due to shunt capacitors. In the same Figure 4.1, (6) and (7) illustrate losses of HVDC and HVAC systems during power transmission. It is shown that an HVDC system has a smaller loss if the same amount of electric power is delivered. Therefore, HVAC transmission is favorable for distances less than about 450 km and HVDC transmission is favorable for distances exceeding 450 km.

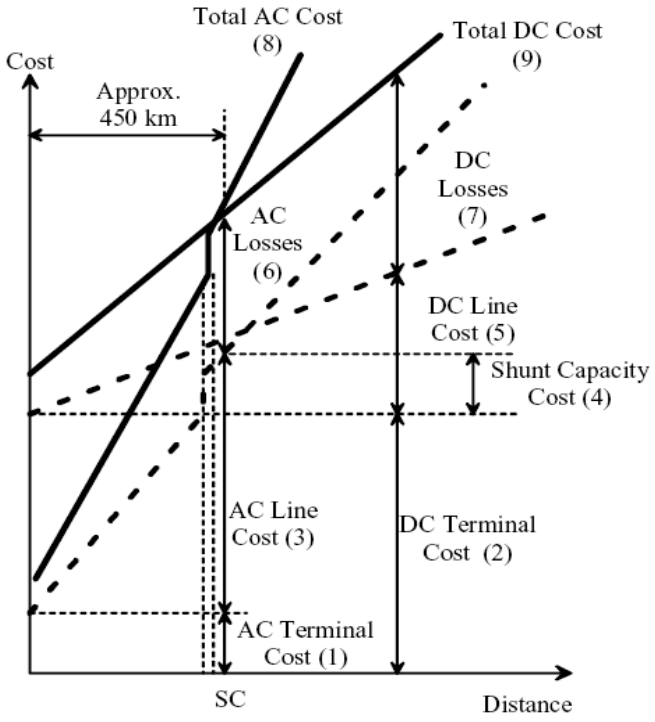

Figure 4.1 : HVDC System Cost

HVDC transmission refers to that the AC power generated at a power plant is transformed into DC power before its transmission. At the inverter (receiving side), it is then transformed back into its original AC power and then supplied to each household. Such power transmission method makes it possible to transmit electric power in an economic way through up-conversion of voltage, which is an advantage in existing AC transmission technology and to overcome many disadvantages associated with AC power transmission as well. The overall structure of an HVDC system and its basic components are described below.

1. **AC Breaker:** This is used to isolate the HVDC system from the AC system when the HVDC system is malfunctioning. This breaker must be rated to carry full load current, interrupt fault current, and energize the usually large converter transformers. The purposes of this breaker are for the interface between AC switch yards or between AC bus bar and HVDC system.
2. **AC Filters and Capacitor Bank:** The converter generates voltage and current harmonics at both the AC and DC sides. Such harmonics overheat the generator and disturb the communication system. On the AC side, a double tuned AC filter is used to remove these two types of harmonics. In addition, the reactive power sources such as a capacitor bank or synchronous compensator are installed to provide the reactive power necessary for power conversion.
3. **Converter Transformer:** This transforms the voltage from the AC system to be supplied to the DC system. It also provides a separation between the AC and DC system. Specifically, when the two units of 6 pulse converters are serially connected to generate a 12 pulse output, a 3-winding converter transformer is used.
4. **Thyristor Converter:** A converter, which is an essential component of HVDC power transmission, is developed using power electronics. It is one of many research areas dealing with the transformation and control of power by switching devices in the power converter. It performs the conversion from AC to DC or from DC to AC. It is mainly comprised of a valve bridge and a transformer with a tap converter.
5. **Smoothing Reactors and DC Filters:** The smoothing reactor reduces the DC ripple current to prevent it from becoming discontinuous at low power levels. Also, the smoothing reactor forms an integral component, together with the DC filter, to protect the converter valve during a commutation failure by limiting the rapid rise of current flowing into the converter.
6. **Line Commutated Current Source Converter and Voltage Source Converter**:. Line Commutated Current Source Converter (LCC), consists of a 12-pulse converter, AC filter and synchronous compensator. LCC depends on the AC system voltage for its proper operation. LCC operates at a lagging power factor, because the firing of the converter has to be delayed relative to the voltage crossing to control the DC voltage.

4.2 HVDC CONFIGRATIONS

The various configurations of HVDC are described as follows:

1) Monopolar HVDC Systems: Monopolar HVDC systems have either ground return or metallic return.

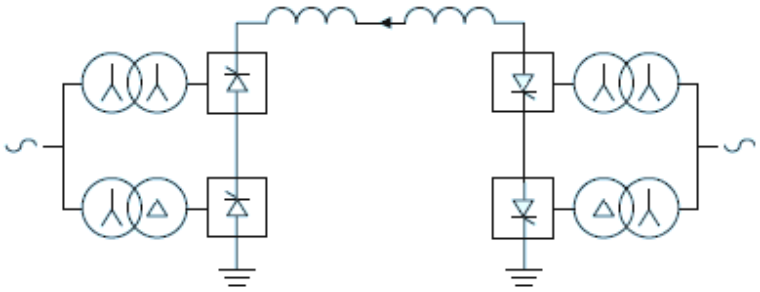

Figure 4.2: A Monopolar HVDC System with Ground Return

A. Monopolar HVDC System with Ground Return: consists of one or more six-pulse converter units in series or parallel at each end, a single conductor and return through the earth or sea, as shown in Figure 4.2. It can be a cost-effective solution for a HVDC cable transmission and/ or the first stage of a bipolar scheme. At each end of the line, it requires an electrode line and a ground or sea electrode built for continuous operation.

B. A Monopolar HVDC System with Metallic Return: It usually consists of one high-voltage and one medium voltage conductor as shown in Figure 4.3. A monopolar configuration is used either as the first stage of a bipolar scheme, avoiding ground currents, or when construction of electrode lines and ground electrodes results in an uneconomical solution due to a short distance or high value of earth resistivity.

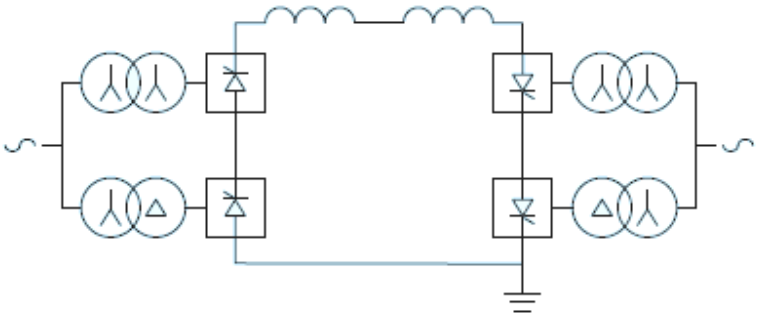

Figure 4.3: A Monopolar HVDC System with Metallic Return

2) Bipolar HVDC Systems: A Bipolar HVDC System consists of two poles, each of which includes one or more twelve-pulse converter units, in series or parallel. There are two conductors, one with positive and the other with negative polarity to ground for power flow in one direction. For power flow in the other direction, the two conductors reverse their polarities. A Bipolar system is a combination of two monopolar schemes with ground return, as shown in Figure 4.4. With both poles in operation, the imbalance current flow in the ground path can be held to a very low value.

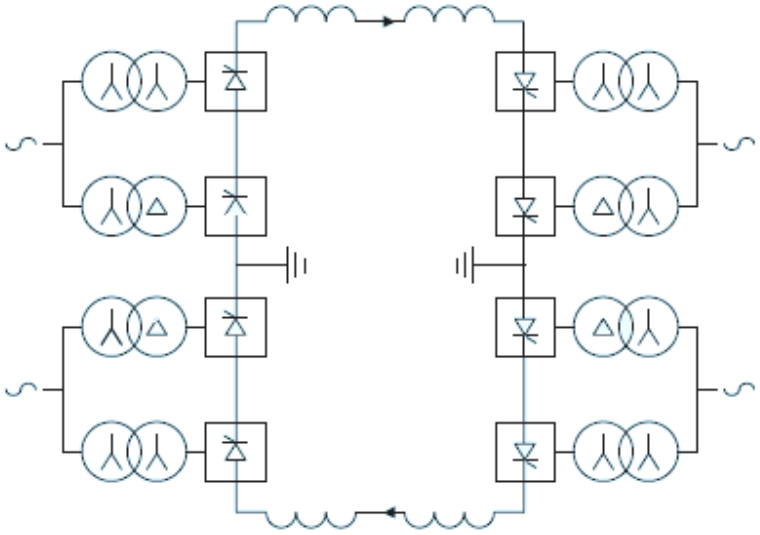

Figure 4.4: Bipolar HVDC System

This is a very common arrangement with the following operational capabilities:

- During an outage of one pole, the other could be operated continuously with ground return or a pole outage, in case long-term ground current flow is undesirable, the bipolar system could be operated in monopolar metallic return mode, if appropriate DC arrangements are provided, as shown in Figure 4.4. Transfer of the current to the metallic path and back without interruption requires a Metallic Return Transfer Breaker (MRTB) and other special-purpose switchgear in the ground path of one terminal. When a short interruption of power flow is permitted, such a breaker is not necessary.
- During maintenance of ground electrodes or electrode lines, operation is possible with connection of neutrals to the grounding grid of the terminals, with the imbalance current between the two poles held to a very low value.

- When one pole cannot be operated with full load current, the two poles of the bipolar scheme could be operated with different currents, as long as both ground electrodes are connected.
- In case of partial damage to DC line insulation, one or both poles could be continuously operated at reduced voltage.
- In place of ground return, a third conductor can be added end-to-end. This conductor carries unbalanced currents during bipolar operation and serves as the return path when a pole is out of service.

3) Back-to-Back HVDC Links: Back-to-back HVDC links are special cases of monopolar HVDC interconnections, where there is no DC transmission line and both converters are located at the same site. For economic reasons each converter is usually a twelve-pulse converter unit and the valves for both converters may be located in one valve hall. The control system, cooling equipment and auxiliary system may be integrated into configurations common to the two converters. DC filters are not required, nor are electrodes or electrode lines, the neutral connection being made within the valve hall.

Generally, for a back-to-back HVDC link from Fig. 4.5, the DC voltage rating is low and the thyristor valve current rating is high in comparison with HVDC interconnections via overhead lines or cables. The reason is that valve costs are much more voltage-dependent, as the higher the voltage the greater the number of thyristors. A low voltage tertiary winding can be built in to the converter transformer for the AC filters and compensation. Smaller reactive power switching steps can thus be achieved. A large back-to-back HVDC system can comprise two or more independent links so that the loss of one converter unit will not cause loss of full power capability.

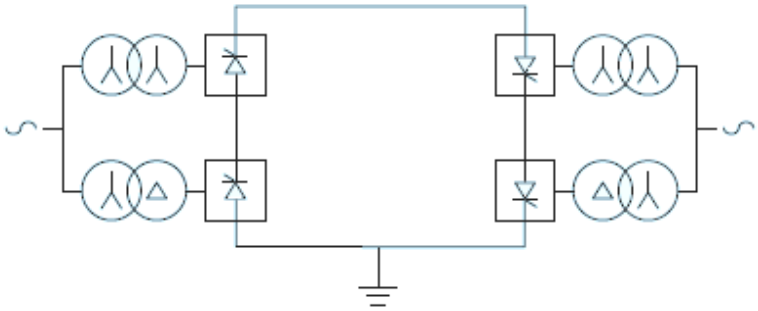

Figure 4.5: Back To Back HVDC Link

4.3 HVDC TRANSMISSION SYSTEM MODEL

Modem power systems are becoming more and more dependent on power electronic control, either for transmission purposes, or for interfacing a potentially wide range of alternative power sources to a network. The issue of how these power electronic circuits interacts with each other through the system interconnection, either through steady state harmonics, or during system transients, is becoming more important.

Power networks are large and complex, as are many of the power electronic devices embedded within them. Complete modeling of such networks is impractical, and network reductions or simplifications must be made. One such simplification involves linearization, which allows fast solutions for large networks, and also allows access to simple and powerful control design and optimization techniques. While linearization is accurate for many network components, for thyristor based power electronic circuits it is a small signal approximation.

4.3.1 HVDC GRAETZ BRIDGE MODEL

In the steady state, free from system distortion, the HVDC converter operates at its base case operating point, producing characteristic harmonics. Converter waveforms and switching instants can be exactly defined. When under system distortion or unbalance, the converter wave-shapes change, and the converter switching instants also change. Linearized model assumes a single source of distortion at a single frequency, and uses the principle of superposition to extend to multiple frequencies or sources of distortion. The effects of the applied distortion are calculated for two circuit configurations; direct conduction and commutation. There are three parts to the solution. The steady state solution, multiplied by a sampling function for the appropriate conduction period, to yield the Partial Steady State spectrum The transient solution, multiplied by the sampling function for the appropriate conduction period, to yield the Partial Transient spectrum The relationship between the switching instant variation and the applied distortion is Linearized, and the resulting spectrum is written as a Pulse Amplitude Modulation Spectrum. This process results in the relationships between waveform distorts around the HVDC converter, which can be written as follows:

$$\begin{bmatrix} \Delta Ip \\ \Delta In \\ \Delta Vd \\ 0 \end{bmatrix} = \begin{bmatrix} a & b & c & d \\ e & f & g & h \\ i & j & k & l \\ m & n & o & -1 \end{bmatrix} \begin{bmatrix} \Delta Vp \\ \Delta Vn \\ \Delta Id \\ \Delta\alpha \end{bmatrix} \tag{4.1}$$

Transfers a to l are derived by the converter model and m, n and o represent the converter control functions. Each transfer is a frequency dependent multiplier. All the variables are small signal variations from the base operating point, and each is a vector of frequencies, specified according to requirements. Subscript d means a DC side variable, subscript ***p*** denotes an AC side variable in positive sequence and subscript *n* an AC side variable in negative sequence. All the transfers are, for small levels of distortion, exact. The model can be used for prediction of harmonic spectra around one or more interconnected HVDC converters, or can be restricted to the terms that describe the feedback paths that govern the transient response of an HVDC system.

4.3.2 HVDC SYSTEM CIRCUIT ANALYSIS

Larson's equation describes the frequency, cross coupling inter-relationships of the converter around a base operating point. Full modeling of the converter must include the time-invariant ac and dc system admittances.

Though linear and time-invariant, the admittances must be represented in the same manner as the full time variant frequency cross-coupling inter-relationships. Hence, the ac and dc system admittances are represented in matrix form and are the same size as the converter frequency cross-coupling matrices, the diagonal representing the admittance frequency. The equation set must be ordered to solve for these dependent vector, the matrix being zero elsewhere.

Nodal analysis provides a convenient way of combining requires indexing of the tensor admittance matrix each converter of the link together with its associated elements for partitioning into the form shown in ac and dc systems. The converter itself can be described in nodal form by rearranging Larson's equation. Figure 4.6 represents the converter in nodal form.

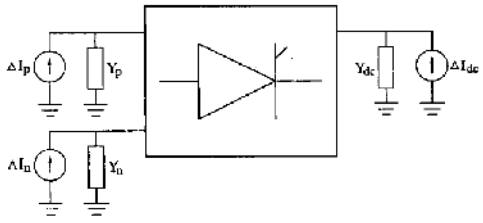

Figure 4.6: Nodal current injections for a single converter

Implicitly incorporating the control, and rearranging Larson's equation to nodal form gives:

$$\begin{bmatrix} Ip \\ In \\ Id \end{bmatrix} = \begin{bmatrix} Y11+Yp & Y12 & Y13 \\ Y21 & Y22+Yn & Y23 \\ Y31 & Y32 & Y33+Yd \end{bmatrix} \begin{bmatrix} Vp \\ Vn \\ Vd \end{bmatrix} \qquad (4.2)$$

Where Y_{I1} to Y_{33} are the converter frequency cross coupling admittance matrix transfers, rearranged from Larson's equation and Y_p, Y_n and Y_{dc} are diagonal matrices representing the frequency dependent system admittances. This generalized nodal system approach means large systems of Linearized time-variant power electronic devices can be built up with their time invariant ac and dc systems easily and solved for the particular distortions of interest.

4.3.3 SOLUTION OF NODAL EQUATION SET

The known of the nodal equation set are all, current injections at all frequencies (except fundamental negative sequence on the rectifier side), as well as the fundamental negative sequence terminal voltage at the rectifier. The unknowns are the fundamental negative sequence current injection at the rectifier and all voltages around the link (except the negative sequence fundamental voltage at the rectifier). This is the general method adopted for rearranging the matrix equations to solve for the unknowns.

4.4 DYNAMIC MODELING

System oscillations associated with power electronic devices are electromagnetic in nature and in the frequency range of approximately 2 to 200 Hz. The use of small signal linearisation methods based on analytical models is a very powerful method of analysis which provides analytical insight into system dynamics, and facilitates the use of classical and modern control design methods.

The configuration of the HVDC transmission system model is shown in Figure 4.7. The purpose of the model is the representation of electromagnetic modes of oscillation, in the DC side frequency range from 2 to 200 Hz**,** which interact with the fastest level of converter controls. The electromechanical dynamics of the power system are not represented, as they are considered to below the frequency range of interest. The HVDC system is modeled using 9 sub-systems, which are the rectifier and inverter AC systems, the rectifier and inverter AC filters and shunt capacitors, the DC system, the rectifier and inverter HVDC converters, and the rectifier and inverter Phase Locked Loops (PLL'S).

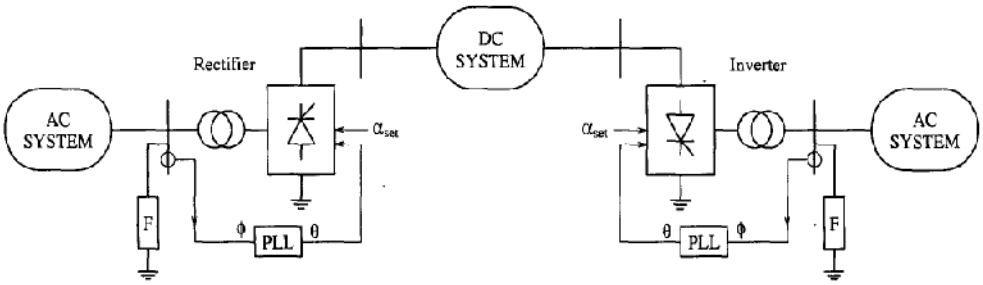

Figure 4.7: HVDC System

4.4.1 STATE MODEL FORMULATION

The formation of a state model is a straightforward process in the case of control sub-systems defined in the s-domain and linear electrical sub-systems, which are described using discrete IUC components. When a sub-system is described in terms of frequency response data it is necessary to fit an s-domain transfer function to the frequency response, which is then converted to a state model. Once the state models of the sub-systems are formed they can be connected together to form a state model of the HVDC system. The state model can be used in conjunction with both classical and modern control theory, for steady state stability analysis and controller design.

4.4.2 AC SYSTEM AND FILTERS

The converter model is derived using AC variables represented in sequence components. To enable the direct connection of sub-systems without the need for variable transformations all AC electrical variables are also represented using sequence components. It is assumed that the positive and negative sequence admittances of the AC system, Y**,** are the same, and that there is no coupling between the sequences. The frequency conversion process of the converter is

accounted for by frequency shifting the AC system equations. This is achieved by representing the admittance Y**,** in zero-pole transfer function form and then adding $\pm$, to the values of the zeroes and poles, as described by equation 4.3 and 4.4.

$$Y_{acp}(s) = Y_{ac}(s + j\omega_o) \quad (4.3)$$

$$Y_{acn}(s) = Y_{ac}(s - j\omega_o) \quad (4.4)$$

It is these two frequencies, with the associated frequency on the DC side, which govern the transient response of the overall system. As the transfer function zeroes and poles have been shifted in opposite directions, the poles of the subsystem still form complex conjugate pairs. The frequency shifted transfer functions are required to be converted into state model form.

4.4.3 DC SYSTEM

The DC system has two electrical terminals which are connected to the DC terminals of the rectifier and inverter. The series inductive nature of the DC system (smoothing reactor and DC transmission line) means that the system is best described in admittance form. This representation is compatible with the converter DC terminal current input and voltage output variables.

$$\begin{bmatrix} I1 \\ I2 \end{bmatrix} = \begin{bmatrix} Y11 & Y12 \\ Y21 & Y22 \end{bmatrix} \begin{bmatrix} V1 \\ V2 \end{bmatrix} \quad (4.5)$$

4.4.4 HVDC CONVERTER

The state model of the HVDC converter used in this paper was obtained from the frequency domain model**.** An examination of the dominant transfers of the frequency domain model shows that, while all transfers exhibit some frequency dependence, this is largely above the frequency range of interest. The change in the HVDC system dynamics, resulting from the use of converter models which take into account varying degrees of frequency dependence in the transfers, indicates that a model where the transfers are approximated as constants is of sufficient accuracy. The constants are naturally chosen to be the value of the frequency domain transfers at zero frequency on the DC side, and are consistent with the differentiation of the standard steady state converter equations. Transfer ***k,*** from dc current to dc voltage, has the form of a zero and is the only case where a constant approximation is inappropriate.

4.4.5 PHASE LOCKED LOOP (PLL)

The PLL is a negative feedback control system which tracks the changes in the angle of the positive sequence fundamental frequency component of the AC commutating bus voltage. The output of the PLL adjusts the position of the firing angle ramp references so that the thyristor firing instants are synchronized to the AC voltage.

The PLL system modeled is of the DQZ type, the major components of which are a frequency modulator, voltage controlled oscillator (VCO), and controller. The development of the PLL small signal model is represented by the block diagram of Figure 4.8**.** The input to the model is the angle of the AC bus voltage, which is obtained from a sequence or *d-q* components representation of the AC voltage. The open loop transfer function consists of the series combination of a non-linear gain *K***,** a PI controller, and an integrator which represents the operation of the VCO. The non-linear gain is the magnitude of the AC bus voltage, and is approximated by a constant using the operating point AC voltage of the system.

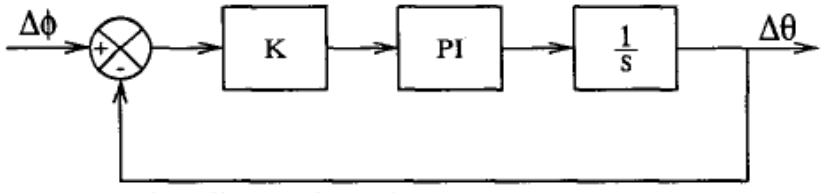

Figure 4.8: Small signal model of the Phase Locked Loop

The gain of the controller is normally set such that the bandwidth of the PLL is in the order of *5* Hz. This limits the possibility of the PLL interacting with the dominant electromagnetic modes of system oscillations which are typically at higher frequencies. The inclusion of the PLL improves the accuracy of system models in the low frequency range.

4.5 SIMULATION OF HVDC SYSTEM

A High Voltage Direct Current Transmission system is been simulated on the MATLAB Simulink package. It's a monopolar system with only one rectifier and one inverter provided at each converter station. The DC line current is been carried by the long distance HVDC Line. The simulated system is shown in Figure 4.9.

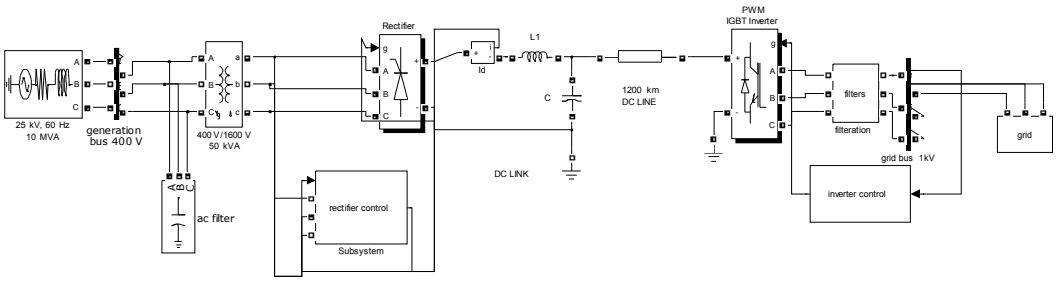

Figure 4.9: Simulation of a HVDC Transmission System

The ac voltage is generated at 400 Volts with a power rating of the 10MVA. The ac voltage is then stepped up and provided to a thyristor based rectifier. To avoid harmonics at the ac supply side, a capacitor is been provided as an ac filter.

The rectifier is a six pulse rectifier system getting its pulses from a synchronized 6-pulse generator and a PI current regulator. The rectifier control system is shown in figure 4.10.

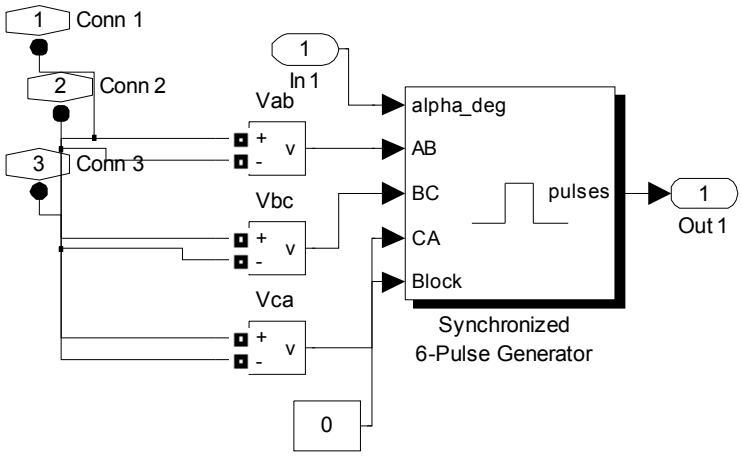

Figure 4.10: Simulated Rectifier Pulse Generator and PI current regulator

The rectified dc is then made to pass through a smoothing reactor and a DC link. From, the DC link, the dc voltage is transmitted via a long distance HVDC line. At the inverter station, the transmitted dc voltage is inverted to get the ac voltage. The inverter uses PWM modulation to get the sinusoidal waveform. The control system of inverter is shown in Figure 4.11.

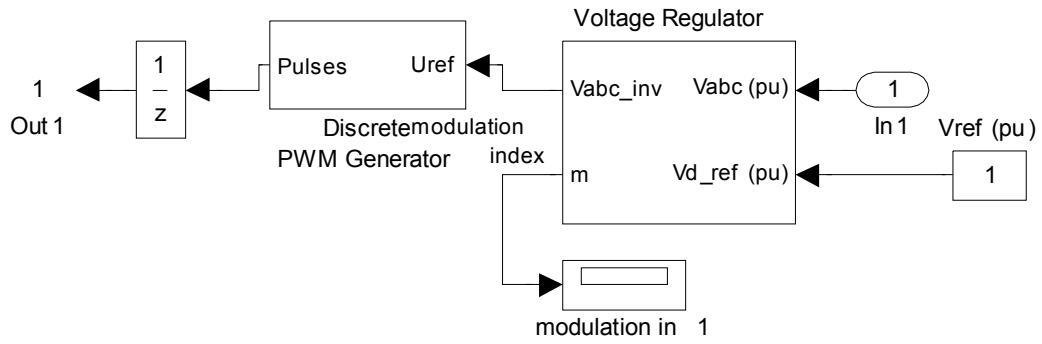

Figure 4.11: Simulated PWM Discrete Pulse Generation for Inverter

The ac voltage obtained from inverter is then filtered by a system of filters containing inductors and capacitors. A filter system is shown in Figure 4.12.

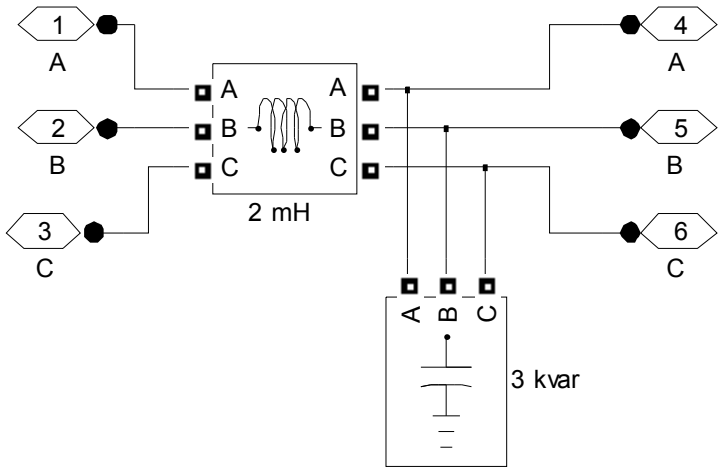

Figure 4.12: Simulation of Filter System

The filtered voltage is now free from harmonics and stepped down and fed to a grid simulated by using a smoothing reactor and a programmable voltage source as shown in Figure 4.13.

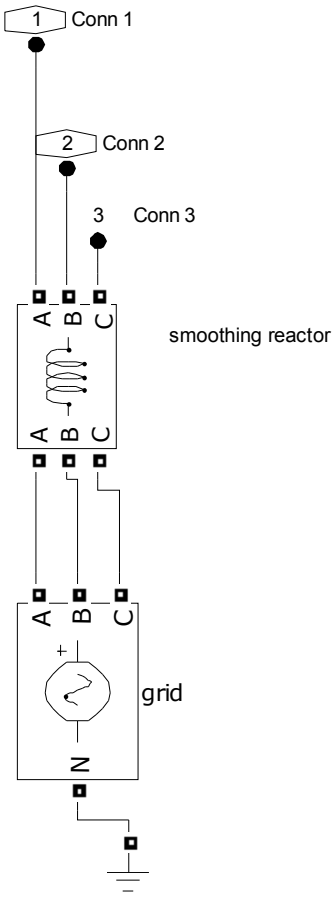

Figure 4.13: Simulation of a Three Phase AC Grid

CHAPTER 5

RESULTS AND DISCUSSIONS

The developments of dynamic models of various components and their implementation under SIMULINK environment have been discussed in Chapter 3. The mono-polar HVDC transmission line has been modeled in Chapter 4. The SIMULINK uses a solver based on trapezoidal rule using free interpolant. The study of the various renewable and conventional resources along with HVDC Transmission has been carried out and their characteristics have been studied.

The performance of the systems is analyzed on the basis of following three cases:

- Single phase AC voltage obtained at the generator side
- DC voltage fed into the transmission line
- Single phase AC voltage obtained at the grid side

5.1 PERFORMANCE OF THE WIND-HVDC LINK SYSTEM

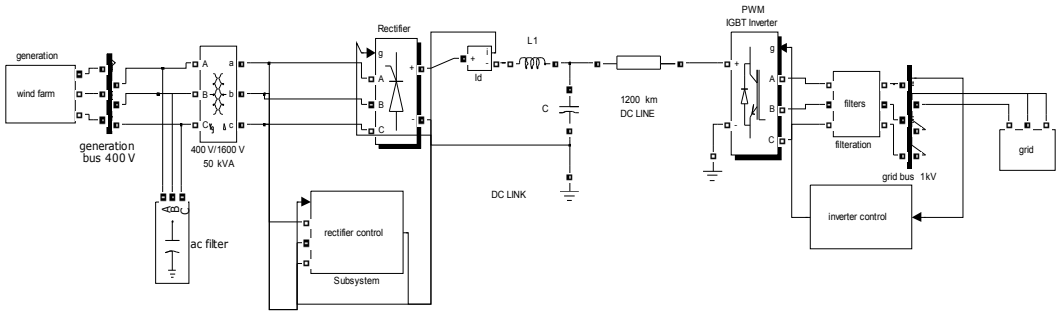

Figure 5.1: Wind Farm Connected With Mono-polar HVDC Transmission System

Wind farm is connected to the grid with the help of mono-polar HVDC transmission system as shown in Figure 5.1. The wind farm consists of forty induction generators of 0.3MW each these generators are connected in parallel to give 12 MW at 400V. The AC filter used to prevent flow of harmonics into generation side is rated to give power of 0.3MVAr. The step up transformer is rated as 5MVA and nominal voltage ratio 0f 400V/1.6KV. Six pulse rectifier uses double pulsing with pulse width of 10 degrees. The frequency of synchronization of voltage is 50 Hz. The DC

link uses smoothing reactor of 0.2 mH and DC capacitor of 5nF. The DC line has R, L, C parameters as 0.015 ohms, 0.792mH and 14.4 nF per kilometer respectively. The inverter uses PWM technology for conversion of DC line voltage to AC. The AC filters are carrying inductance of 200 mH and capacitive reactive power of 300kVAr. The rated voltage of grid is 400V.

The waveforms of the single phase AC voltage at generation side, DC voltage fed to the link and the single phase AC of Wind-HVDC link are shown in Figure 5.2(a) to 5.2(c).

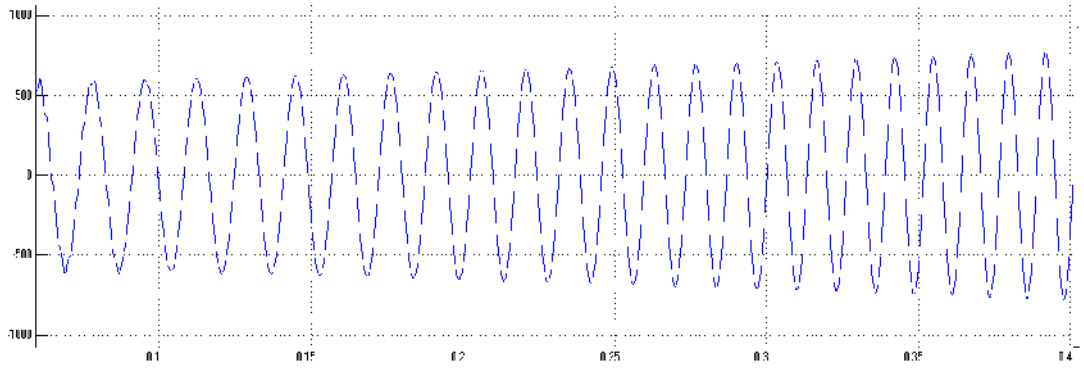

Figure 5.2(a): Generated AC Voltage of Wind-HVDC System

The line to line AC voltage produced at the generating side of wind farm is shown in Figure 5.2(a). It initially has a voltage of 500 V in the beginning and then it rises to a constant voltage of 700 V. This rise of voltage is due to the voltage build up caused by the capacitors connected at the beginning of each induction generator in the wind farm.

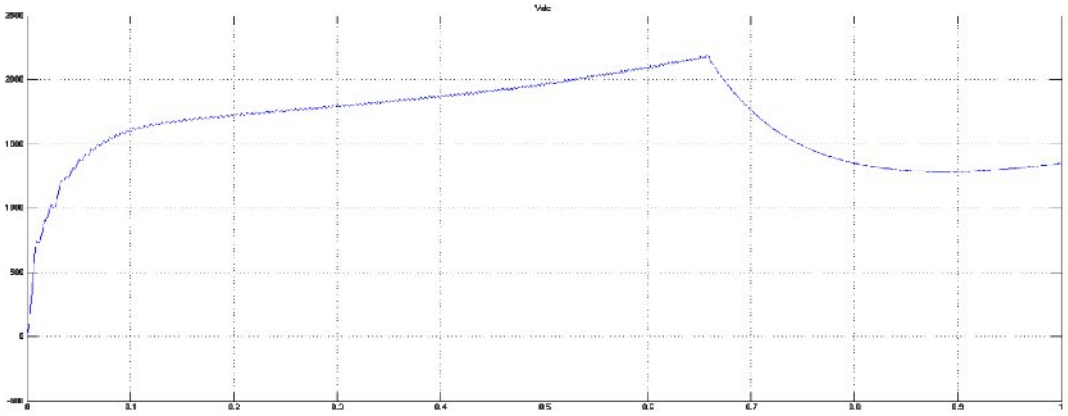

Figure 5.2(b): DC Voltage of Wind HVDC System Transmitted into the Line

The rectified DC voltage going into the line is shown in Figure 5.2(b). The rectified DC voltage 1.5 KV at 0.05 seconds and keeps on increasing till 0.65 seconds and then decreases to steady 1.4 KV from 0.8 seconds and onwards.

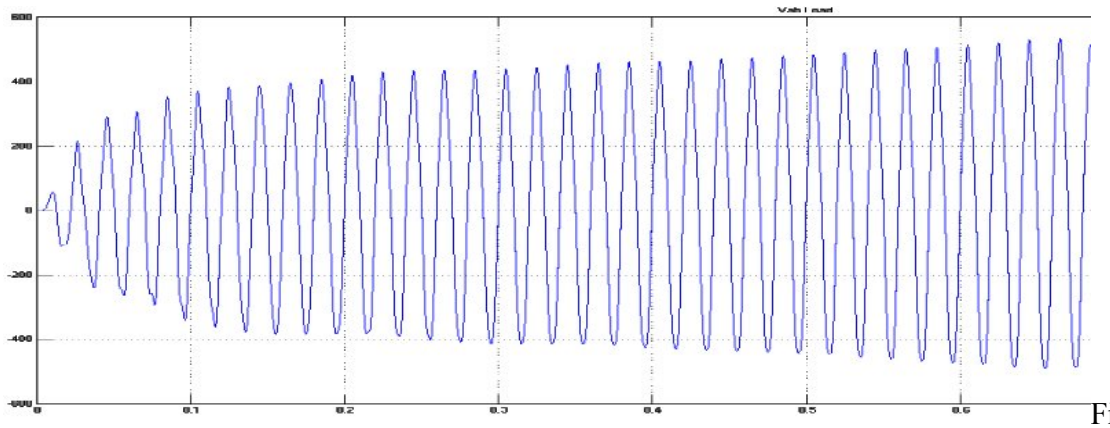

Figure 5.2(c): Single Phase AC Voltage of Wind HVDC System at Grid

Figure 5.2(c) shows the single phase line to line AC voltage waveform at the grid side. It builds up to a value of 400 Volts till 0.15 seconds and then increases to constant value of 450 V throughout.

5.2 PERFORMANCE OF DIESEL HVDC LINK SYSTEM

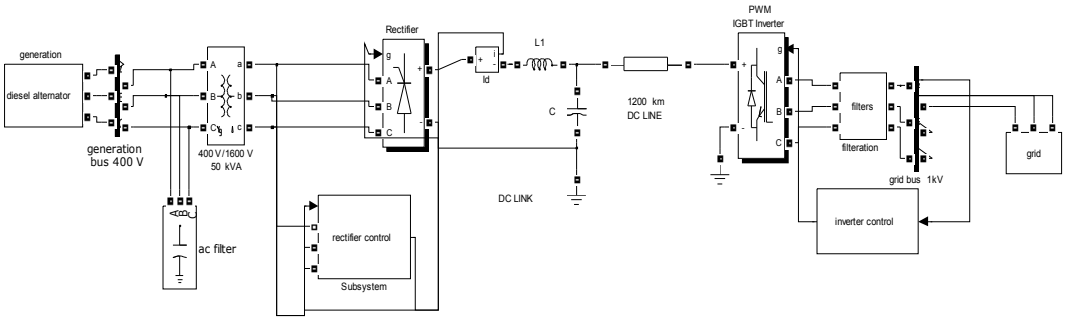

Figure 5.3: Diesel Alternator Connected with a Mono-polar HVDC Transmission System

Diesel alternator connected with a mono-polar HVDC transmission system is connected to grid as shown in Figure 5.3. The diesel alternator is rated to give 12 MVA at 400V. The AC filter used to prevent flow of harmonics into generation side is rated to give power of 0.3MVAr at 400V. The step up transformer is rated as 5MVA and nominal voltage ratio 0f 400V/1.6KV. Six pulse rectifier uses double pulsing with pulse width of 10 degrees. The frequency of

synchronization of voltage is 50 Hz. The DC link uses smoothing reactor of 0.2 mH and DC capacitor of 5nF. The DC line has R, L, C parameters as 0.015 ohms, 0.792mH and 14.4 nF per kilometer respectively. The inverter uses PWM technology for conversion of DC line voltage to AC. The AC filters are carrying inductance of 200 mH and capacitive reactive power of 300kVAr. The rated voltage of grid is 400V.

The waveforms showing single phase AC voltage at generation side, DC voltage fed to the link and the single phase AC of diesel HVDC link system are shown in Figure 5.4(a) to 5.4(c).

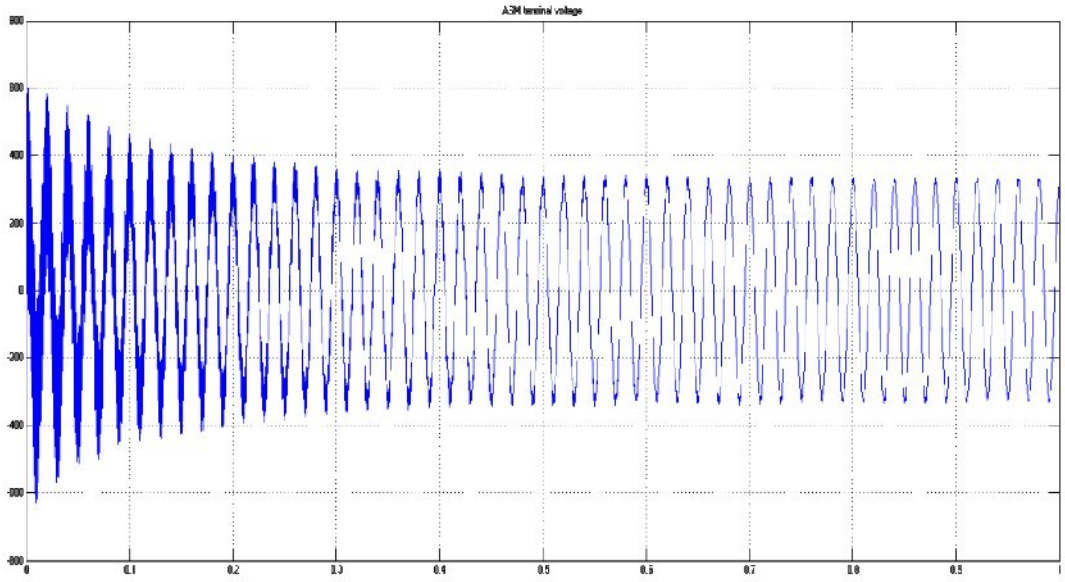

Figure 5.4(a): Generated AC Voltage of Diesel HVDC System

The line to line AC voltage produced at the generating side of diesel alternator is shown in Figure 5.4(a). It initially has a voltage of 600 V in the beginning then it settles to a constant voltage of 380 V after 0.2 seconds. This rise of voltage in the beginning is due to the capacitor connected at the generator side as an AC filter to avoid harmonics from DC side to flow into AC side.

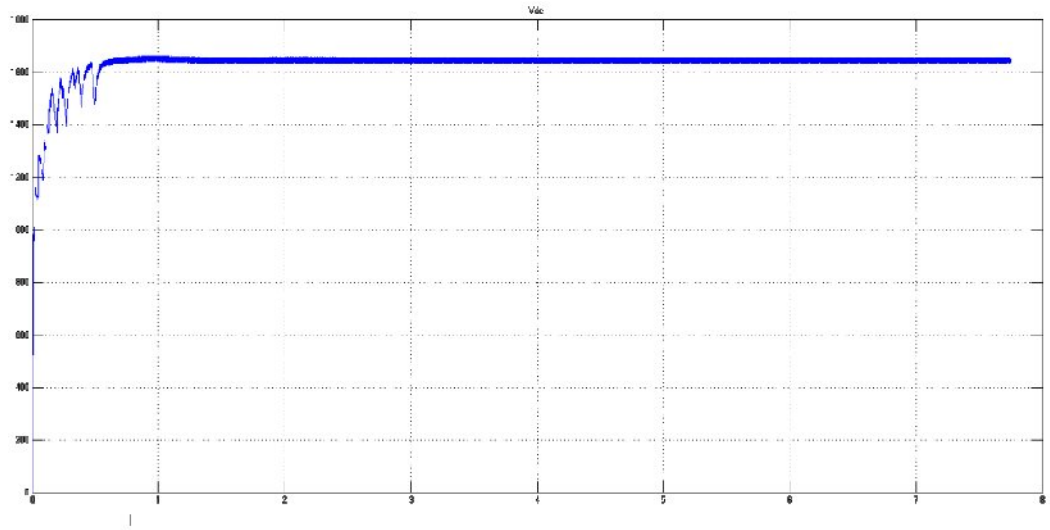

Figure 5.4b: Rectified DC Voltage of Diesel HVDC System Fed to the Line

The rectified DC voltage from generated AC going into the line is shown in Figure 5.4(b). The rectified DC voltage is having few oscillations in beginning till 0.07 seconds then it finally settles to 1.6 KV from 1 second and onwards. These oscillations in beginning are due the same reason as in case of single phase line to line voltage of generation side.

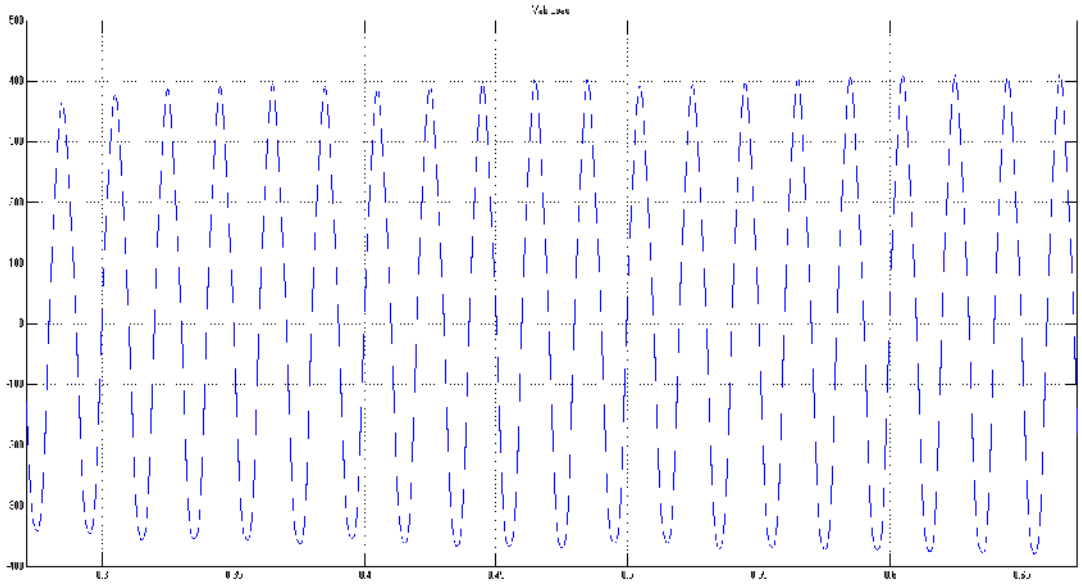

Figure 5.4(c): Single Phase AC Voltage Waveform of Diesel HVDC System at the Grid Side

Figure 5.4(c) shows the single phase line to line AC voltage waveform at the grid side. It is having a constant value of 400 Volts throughout without having any transients, which had been removed by the filters used after inverter end.

5.3 PERFORMANCE OF HYDRO-HVDC LINK SYSTEM

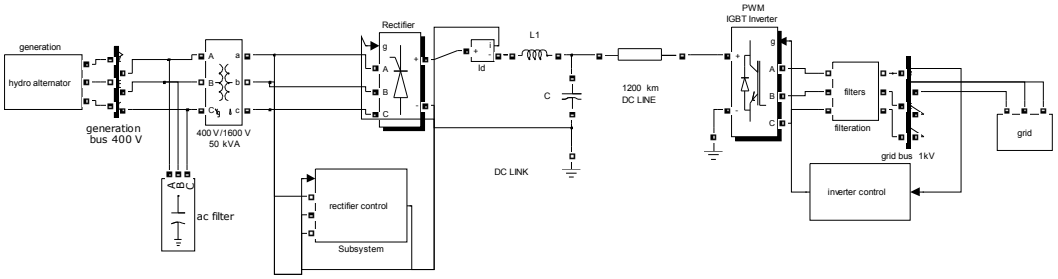

Figure 5.5: Hydro electric Generator Connected with Mono-polar HVDC Transmission and Grid

Hydro electric generator is connected with a Mono-polar HVDC transmission system connected to grid as shown in Figure 5.5. The hydro generator is rated to give 16 MVA at 400V. The AC filter used to prevent flow of harmonics into generation side is rated to give power of 0.3MVAr. The step up transformer is rated as 5MVA and nominal voltage ratio 0f 400V/1.6KV. Six pulse rectifier uses double pulsing with pulse width of 10 degrees. The frequency of synchronization of voltage is 50 Hz. The DC link uses smoothing reactor of 0.2 mH and DC capacitor of 5nF. The DC line has R, L, C parameters as 0.015 ohms, 0.792mH and 14.4 nF per kilometer respectively. The inverter uses PWM technology for conversion of DC line voltage to AC. The AC filters are carrying inductance of 200 mH and capacitive reactive power of 300kVAr. The rated voltage of grid is 400V.

The waveforms showing single phase AC voltage at generation side, DC voltage fed to the link and the single phase AC of hydro-HVDC system are shown in Figure 5.6(a) to 5.6(c).

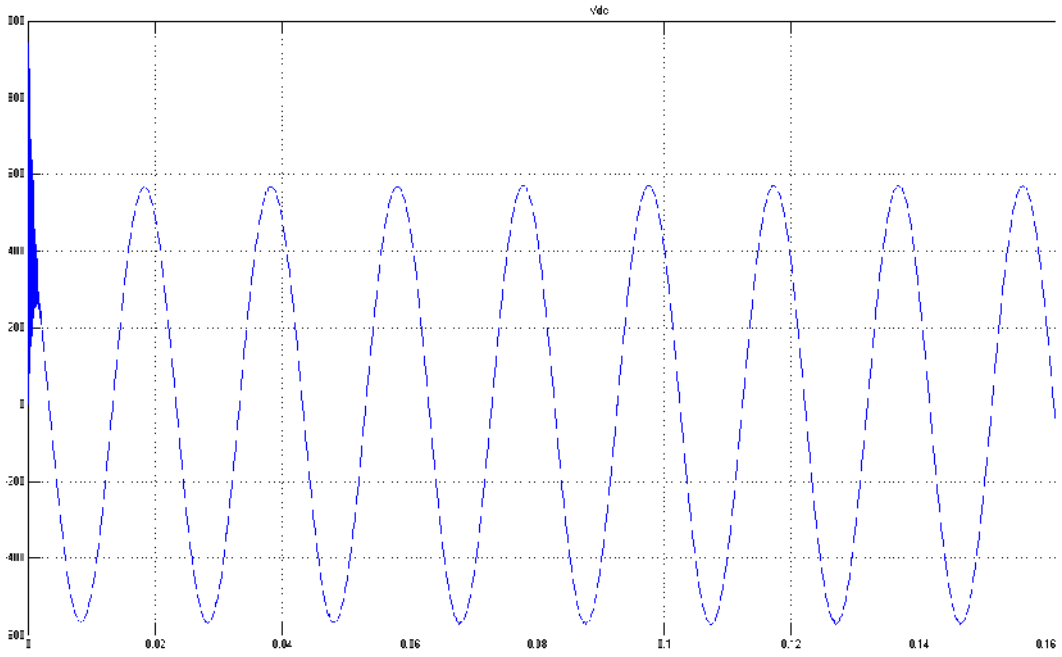

Figure 5.6(a): Generated AC Voltage of Hydroelectric HVDC System

The generated line to line single phase voltage is shown in Figure 5.6(a). Initially due to hunting its having a very large value to 1KV. Then it decreases and finally settles to 500V from 0.01 seconds and remains constant throughout.

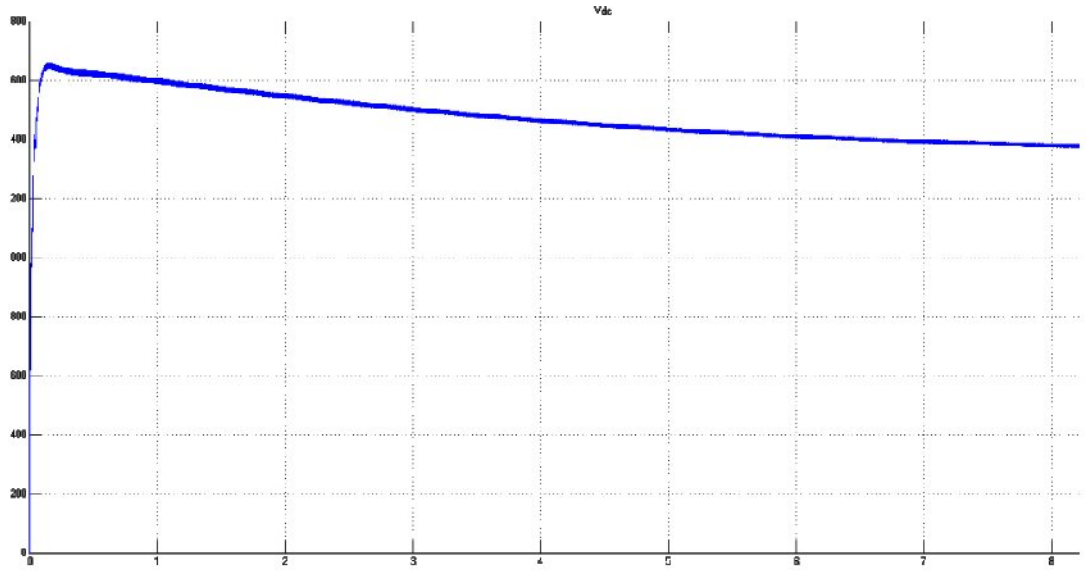

Figure 5.6(b): Rectified DC Voltage of Hydroelectric System Fed to the Transmission Line

The rectified DC voltage going into the line is shown in Figure 5.6(b). The rectified DC voltage increases sharply to 1.6 KV at 0.01 seconds and slowly decreases till 1 second and settles to steady 1.4 KV from 6 seconds and onwards.

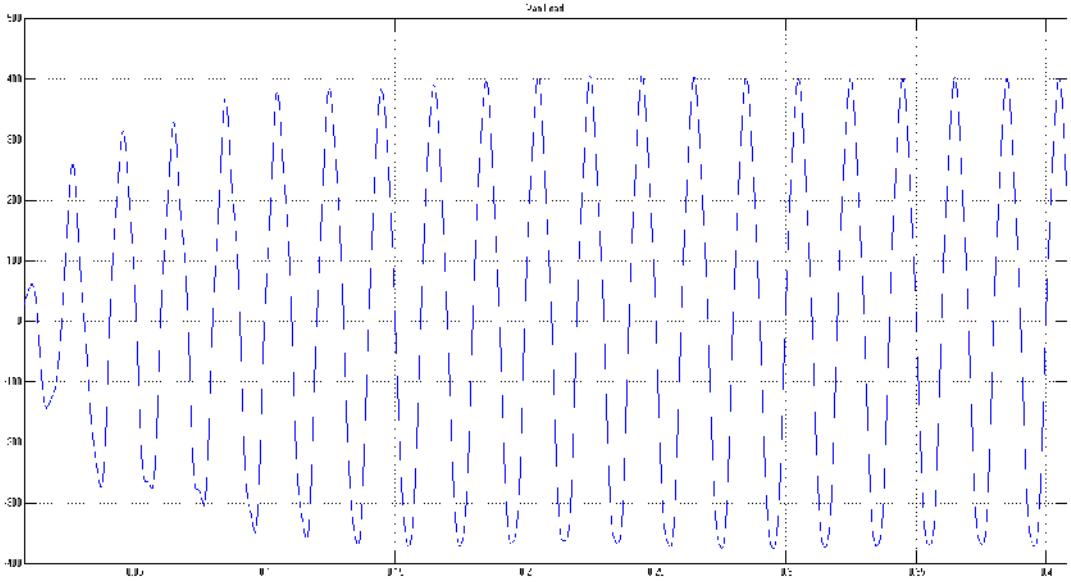

Figure 5.6(c): Single Phase AC Voltage Waveform of hydroelectric system at Grid Side

Figure 5.6(c) shows the single phase line to line AC voltage waveform at the grid side. It is having initially a value of 300 Volts then it builds up to a constant value of 400 V throughout.

5.4 PERFORMANCE OF SOLAR HVDC LINK SYSTEM

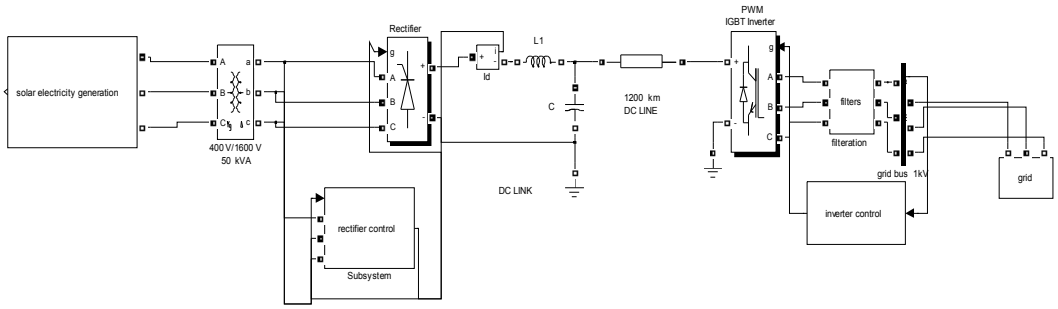

Figure 5.7: Solar Electricity System with Monopolar HVDC Transmission line

Solar is connected with a monopolar HVDC transmission system connected to grid as shown in Figure 5.7.Firstly, the DC voltage from solar cells is converted to AC voltage by a PWM

inverter. The output voltage of inverter is carrying a lot of harmonics is made to pass through a filter and then stepped up.

Large numbers of solar cells are connected in series to give 400V at 400MW. The step up transformer is rated as 5MVA and nominal voltage ratio 0f 400V/1.6KV. six pulse rectifier uses double pulsing with pulse width of 10 degrees. The frequency of synchronization of voltage is 50 Hz.. The DC link uses smoothing reactor of 0.2 mH and DC capacitor of 5nF. The DC line has R, L, C parameters as 0.015 ohms, 0.792mH and 14,4 nF per kilometer respectively. The inverter uses PWM technology for conversion of DC line voltage to AC. The AC filters are carrying inductance of 200 mH and capacitive reactive power of 300kVAr. The rated voltage of grid is 400V.

The waveforms showing single phase AC voltage at generation side, DC voltage fed to the link and the single phase AC of Solar-HVDC system are shown in Figure 5.8(a) to 5.8(c).

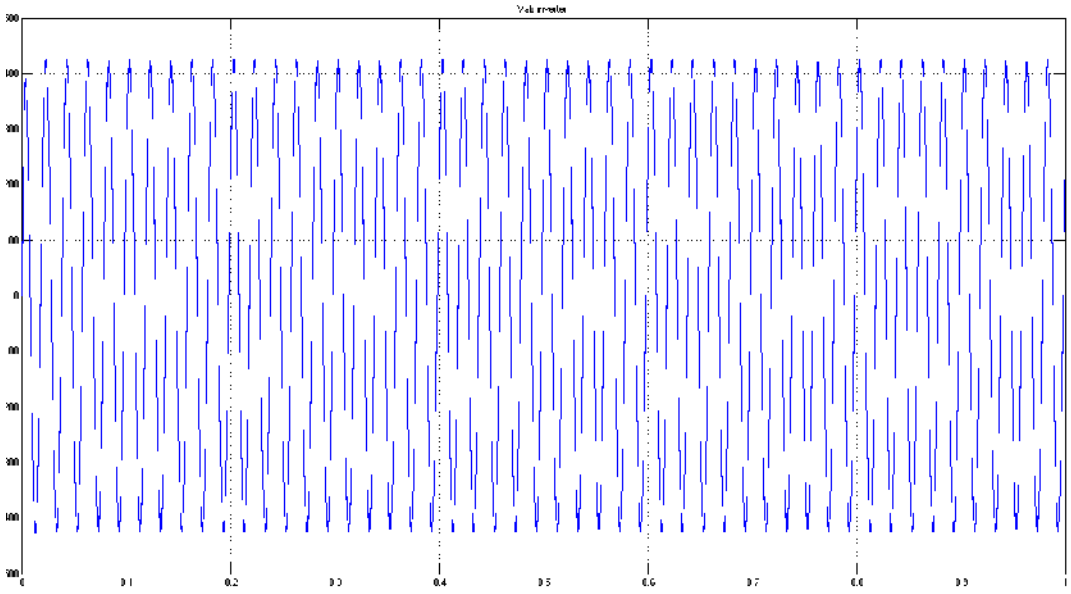

Figure 5.8(a): Obtained AC voltage of Solar Cells after Inversion

Figure 5.8(a) shows AC voltage obtained after inversion of DC voltage after getting stepped up from transformer and passing through filters. It is having value of 400V line to line.

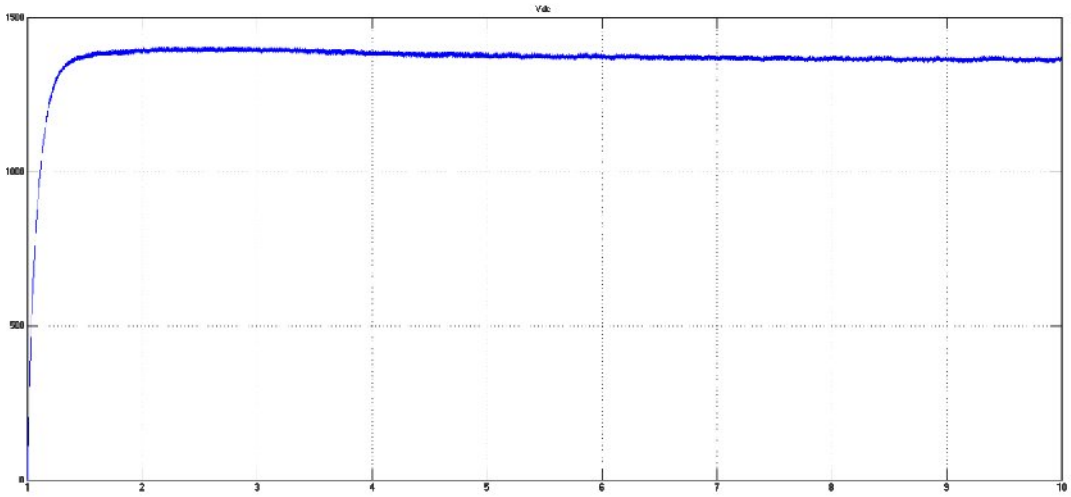

Figure 5.8(b): Rectified DC voltage of solar-HVDC Fed to the Line

The rectified DC voltage from generated AC going into the line is shown in Figure 5.8(b). The rectified DC voltage rises abruptly at 0.05 seconds to steady state value of 1.3 KV and remains constant.

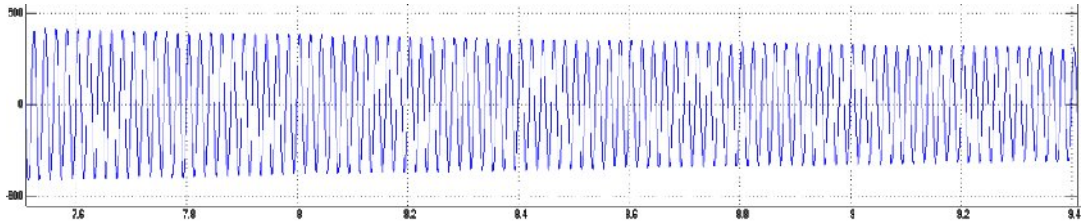

Figure 5.8(c): Single Phase AC Voltage Waveform of Solar-HVDC System at the Grid Side

Figure 5.8(c) shows the single phase AC voltage waveform at the grid side. It appears to be having a constant value of 400 Volts throughout but due to transients.

5.5 PERFORMANCE OF STEAM HVDC LINK SYSTEM

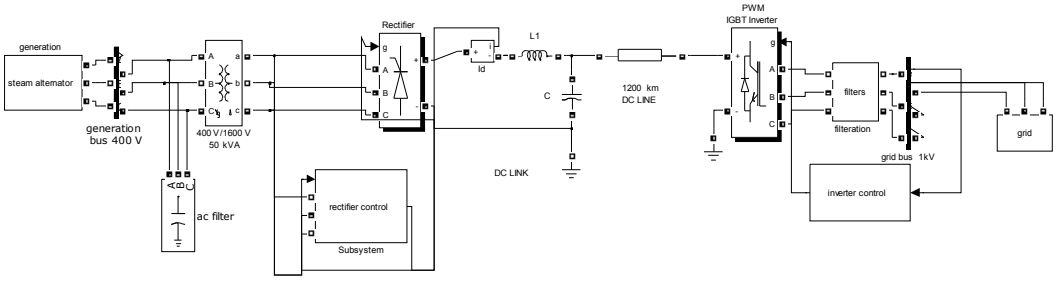

Figure 5.9: Steam Alternator Connected with a Monopolar HVDC Transmission System

Steam alternator is connected with a monopolar HVDC transmission system connected to grid as shown in Figure 5.9. The steam alternator is rated at 12 MVA at 400V. The AC filter used to prevent flow of harmonics into generation side is rated to give power of 0.3MVAr. The step up transformer is rated as 5MVA and nominal voltage ratio 0f 400V/1.6KV. six pulse rectifier uses double pulsing with pulse width of 10 degrees. The frequency of synchronization of voltage is 50 Hz. The DC link uses smoothing reactor of 0.2 mH and DC capacitor of 5nF. The DC line has R, L, C parameters as 0.015 ohms, 0.792mH and 14,4 nF per kilometer respectively. The inverter uses PWM technology for conversion of DC line voltage to AC. The AC filters are carrying inductance of 200 mH and capacitive reactive power of 300kVAr. The rated voltage of grid is 400V.

The waveforms showing single phase AC voltage at generation side, DC voltage fed to the link and the single phase AC are shown in Figure 5.10(a) to 5.10(c).

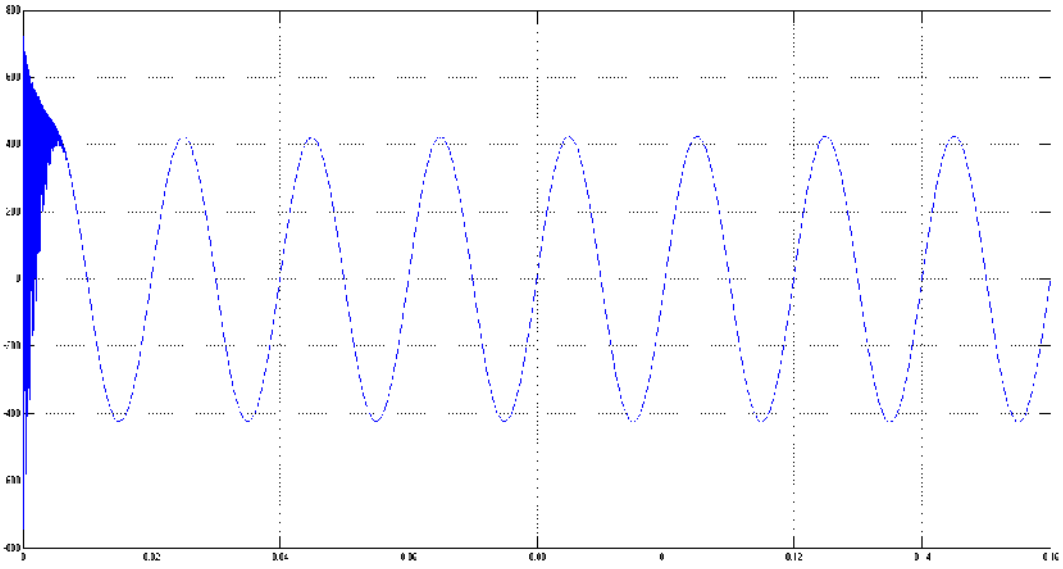

Figure 5.10(a): Generated AC voltage of Steam-HVDC System

Figure 5.10 (a) shows generated single phase line to line voltage of steam alternator. Having few transients in beginning due to hunting of alternator it is having a constant steady value of 400 Volts throughout.

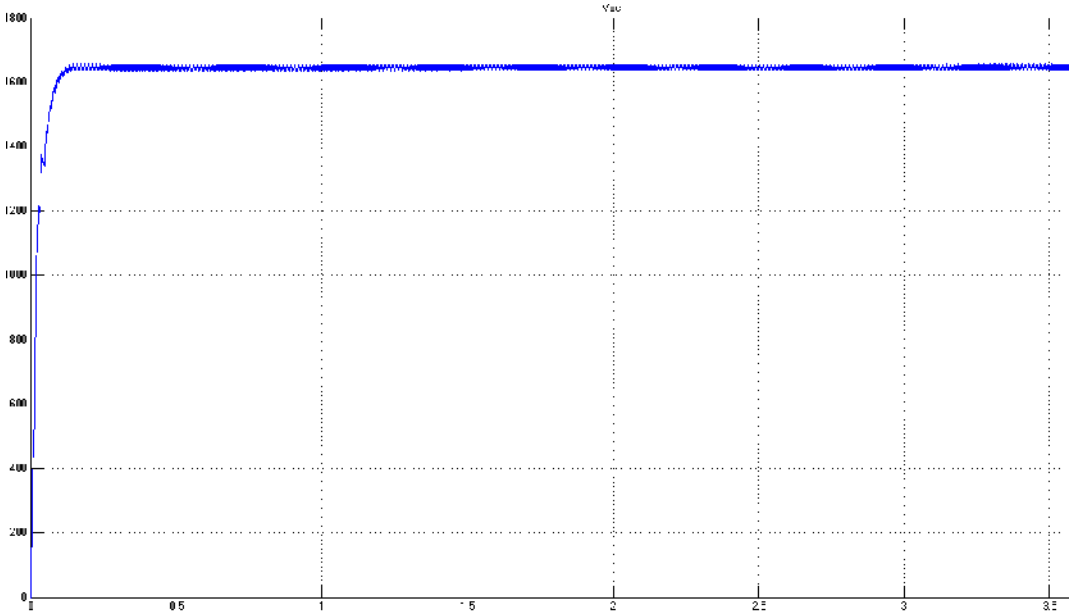

Figure 5.10(b): Rectified DC voltage of Steam system Fed to the Line

The rectified DC voltage from generated AC going into the line is shown in Figure 5.10(b). The rectified DC voltage rises sharply to 1.62 KV in just 0.2 seconds and reaches steady state immediately.

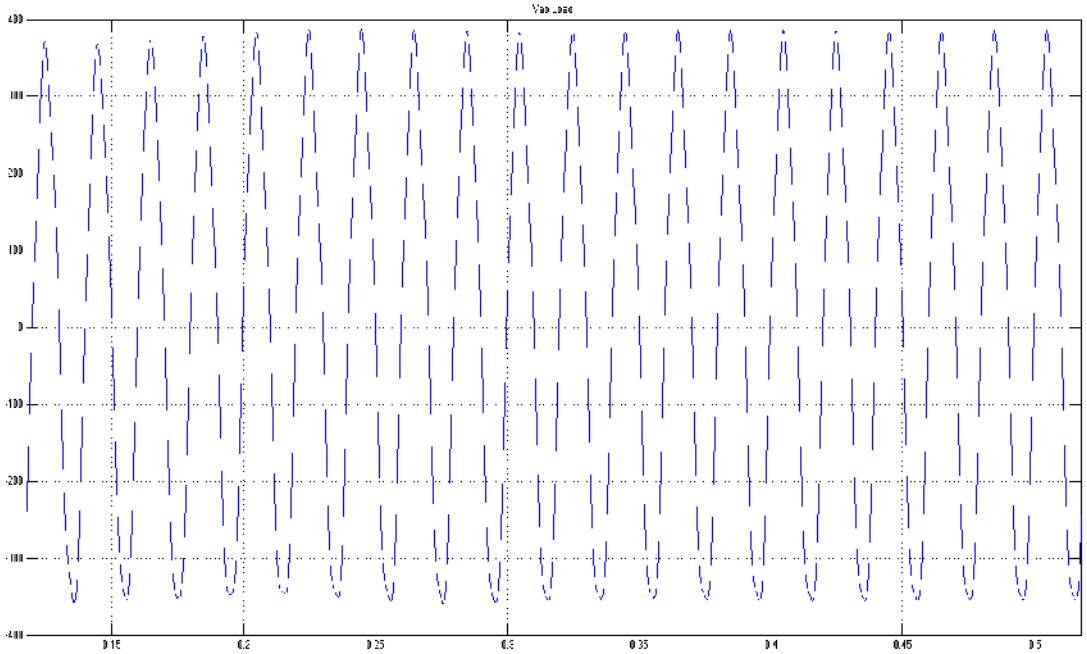

Figure 5.10(c): Single Phase AC Voltage Waveform of Steam-HVDC System at the Grid Side

Figure 5.10(c) shows the single phase AC voltage waveform at the grid side. It is having a constant value of 390 Volts throughout.

5.6 INTERCONNECTION OF VARIOUS RESOURCES WITH HVDC TRANSMISSION LINE

In the above sections simulation has been carried out showing the various sources feeding power to the grid through HVDC line individually. In this section, simulation is carried out showing all the sources feeding power to a common grid by their independent transmission lines. The simulation model showing all these sources connected to grid through HVDC is shown in Figure 5.11.

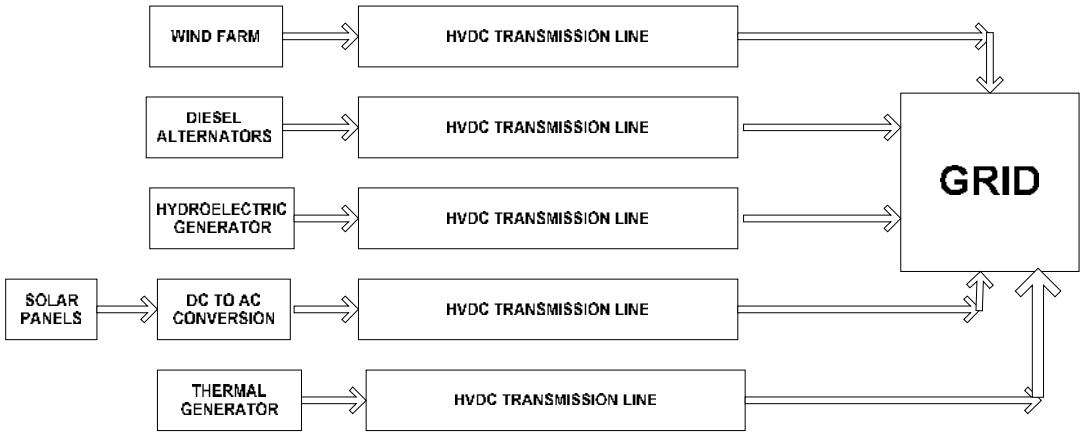

Figure 5.11: Various Sources Connected to Common Grid through Different HVDC Line

5.6.1 PERFORMANCE OF THE WIND-HVDC LINK SYSTEM AFTER INTERCONNECTION

The waveforms showing single phase AC voltage at generation side, DC voltage fed to the link and the single phase AC are shown in Figure 5.12(a) to 5.12(c). These waveforms are corresponding to the wind-HVDC link system after connecting it with the common grid.

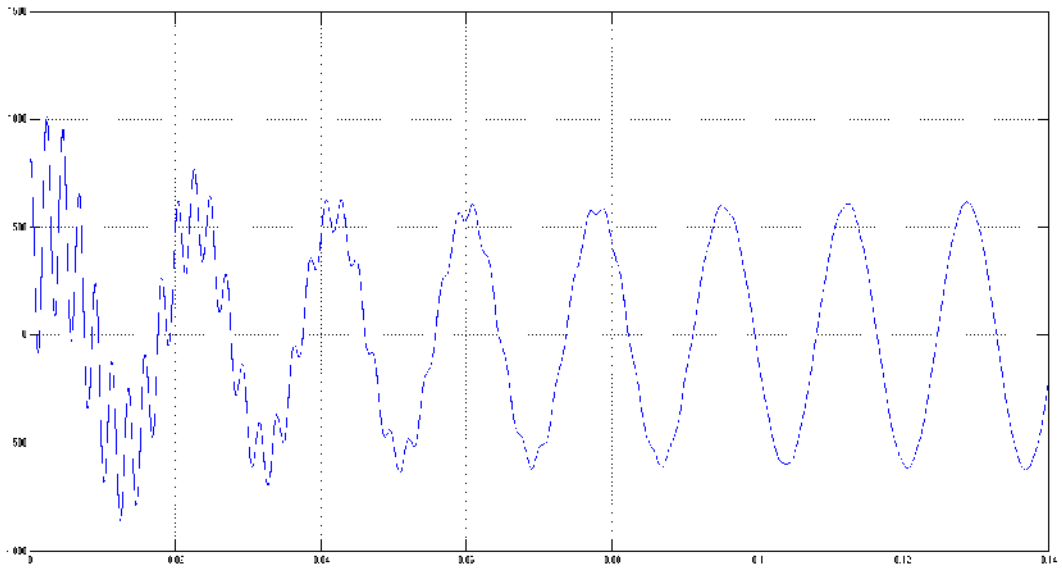

Figure 5.12(a): Generated AC Voltage of Wind HVDC link after interconnection

The line to line AC voltage produced at the generating side of wind farm after interconnection is shown in Figure 5.12(a). It initially has a lot of transients and voltage ranging up to 100 Volts. After 0.09 seconds it finally settles down to constant value of voltage of 500 V. though the magnitude is same as before interconnection but the voltage waveform suffers from serious distortions.

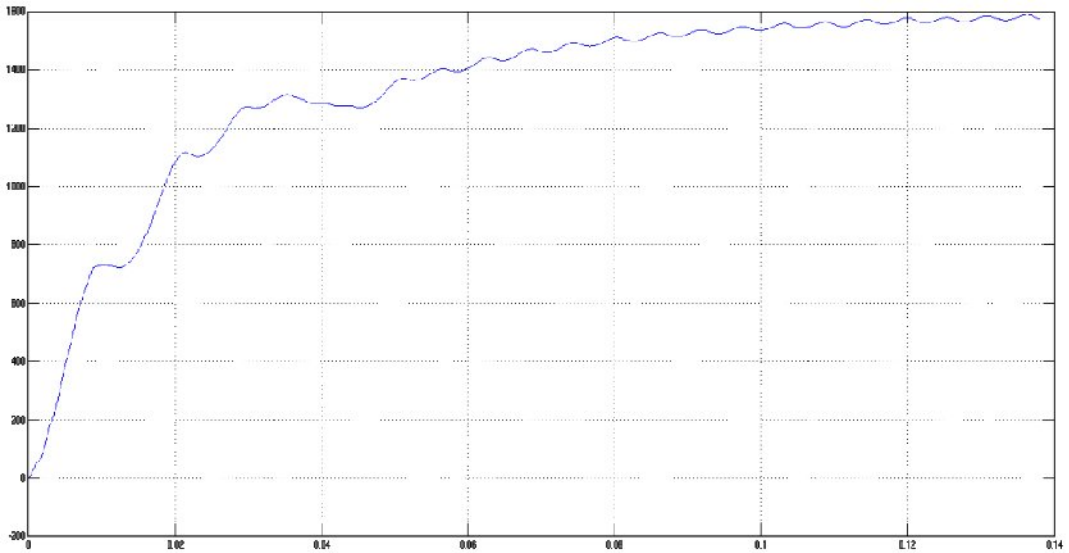

Figure 5.12(b): DC Voltage of Wind HVDC Link System Transmitted into the Line after interconnection

Figure 5.12(b) shows DC voltage of Wind HVDC link system transmitted into the line after its interconnection with common grid. It is showing transient behavior and could only settle after 120 milliseconds having steady state value of 1.5 KV as compared to 1.2 KV when it is connected alone with the grid.

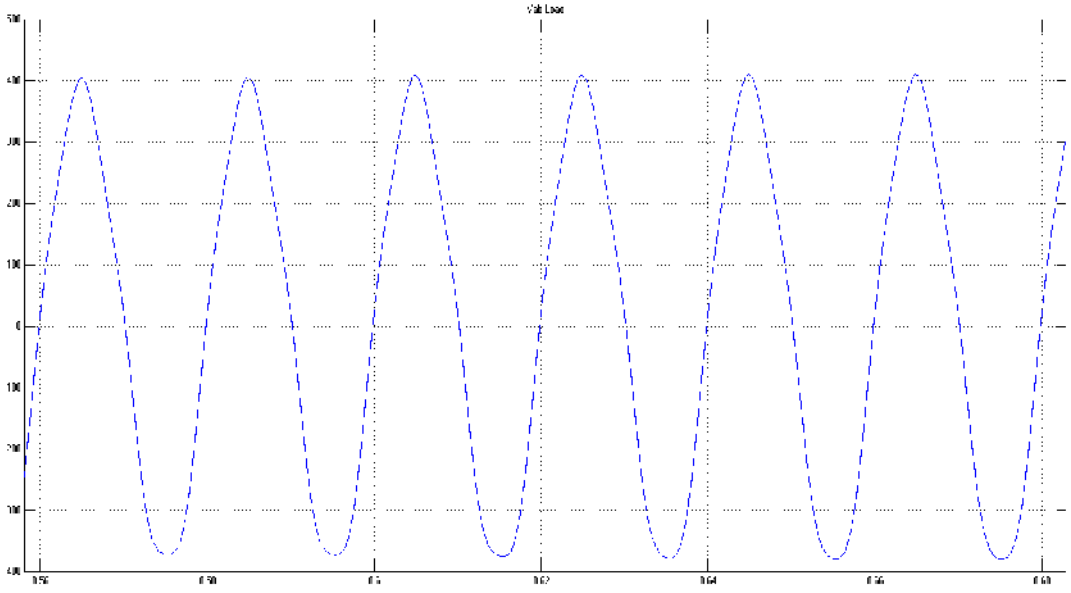

Figure 5.12(c): Single Phase AC Voltage of Wind HVDC System Obtained at Common Grid after interconnection

Figure 5.12(c) shows the single phase line to line AC voltage waveform at the grid side after interconnection. It shows constant voltage of 400V throughout with positive peak slightly higher than negative peak which is due to DC offset. Before interconnection it is having magnitude 450 V after interconnecting it settles to 400 V.

5.6.2 PERFORMANCE OF THE DIESEL-HVDC LINK SYSTEM AFTER INTERCONNECTION

The waveforms showing single phase AC voltage at generation side, DC voltage fed to the link and the single phase AC of Diesel-HVDC system are shown in Figure 5.13(a) to 5.13(c). These waveforms are corresponding to the diesel-HVDC link system after connecting it with the common grid.

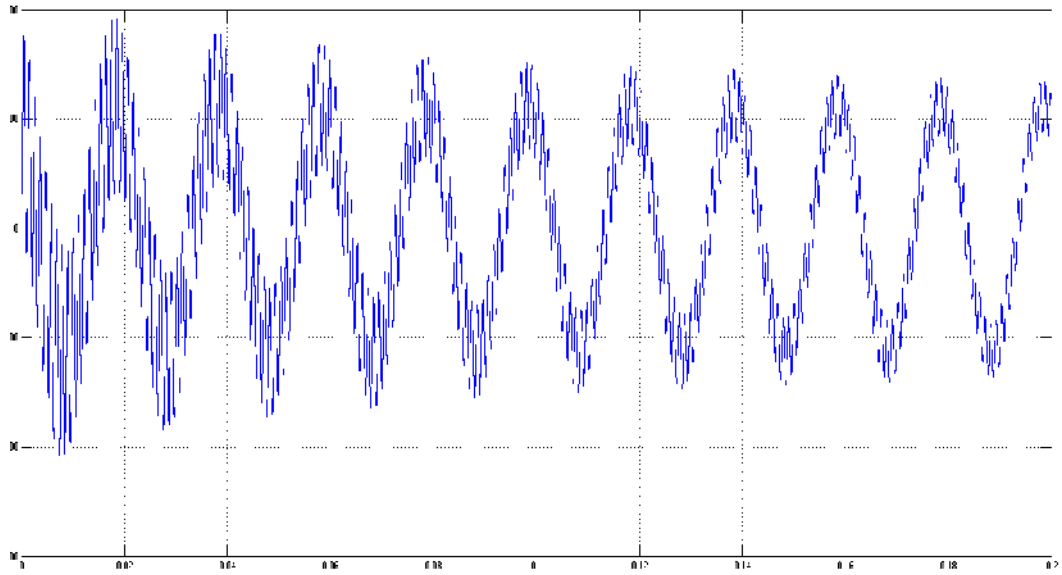

Figure 5.13(a): Generated AC Voltage of Diesel HVDC link after interconnection

The line to line AC voltage produced by diesel alternator after integrating with common grid is shown in Figure 5.13(a). It is showing highly distorted sinusoidal waveform of value 400V which settles to 350V after 120 milliseconds. In comparison to before interconnection, the voltage has been observed to has lot of distortions and decreased in magnitude from 380V to 350V at steady state.

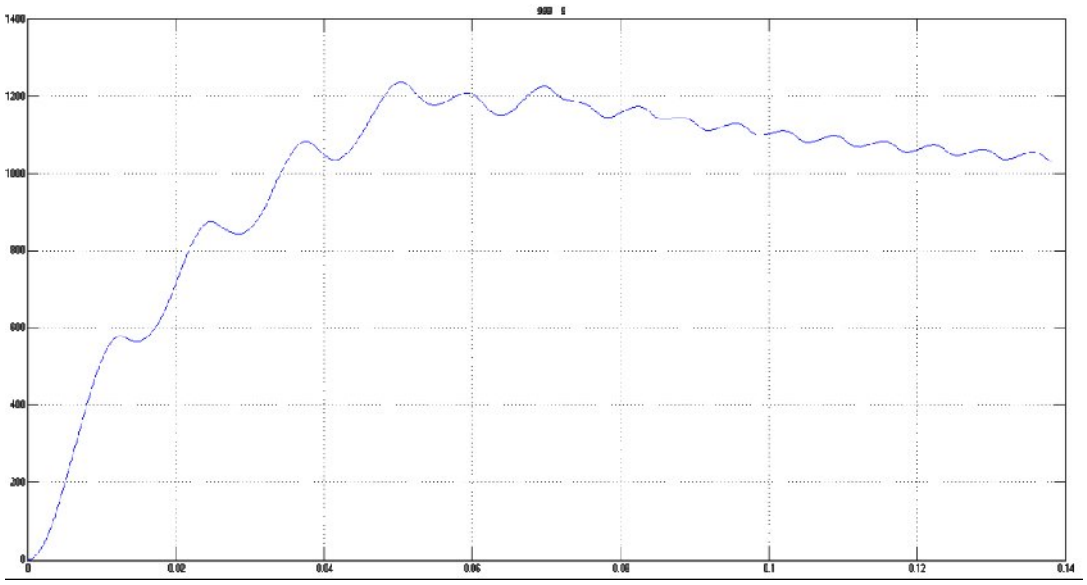

Figure 5.13(b): DC Voltage of Diesel HVDC Link System Transmitted into the Line after interconnection

Figure 5.13(b) shows DC voltage of diesel HVDC link system transmitted into the line after its interconnection with common grid. It is showing transient and oscillatory behavior like wind as compared to its stable behavior when connected alone to grid. After interconnection, it could only settle after 140 milliseconds to a steady value of 1KV as compared to 1.6 KV earlier.

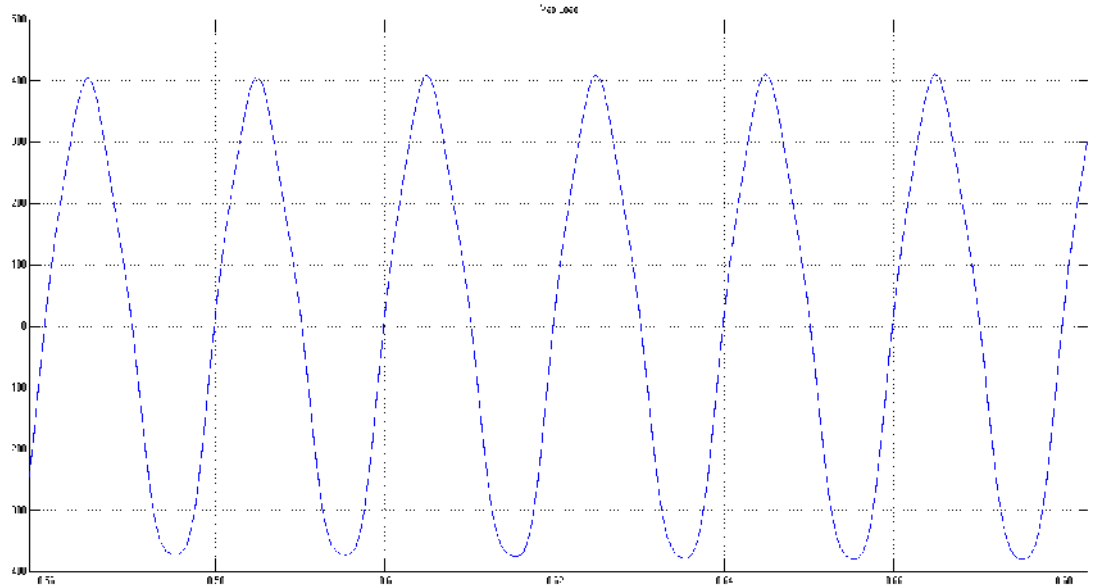

Figure 5.13(c): Single Phase AC Voltage of Diesel HVDC System Obtained at Common Grid after interconnection

Figure 5.13(c) shows the single phase line to line AC voltage waveform at the grid side after interconnection. It shows constant voltage of 400V throughout with positive peak slightly higher than negative peak which is due to DC offset. In comparison to previous waveform of before interconnection, it is having same magnitude 0f 400V but got little distorted.

5.6.3 PERFORMANCE OF THE HYDRO-HVDC LINK SYSTEM AFTER INTERCONNECTION

The waveforms showing single phase AC voltage at generation side, DC voltage fed to the link and the single phase AC are shown in Figure 5.14(a) to 5.14(c). These waveforms are corresponding to the hydro-HVDC link system after connecting it with the common grid.

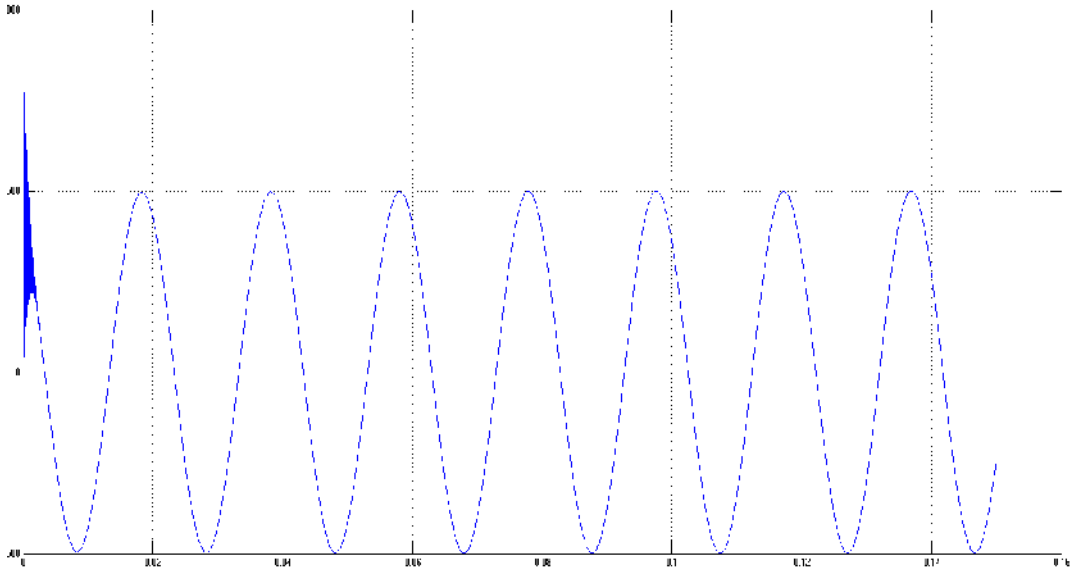

Figure 5.14(a): Generated AC Voltage of Hydro HVDC link after interconnection

The line to line AC voltage produced at the generating side of hydro-HVDC is shown in Figure 5.14(a). It initially has a few transient but has mostly constant voltage throughout of 500 V which is same as before interconnection.

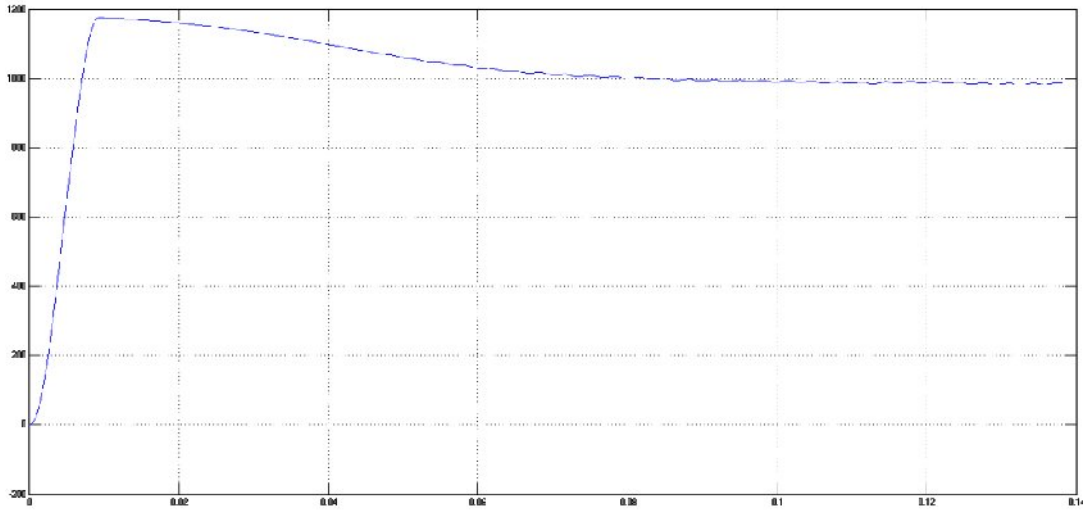

Figure 5.14(b): DC Voltage of Hydro HVDC Link System Transmitted into the Line after interconnection

Figure 5.14(b) shows DC voltage of hydro HVDC system transmitted into the line after its interconnection with common grid. It does not show any transient behavior and rises to 1.19 KV in 10 milliseconds and settles fast to 1 KV in 80 milliseconds as compared to 1.4 KV earlier.

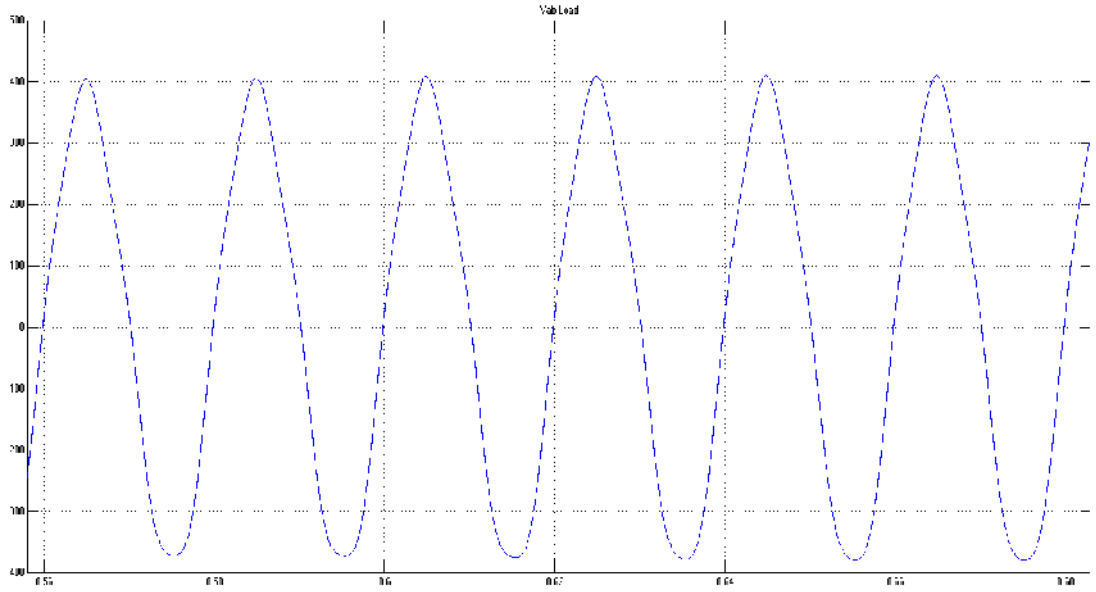

Figure 5.14(c): Single Phase AC Voltage of Hydro HVDC System Obtained at Common Grid after interconnection

Figure 5.14(c) shows the single phase line to line AC voltage waveform at the grid side after interconnection. It shows constant voltage of 400V throughout with positive peak slightly higher than negative peak which is due to DC offset.

5.6.4 PERFORMANCE OF THE SOLAR-HVDC LINK SYSTEM AFTER INTERCONNECTION

The waveforms showing single phase AC voltage at generation side, DC voltage fed to the link and the single phase AC of solar-HVDC link after connecting it with the common grid are shown in Figure 5.15(a) to 5.15(c).

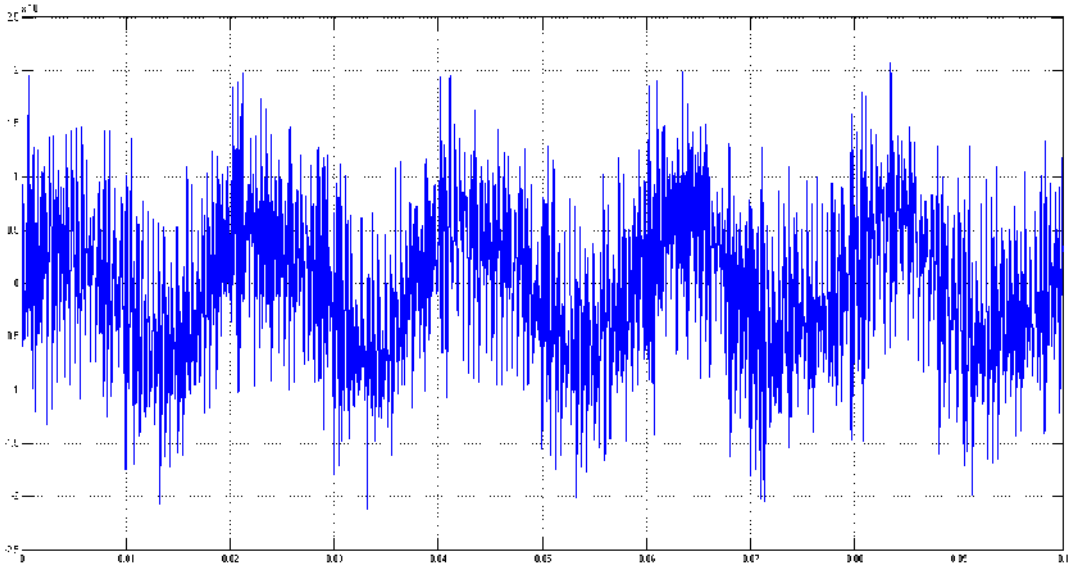

Figure 5.15(a): Generated AC Voltage of Solar HVDC link after interconnection

The line to line AC voltage produced at the generating side of solar-HVDC system is shown in Figure 5.15(a). It is having highly distorted waveform of magnitude 150V after interconnection. This is due to the fact that solar goes through two conversions, first from DC to AC by inverter and then from DC to AC by rectifier.as compared to previous case of connecting independent source, the voltage has lots both its quality and magnitude upto a large extent.

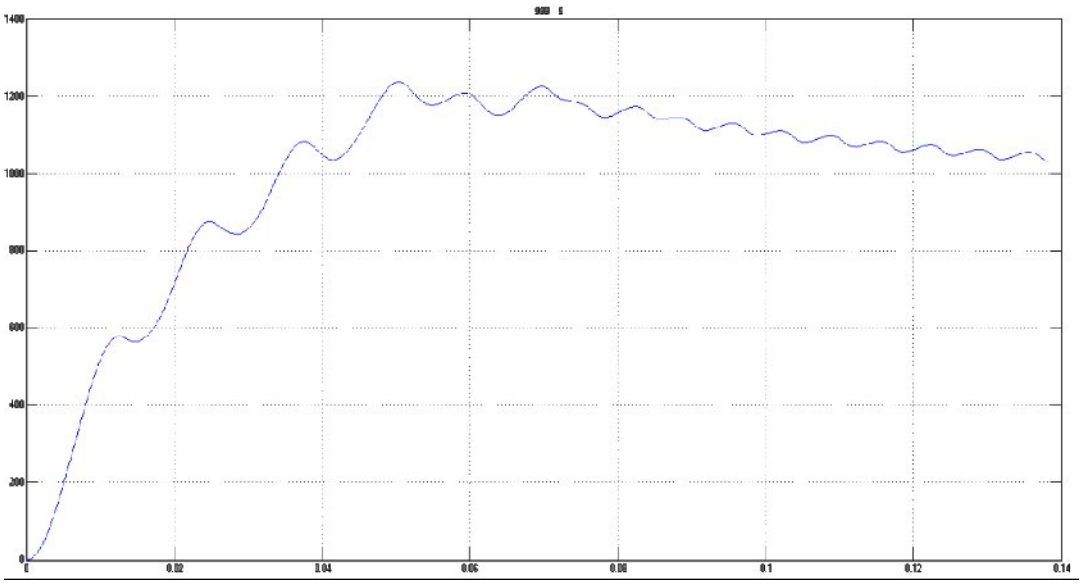

Figure 5.15(b): DC Voltage of Solar HVDC Link System Transmitted into the Line after interconnection

Figure 5.15(b) shows DC voltage of solar HVDC link system transmitted into the line after its interconnection with common grid. It is showing similar nature as like hydro but could achieve steady state before 130 milliseconds. Also its value dropped from 1.63 KV to 0.9 KV after interconnection.

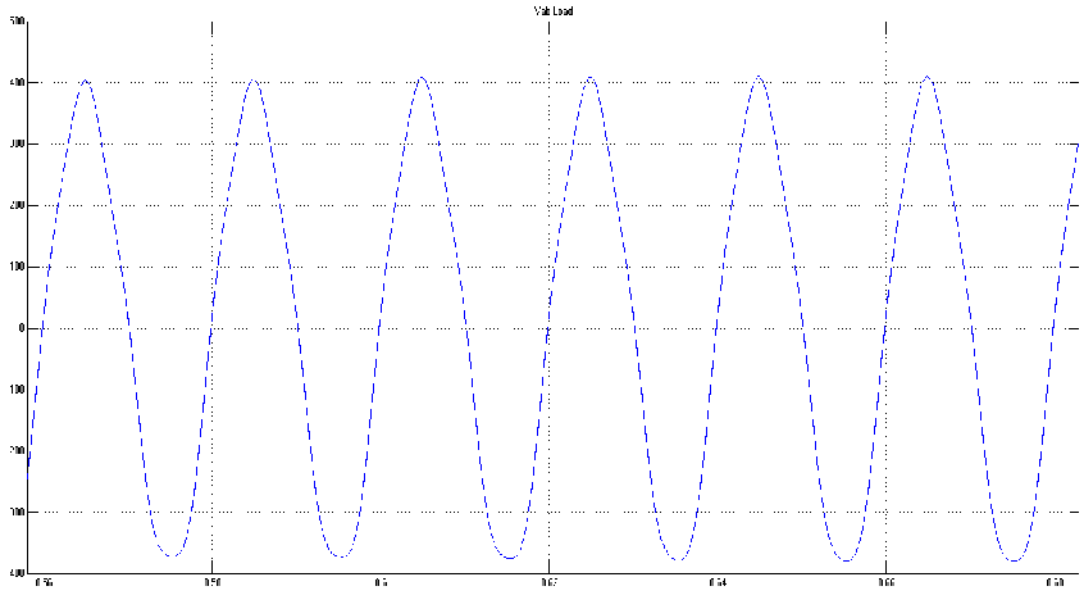

Figure 5.15(c): Single Phase AC Voltage of Solar HVDC System Obtained at Common Grid after interconnection

Figure 5.15(c) shows the single phase line to line AC voltage waveform at the grid side after interconnection. It shows constant voltage of 400V throughout with positive peak slightly higher than negative peak which is due to DC offset.

5.6.5 PERFORMANCE OF THE STEAM-HVDC LINK SYSTEM AFTER INTERCONNECTION

The waveforms showing single phase AC voltage at generation side, DC voltage fed to the link and the single phase AC are shown in Figure 5.16(a) to 5.16(c). These waveforms are corresponding to the steam-HVDC link system after connecting it with the common grid.

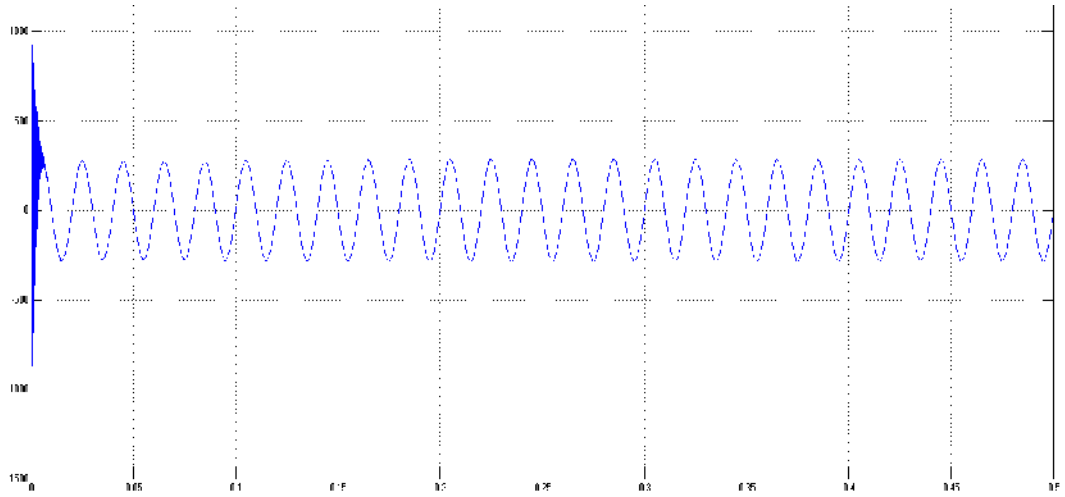

Figure 5.16(a): Generated AC Voltage of Steam HVDC link after interconnection

The line to line AC voltage produced at the generating side of steam HVDC system after interconnection is shown in Figure 5.16(a). It initially has few transients but is constant throughout having voltage of 350 V.

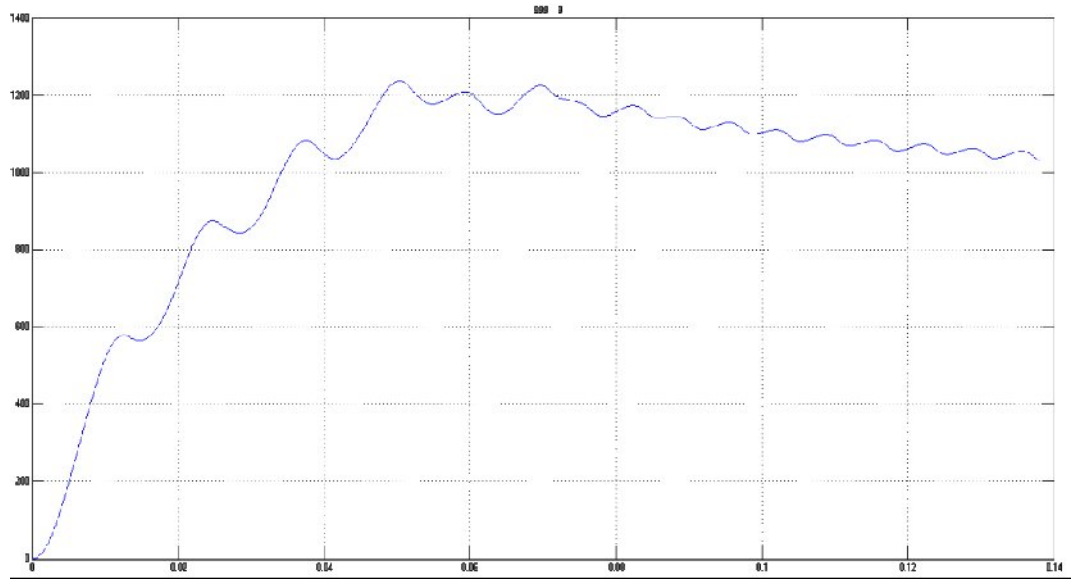

Figure 5.16(b): DC Voltage of Steam HVDC Link System Transmitted into the Line after interconnection

Figure 5.16(b) shows DC voltage of steam HVDC link system transmitted into the line after its interconnection with common grid. It is showing similar nature as like hydro but could achieve

steady state before 130 milliseconds. Also its value dropped from 1.63 KV to 0.9 KV after interconnection.

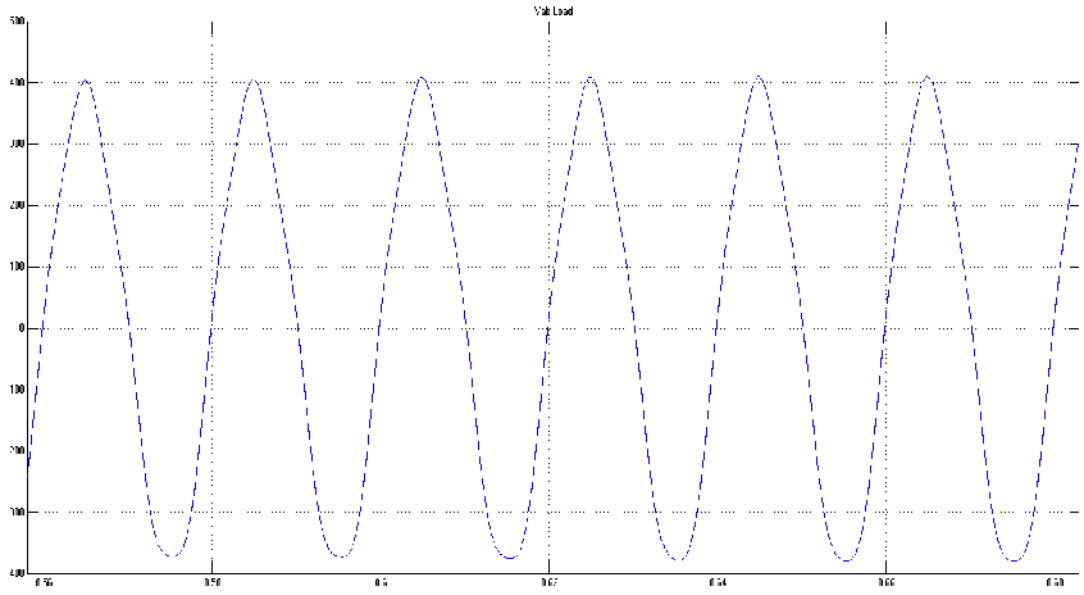

Figure 5.16(c): Single Phase AC Voltage of Steam HVDC System Obtained at Common Grid after interconnection

Figure 5.16(c) shows the single phase line to line AC voltage waveform at the grid side after interconnection. It shows constant voltage of 400V throughout with positive peak slightly higher than negative peak which is due to DC offset.

CHAPTER 6

CONCLUSIONS AND FUTURE SCOPE OF WORK

6.1 CONCLUSIONS

The system having both conventional and renewable generating sources located at far distant locations and connected through HVDC transmission system as its backbone has been simulated. Power from sources has been fed individually to grid through HVDC line. Thereafter, Simulation is carried out with all the sources feeding power to the common grid collectively from their own line. All the simulations are carried out under MATLAB Simulink environment. Following conclusions can be drawn:

1) Renewable and non-renewable sources of power located at remote locations can be integrated to give power to a common grid by using HVDC Transmission system.

2) All the sources after integrating with the grid, give same voltage magnitude as rated voltage of grid.

3) Wind HVDC link system and Solar HVDC link system suffers from serious distortions in the voltages at the generation side and DC link.

4) Both hydro and Diesel shows almost same behavior. Both the systems have same loss in voltage in DC link. Also, both the systems come to steady state in same time and faster than the other sources.

5) Steam doesn't undergo from any serious distortions both in magnitude and wave shape but could not achieve steady state as readily as hydro and diesel.

6.2 SCOPE FOR FUTURE WORK

After the completion of the simulation work, the scope is been identified as:

- Study of various switching & fault conditions for the proposed system.
- Investigate the minimum cost of generation and transmission for the proposed system.
- Implementation of whole system with bipolar HVDC system instead of mono-polar with ground return.

REFERANCES

1) Ahshan, R.; Iqbal, M.T.; Mann G.K.I.; Quaicoe J.E.; ‘‘Micro-grid System Based on Renewable Power Generation Units’’, Proceedings of IEEE 23rd Canadian Conference on Electrical and Computer Engineering, Alberta, Canada, pp. 1-4, May 2-5,2010.

2) Asplund, G.; **‘‘**Sustainable energy systems with HVDC transmission**’’,** Proceedings of IEEE Power Engineering Society General Meeting, Denver, CO, USA, pp.2299-2303, June 6-10, 2004.

3) Jain, A.; Garg, K.; ‘‘Variable Renewable Generation and Grid Operation’’, Proceedings of IEEE International Conference on Power System Technology, Hangzhou, China, pp. 1-8, October 24-28, 2010.

4) Karlis, A.; Dokopoulos, P.; ‘‘Small Power Systems Fed by Hydro, Photovoltaic, Wind Turbines and Diesel Generators’’, IEEE Proceedings 3rd International Conference on Electronic Circuits, Rodos, Greece, Vol. 2, pp. 1013-1016, October 13-16, 1996.

5) Chan, T.T.; ‘‘Transient analysis of integrated solar/diesel hybrid power system using MATLAB Simulink’’, Proceedings of International Conference of Engineers and Computer Scientists, Hong Kong, March 17-19, 2010.

6) IEEE committee report, "Dynamic models for steam and hydro turbines in power system studies", IEEE Transactions on Power Apparatus and Systems, Vol.PAS-92, No.6, 1973, pp.1904-1915.

7) IEEE committee report, "Dynamic models for steam and hydro turbines in power system studies", IEEE Transactions on Power Apparatus and Systems, Vol.PAS-92, No.6, 1973, pp.1904-1915.

8) Eggenberger, M.A.; "A Simplified Analysis of the No Load Stability of Mechanical-Hydraulic Speed Control System for Steam Turbines", ASME Paper 60-WA-34, December 1960.

9) IEEE Committee Report, "Computer Representation of Excitation Systems", IEEE Transactions on Power Apparatus and Systems, vol. PAS-87, No. 6 pp. 1460-1468, June 1968.

10) Birnbaum M.; Noyes E.G.; "Electro Hydraulic Control for Improved Availability and Operation of large Steam Turbines", ASME-IEEE National Power Conference, Albany, New York, September 19-23, 1965.

11) Sharaf, A.M.; Aljankawey, A.; "Voltage Stabilization Using A Fact Modulated Power Filter ", Industrial Electronics, 2006 IEEE International Symposium, Montréal, Quebec, Canada on Vol. 3, pp. 1937-42, July 2006.

12) Khennas, S.; Dunnett, S.; Piggott, H.; "Small Wind Systems for Rural Energy Services", ITDG Publishing, 2003, ISBN 1853395552.

13) Anderson, P. M.; Bose, A.; ''Stability Simulation of Wind Turbine Systems", IEEE Transactions on Power Apparatus and Systems, Vol. PAS-102, no. 12, December 1983, pp. 3791-3795.

14) Heier, S.; ''Grid Integration of Wind Energy Conversion Systems'', John Wiley & Sons Ltd, 1998, pp. 385.

15) Akhmatov, V.; ''Modeling and transient stability of large wind farms'', Electrical Power and Energy System, vol. 25, issue 2, February 2003, pp. 123-144.

16) Dusonchet, L. ; Massaro, F. ; Telaretti, E. , ''Transient stability simulation of a fixed speed wind turbine by Matlab/Simulink'', IEEE Proceedings International Conference on Clean Electric Power, Capril, Italy, pp. 651-655, May 21-23,2007.

17) Sharaf, A.M.; Aljankawey, A.S.; Altas, I.H.; ''Dynamic Voltage Stabilization of Stand-Alone Wind Energy Schemes'', IEEE Proceedings Electric Power Conference, Quebec, Canada, pp. 14-19, October 25-26,2007.

18) IEEE Working Group on Prime Mover and Energy Supply Models for System Dynamic Performance Studies, "Hydraulic Turbine and Turbine Control Models for Dynamic Studies", IEEE Transactions on Power Systems, Vol.7, No.1, February, 1992, pp. 167-179

19) IEEE Committee Report, "Dynamic Models for Steam and Hydro Turbines in Power System Studies", IEEE Trans. Power Apparatus and System, Vol. 92, pp 1904-1915.

20) Woodward, J.L.; "Hydraulic-Turbine Transfer Function for Use in Governing Studies", IEE Proceedings on Generation, Transmission and Distribution, Vol. 115, pp. 424-426, March 1968.

21) Smith J.R.; *et al,* ‘‘Assessment of Hydro turbine Models for Power System Studies", IEE Proceedings on Generation, Transmission and Distribution, Vol. 130, No. 1, January 1983.

22) Agnew P.W.; “The Governing of Francis Turbines”, Water Power, pp. 119-127, April 1974.

23) Oldenburger, R.; Donelson, J.; ‘‘Dynamic Response of a Hydroelectric Plant", Trans. AIEE, Vol. 81, Pt. 111, pp. 403-418, 1962.

24) Undriil, J.M.; Woodward, J.L.; ‘‘Non-Linear Hydro Governing Model and Improved Calculation for Determining Temporary Droop’’, IEEE Trans., Vol. PAS-86, No. 4, pp. 443-453, April 1967.

25) Deny E.; Malley M.O.; “Wind generation, power system operation, and emission reduction”, IEEE Trans. Power System, Vol. 21,No.1, Feb 2006. pp. 341-347.

26) Ummels B.C.; *et al;*“Impacts of Wind Power on Thermal Generation Unit Commitment and Dispatch”, IEEE Trans on Energy Conversion, Vol. 22, No.1, March 2007.

27) Oparaku, O.U.; “Design criteria of solar water pumping systems for agricultural production”, Nigerian J Solar Energy, Vol.14, pp 62–75, 2003.

28) Ugwuoke, P.E.; Oparaku, O.U.; Okeke, O.E.; “Computer-aided design of a 7 kW power stand-alone photovoltaic system for a hypothetical household application at a remote location in Nsukka”, Nigerian J Solar Energy, Vol. 14, pp 73–81, 2003.

29) Maduekwe, A.H.L.; Iheonu, E.E.; Akingbade, F.O.A.; “Verification of some simple solar radiation models in the Nigerian environment”, Nigerian J Renewable Energy, Vol.10, pp 4-11, 2002.

30) Ododo, J.C., Abdourahamane, I.I., Sambo, G.B.; “Applicability of the Swartman–Ogunlade equations to Nigerian stations”, Nigerian J Solar Energy, Vol. 15, pp93–114, 2005.

31) Wood A. R.; Osauskas C. M.; Hume D. J., ‘‘SMALL SIGNAL MODELLING OF HVDC TRANSMISSION SYSTEMS’’, IEEE 7th International Conference on AC-DC Power Transmission, pp. 107-112, London, United Kingdom, November 28-30, 2001.

32) "Recommended Practice for Excitation System Models for Power System Stability Studies’’, IEEE Standard 421.5-1992, August, 1992.